

**NIST GCR 95-676**

---

---

**New Mass Transport Elements and Components  
for the NIST IAQ Model**

---

---

James W. Axley  
School of Architecture  
Yale University

July 1995

Prepared for:  
Indoor Air Quality and Ventilation Group  
Building Environment Division  
Building and Fire Research Laboratory  
National Institute of Standards and Technology  
Gaithersburg, MD 20899



**U. S. Department of Commerce**  
Ronald H. Brown, *Secretary*  
Mary L. Good, *Under Secretary for Technology*  
National Institute of Standards and Technology  
Arati Prabhakar, *Director*

## **ABSTRACT**

This report presents new mass transport elements for the next generation of the NIST IAQ Model that may be used to model a) homogenous (bulk-air) chemistry within well-mixed chamber, b) aerosol mass transport within well-mixed chambers and fractional particle filtration in building filtration devices, and c) heterogeneous (surface-related) physical processes and chemical transformations including those governing the behavior of gas-phase air cleaning devices. In an effort to maintain rigor, generality, and flexibility, each transport process is formulated in terms of the elemental mass transport steps that together govern the overall process. In this way, the more complex processes may be represented as *component equations* that are *assembled* from *fundamental element equations*.

The element/component assembly method, upon which the NIST IAQ Model is based, provides a general and modular approach to the formulation of systems of equation governing the mass and air transport in buildings to effect indoor air quality analysis. In this approach, the solution of the *system equations* is a computationally distinct task that may be achieved using a variety of numerical methods. The third chapter of this report discusses numerical and computational strategies for the solution of the system equations that are compatible with both the existing and proposed new mass transport elements and presents candidate strategies that appear to be most promising.

Finally the fourth chapter of this report considers user interface strategies to implement the proposed new mass transport elements and components.

**Keywords:** contaminant dispersal, filtration, indoor air quality, mass transport, modeling, ventilation

## TABLE OF CONTENTS

Abstract.....	1
Table of Contents.....	3
1. Introduction.....	5
2. Elemental/Component Equations.....	7
2.1 Homogeneous Chemistry.....	7
2.1.1 Gas-Phase Chemistry.....	8
2.1.1.1 Unimolecular Reactions & Photochemical Dissociation.....	9
2.1.1.2 Bimolecular and Termolecular Reactions.....	10
2.1.1.3 Temperature Dependencies.....	11
2.1.1.4 Other Rate Reactions.....	12
2.1.1.5 Formulation for IAQ Analysis - Well-Mixed Zone Idealization.....	12
2.1.1.6 Example Application - Single Well-Mixed Zone w/ Bimolecular Chem..	14
2.1.1.7 The Pseudo Uncoupled Linear Form.....	15
2.1.1.8 Solution Methods - PSSA and Newton-Raphson Methods.....	17
2.1.1.9 Initial Concentrations, Outdoor Concs., and Steady State Concs.....	21
2.1.1.10 Heterogeneous Loss.....	22
2.1.1.11 Recommendations for the Next Generation NIST IAQ Model.....	23
2.1.2 Aqueous- & Aerosol-Phase Chemistry.....	26
2.2 Aerosol Transport & Fractional Particle Filtration.....	27
2.2.1 Aerosol Representation.....	28
2.2.2 [Nazaroff's] Basic Model Postulate.....	30
2.2.3 Ventilation and Filtration.....	30
2.2.3.1 Fractional Aerosol Filtration.....	32
2.2.3.2 Fractional Filtration Efficiency - The Empirical Approach.....	33
2.2.3.3 Fractional Filtration Efficiency - The Theoretical Approach.....	35
2.2.4 Aerosol Deposition onto [Room] Surfaces.....	35
2.2.5 Coagulation.....	39
2.3 Heterogeneous Processes.....	43
2.3.1 Elemental Mass Transport Processes.....	44
2.3.1.1 Boundary Layer Diffusion.....	45
2.3.1.2 Mass Transfer Resistance.....	47
2.3.1.3 Equilibrium Constraints.....	49
Absorption.....	50
Adsorption.....	51
Vaporization and Sublimation.....	55
2.3.1.4 1D Simple Diffusion.....	57
2.3.1.5 1D Equilibrium-Constrained Diffusion in Porous Solids.....	58
Sheet-Like Porous Solids.....	58
Granulated Porous Solids.....	60
2.3.1.6 1D Convection-Diffusion.....	61
Porous Solid Sheets.....	61
Packed Beds of Porous Adsorbents.....	62
2.3.1.7 Surface Chemistry.....	63
Unimolecular Decomposition.....	64
Bimolecular Interactions.....	65
2.3.2 Applications of the Elemental Transport Equations.....	67
2.3.2.1 Practical Use of Constraint Relations.....	68
Absorption Transport.....	69
Adsorption Transport.....	69
Evaporation Transport.....	70
2.3.2.2 Zero-Capacitance Nodes.....	71
3. Solution of System Equations.....	73
3.1 Solution Methods.....	73
3.2 Structure of System Equations.....	76
4. User Interface Strategies.....	78
4.1 Homogeneous Chemistry.....	78
4.2 Aerosol Transport and Fractional Particle Filtration.....	81
4.3 Heterogeneous Processes.....	83
References.....	84

## 1. INTRODUCTION

The NIST IAQ Model has now undergone four generations of development marked by the release of the programs CONTAM86, CONTAM87, CONTAM88, and, most recently, CONTAM93/94. CONTAM86 supported single species multizone gas-phase contaminant dispersal analysis, CONTAM87 extended the NIST IAQ Model to account for multiple reactive gas-phase contaminants and the possibility of convection-diffusion mass transport in 1D flow regimes (e.g., ducts), CONTAM88 integrated multizone airflow analysis with the contaminant dispersal analysis of the earlier generations and CONTAM93/94 was developed to provide users with a graphic users interface, more complete libraries of mass transport and airflow elements and better numerics.

During the past eight years of model development, the IAQ research community has not stood still. More complete mathematical models have emerged to account for a) homogeneous (bulk-air) and heterogeneous (surface-related) physical and chemical transformations, b) aerosol/particulate transport, c) pollutant source emissions, and d) sorption and particle filtration devices. Consequently, the time is ripe to begin the development of new mass transport elements and components for the next generation NIST IAQ Model based on these more complete models.

This report is directed toward the development of these needed mass transport elements and is organized into three chapters – *formulation of element equations, identification of strategies for solution of system equations and development of user interface strategies for computational implementation.*

In preparation for this report, the literature was reviewed to assemble a) available mathematical models for the transport processes enumerated above and b) user interface strategies used to implement these models computationally. From these reviews the most promising models for homogeneous chemistry, aerosol transport, and filtration were selected. For source emission modeling, on the other hand, a new approach was taken. Elemental transport relations were collected for the fundamental transport steps that may be expected to govern the actual physical mechanisms governing emission for a variety of possible sources. These elemental relations were then used to assemble a series of examples of physically-based emission models without any attempt to be comprehensive. Empirically-based emission models were not considered.

Few of the available models are presented in the necessary *element equation* form most suitable for computational implementation within the CONTAM element assembly framework. Therefore, the available models were (re)formulated as element equations. In an effort to maintain rigor, generality, and flexibility, each transport process was reformulated in terms of the elemental mass transport steps that together govern the process. In this way, the more complex processes may be represented as *component equations* that are *assembled from fundamental element equations*. Thus, for example, sorption filtration *components* are developed as assemblages of *elements* modeling boundary layer diffusion, pore diffusion, and sorption.

The element assembly method, upon which the CONTAM family of program is based, provides a general and modular approach to the formulation of systems of equations governing the mass and air transport in buildings to effect indoor air quality analysis. In this approach, the solution of the *system equations* is a computationally distinct task that may be achieved using a variety of numerical methods. The choice of numerical method used is, however, limited by the mathematical character of element equations being assembled. The third chapter of this report discusses numerical and computational strategies for the solution of the system equations that are compatible with both the existing and proposed new mass transport elements and presents candidate strategies that appear to be most promising.

The methods used to communicate input to a program (i.e., building *idealization, representation,* and program *interface* conventions) and computed results to the user demand careful consideration. The last chapter attempts to develop user interface strategies, based on the review of conventions used in related programs, for the implementation of the proposed new mass transport elements.

√ Throughout the report, text marked, as this paragraph is marked, by a √ in the left margin and a dotted line in the right margin provide specific recommendations for the next generation of the NIST IAQ Model – CONTAMxx.

## 2. ELEMENT/COMPONENT EQUATIONS

Fundamental theory and equations derived to be integrable with current multizone indoor air quality analysis models – most importantly, the NIST IAQ Model – will be presented in this chapter to add mass transport modeling capabilities for:

- Homogeneous Chemistry
- Aerosol Transport & Fractional Particle Filtration
- Heterogeneous Processes
  - Elemental Mass Transport Processes
  - Room Sorption Transport
  - Sorption Filtration
  - Fundamentally-Based Air Pollutant Source Models

User interface requirements and numerical methods to form and/or solve systems of equations assembled from the element or component equations presented will be discussed within the individual sections of this chapter. Chapters 3 and 4 of this report will then attempt to review these individual interface requirements and numerical methods to formulate strategies to efficiently a) form and solve systems of equations assembled from these new and existing element or component models and b) communicate input data and output results with the users of programs based on these new and existing models.

### 2.1. Homogeneous Chemistry

Indoor air quality may be affected by chemical reactions that occur homogeneously within the *bulk air phase*<sup>1</sup> contained within building rooms or zones. Three broad classes of homogeneous chemistry will be distinguished here – *gas-phase*, *aqueous-phase*, and *aerosol-phase* chemistry – where aqueous-phase homogeneous chemistry is a special, but important, subclass of aerosol-phase chemistry involving chemistry occurring within or on individual particles of a homogeneously distributed aerosol. It is presumed, here, that the dynamics of these three classes of homogeneous chemistry (i.e., as controlled by both the kinetics of the chemistry in question and the mass transport processes that may affect this chemistry) may be modeled using the vast body of theory, knowledge, and information developed in the closely related field of (outdoor) tropospheric, atmospheric chemistry (1-4).

This report will limit consideration to the development of new gas-phase homogeneous chemistry mass transport elements for the next generation NIST IAQ model leaving aqueous-phase and aerosol-phase chemistry to future efforts. Recent research has indicated that gas-phase chemistry

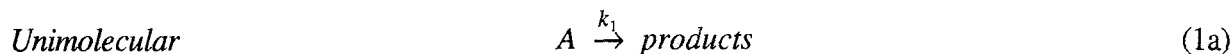
---

<sup>1</sup> *bulk air-phase* – used in chemical engineering literature to refer to the main or greater part of a volume of air as distinguished from that part of the air volume associated with surface layers at the boundaries of a volume of air.

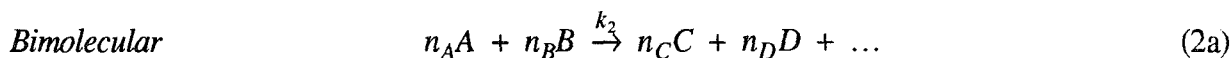
may play a significant role in indoor air at times (5-10) and aqueous-phase chemistry is presently coming under closer scrutiny (11-13). For this reason, issues relating to aqueous-phase and aerosol-phase chemistry will be reviewed to aid the planning of future development efforts.

### 2.1.1. Gas-Phase Chemistry

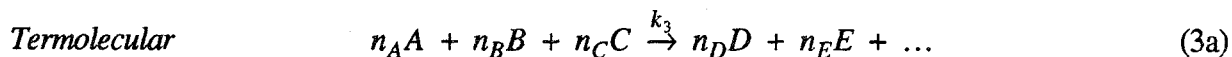
Fortuitously, the detailed mechanism and associated kinetics of gas-phase atmospheric chemistry can, most often, be described in terms of either unimolecular, bimolecular, or termolecular *elementary* reactions and their kinetic rate expressions as:



$$\frac{d[A]}{dt} = -k_1[A] \quad (1b)$$



$$\frac{1}{n_A} \frac{d[A]}{dt} = \frac{1}{n_B} \frac{d[B]}{dt} = -k_2[A][B] = \frac{-1}{n_C} \frac{d[C]}{dt} = \frac{-1}{n_D} \frac{d[D]}{dt} = \dots \quad (2b)$$



$$\frac{1}{n_A} \frac{d[A]}{dt} = \frac{1}{n_B} \frac{d[B]}{dt} = \frac{1}{n_C} \frac{d[C]}{dt} = -k_3[A][B][C] = \frac{-1}{n_D} \frac{d[D]}{dt} = \frac{-1}{n_E} \frac{d[E]}{dt} = \dots \quad (3b)$$

where  $[A]$ ,  $[B]$ , ... are concentrations conventionally expressed in terms of either molecules-species·cm-air<sup>-3</sup> or ppm (i.e., molecules-species·10<sup>6</sup>-molecules-air<sup>-1</sup> or mole-species·10<sup>6</sup>-mole-air<sup>-1</sup>);  $n_A$ ,  $n_B$ , ... are the number of molecules or moles stoichiometrically involved in each reaction; and  $k_1$ ,  $k_2$ ,  $k_3$  are first, second, and third order rate constants respectively.

Given one mole or  $6.023 \times 10^{23}$  molecules occupies a volume ( $V_s$ ) of 22,400 cm<sup>3</sup> at standard conditions of temperature ( $T_s = 273$  °K) and pressure ( $P_s = 1$  atm) or a volume  $V$  at any other state of temperature  $T$  (°K) and pressure  $p$  (atm):

$$V = V_s \left( \frac{P_s}{P} \right) \left( \frac{T}{T_s} \right) \quad (4)$$

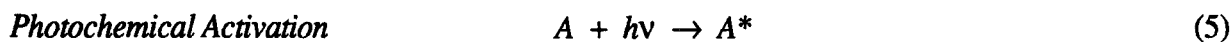
the conventional units of the rate constants used above –  $k_1$ ,  $k_2$ , and  $k_3$  – and the conversion factor between these units may be derived as tabulated below (see (1) Appendix 4.A.1 for details):

Table 1: Conventional kinetic rate constant units and their conversion.

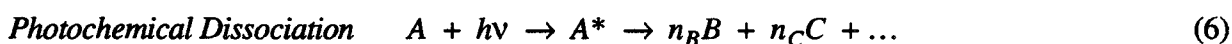
	Conventional Units		Conversion Relation
[X]	[X] molecule·cm <sup>-3</sup>	[X] <sub>ppm</sub> ppm	$[X]_{ppm} = [X] \frac{22,400(1/p)(T/273) \times 10^6}{6.023 \times 10^{23}}$
k <sub>1</sub>	k <sub>1</sub> s <sup>-1</sup>	k <sub>1ppm</sub> min <sup>-1</sup>	$k_{1ppm} = 60 k_1$
k <sub>2</sub>	k <sub>2</sub> cm <sup>3</sup> ·molecule <sup>-1</sup> ·s <sup>-1</sup>	k <sub>2ppm</sub> ppm <sup>-1</sup> ·min <sup>-1</sup>	$k_{2ppm} = 4.40 \times 10^{17} \left(\frac{p}{T}\right) k_2$
k <sub>3</sub>	k <sub>3</sub> cm <sup>6</sup> ·molecule <sup>-2</sup> ·s <sup>-1</sup>	k <sub>3ppm</sub> ppm <sup>-2</sup> ·min <sup>-1</sup>	$k_{3ppm} = 3.23 \times 10^{33} \left(\frac{p}{T}\right)^2 k_3$

### 2.1.1.1. Unimolecular Reactions & Photochemical Dissociation

Unimolecular elementary reactions often involve a reactant that is in an excited or *activated* state, A\*. In atmospheric chemistry, photochemical conversion resulting from the absorption of a photon,  $h\nu$ , provides an important path to activation:



Of the photolytically activated reactions possible, photolytic dissociation (i.e., the fragmentation or separation of the original species A into component constituents) is most important:



The photolytic dissociation of trace air pollutants may be represented as a first order process, Equation 1A, with the rate constant,  $k_1$ , dependent on the integral of the product of the *actinic irradiance density*,  $I(\lambda)$  (photons·cm<sup>-3</sup>·sec<sup>-1</sup>) – a measure of the spectral distribution of radiant flux or radiant intensity (photons·cm<sup>-2</sup>·sec<sup>-1</sup>) per unit wavelength (cm<sup>-1</sup>), the *absorption cross-section* of the molecule A,  $\sigma_A(\lambda, T)$  (cm<sup>2</sup>), and the *quantum yield* or *probability* of dissociation of A upon absorption of a photon,  $\phi_A(\lambda, T)$ , over the wavelength interval of interest,  $\langle \lambda_1 .. \lambda_2 \rangle$  (cm), as:

$$\text{Photochemical Dissociation} \quad k_1 = \int_{\lambda_1}^{\lambda_2} \sigma_A(\lambda, T) \phi_A(\lambda, T) I(\lambda) d\lambda \quad (7)$$

where  $T$  is included to account for the temperature dependency of these quantities. Seinfeld notes that in the troposphere  $\langle \lambda_1 .. \lambda_2 \rangle \approx \langle 280 .. 730 \text{ nm} \rangle$  and for practical application Equation 7 is



approximated by a discrete approximation using wavelength intervals,  $\Delta\lambda$ , of from 10 to 20 nm as ( (1) page 113):

$$\text{Photochemical Dissociation} \quad k_1 \approx \sum \overline{\sigma}_A(\lambda_i, T) \overline{\phi}_A(\lambda_i, T) \overline{I}(\lambda_i) \Delta\lambda \quad (8)$$

where the overbars are used to indicate mean values taken from measured data. Table 4.1 in Seinfeld's text, lists the major photochemical dissociation reactions occurring in the lower atmosphere.

The kinetics of a unimolecular reaction may be represented as a pseudo, "zero-order" process with rate  $k_{0\infty}$  when the reactant is abundant and the rate of reaction is so slow that the reactant's concentration does not change significantly during the course of the reaction:

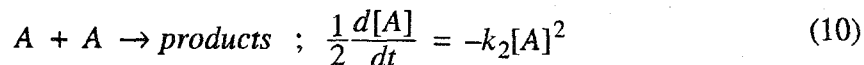
$$\text{Pseudo Zero Order} \quad \frac{1}{n_A} \frac{d[A]}{dt} \approx -k_{0\infty} ; k_{0\infty} = k_1[A] \text{ for } [A] = [A]_{ss} \approx \text{constant} \quad (9)$$

This condition may also be identified as a *pseudo-steady state* condition and thus the *ss* subscript notation above for the reactant  $[A]_{ss}$ .

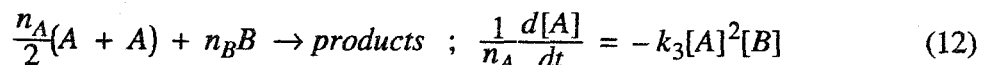
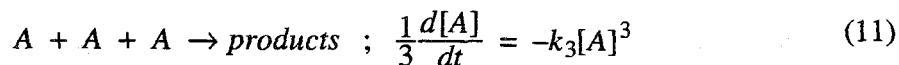
#### 2.1.1.2. Bimolecular and Termolecular Reactions

In atmospheric chemistry, the bimolecular and termolecular reactions described above most often involve equal numbers of reactant groups – that is, unit stoichiometry. This is due to the fact that in the gas-phase these elementary reactions are invariably associated with collisions of individual atoms, molecules, radicals<sup>2</sup>, or ions. Given the probability of simultaneous collision of three atoms, molecules, radicals, or ions is likely to be small, termolecular reactions are uncommon and are likely to proceed at low rates. That is to say, atmospheric chemistry is dominated by (unimolecular and) bimolecular elementary reactions.

Tables 4.10 and 4.11 in Seinfeld's text, lists the important reactions of the oxides of nitrogen occurring in the lower atmosphere showing that they are dominated by bimolecular kinetics and unit stoichiometry of reactants. A closer examination of these tables reveal two generic cases of bimolecular kinetics – that presented above in Equations 2 and the special case:



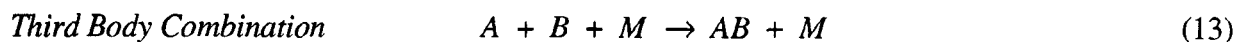
(Note the stoichiometric coefficient of 1/2 here.) By generalization, three generic cases of termolecular kinetics may be identified – that presented above in Equations 3 and the following two special cases:




---

<sup>2</sup> Radicals may be thought to be uncharged (i.e., nonionic) molecular fragments that contain an unpaired electron and, as a result, tend to be highly reactive.

Finally, a special class of termolecular reaction should be noted – the generic *combination* reaction involving a third *body M* of the form:



The mechanisms responsible for this type of reaction are thought to involve a series of two bimolecular elementary reactions (see (1) Appendix 4.A.2 for details) and the rate expression for this reaction is often written in the form of a bimolecular rate expression (i.e., Equation 2b) with the rate constant dependent on the concentration of the third body at the *low-pressure limit*, independent of the third body concentration at the *high-pressure limit*, and a blended combination between as:

$$\textit{Third Body Combination} \quad k_2 \approx \begin{cases} k_{2o}[M] ; \text{ as } [M] \rightarrow 0 \\ \frac{k_{2o}[M]k_{2\infty}}{k_{2o}[M] + k_{2\infty}} F \\ k_{2\infty} ; \text{ as } [M] \rightarrow \infty \end{cases} \quad (14)$$

where  $F$  is the so-called broadening factor used to fine-tune the intermediate relation. That is to say, at the low pressure limit this generic combination reaction is governed by termolecular kinetics while at the high pressure limit the behavior is bimolecular.

In a similar way the kinetics of a bimolecular reaction may be represented as a pseudo, first-order process with rate constant  $k_{1\infty}$  when one of the reactants remains practically constant (e.g., if the reactant is so abundant that its concentration does not change significantly during the course of the reaction) – another example of a pseudo steady state:

*Pseudo First Order*

$$\frac{1}{n_A} \frac{d[A]}{dt} = \frac{1}{n_B} \frac{d[B]}{dt} \approx -k_{1\infty}[A] ; k_{1\infty} = k_2[B]_{ss} \text{ for } [B] = [B]_{ss} \approx \text{constant} \quad (15)$$

### 2.1.1.3. Temperature Dependencies

For ideal elementary reactions, rate constants are dependent on the absolute temperature at which the reaction occurs as defined by the Arrhenius Equation:

$$k = A \exp\left(\frac{-E_{act}}{RT}\right) \quad (16)$$

where  $A$  is the Arrhenius constant with the same units as  $k$ ,  $E_{act}$  is the so-called “activation energy” associated with the given reaction,  $R$  is the universal gas constant ( $8.3145 \text{ J}\cdot\text{mol}^{-1}\cdot\text{K}^{-1}$ ), and  $T$  is the temperature of the reaction ( $^{\circ}\text{K}$ ). See (14) pages 14 to 16 for a general introduction to the Arrhenius relation.

Several specific Arrhenius relations are included in the tables of Seinfeld’s text mentioned above. A close examination of these tables will reveal, however, other temperature dependent – and more

complex – relations (e.g., for the important reaction of oxygen with the oxygen radical to produce ozone:  $O + O_2 + M \rightarrow O_3 + M$ ).

#### 2.1.1.4. Other Rate Relations

Although it is believed that practically all chemical reactions can be represented in terms of unimolecular, bimolecular, and/or termolecular elementary mechanisms these mechanisms may not be known or researchers may have had to limit consideration to the overall reaction that results from the combined elementary steps. As a result, for a few cases only overall or completely empirical rate expressions may be available. As might be expected, such rate expressions assume a large variety of forms and, therefore, must be considered on a case-by-case basis.

#### 2.1.1.5. Formulation for IAQ Analysis – Well-Mixed Zone Idealization

Thus far, all rate expressions have been presented in the conventional format utilized in the field of kinetics. For indoor air quality analysis, the conventions are different – we seek to consider the dynamic change of zone (mean) air pollutant concentrations  $C_A, C_B, C_C, \dots$ , expressed in terms of mass fraction (mass-A·mass-air<sup>-1</sup>, etc.), within a collection of well-mixed zones. The mass fraction of a species  $B$ , for example, is related to the concentration expressed in terms of molecule·cm<sup>-3</sup> as:

$$C_B \left( \frac{\text{grams-B}}{\text{grams-air}} \right) = [B] \left( \frac{\text{molecules-B}}{\text{cm}^3\text{-air}} \right) \frac{1}{N_A} \left( \frac{\text{mol-B}}{\text{molecules-B}} \right) M_B \left( \frac{\text{grams-B}}{\text{mol-B}} \right) \frac{1}{\rho_{air}} \left( \frac{\text{cm}^3\text{-air}}{\text{grams-air}} \right)$$

or

$$C_B = [B] \frac{M_B}{N_A \rho_{air}} \quad (17)$$

where  $N_A$  is Avogadro's constant ( $6.022 \times 10^{23}$  molecules·mol<sup>-1</sup>),  $M_B$  is the molecular weight of species  $B$  (grams-B·mol-B<sup>-1</sup>), and  $\rho_{air}$  is the density of air within the well-mixed zone (grams-air·cm<sup>-3</sup>). For non-trace analysis one must be careful to use the (current value of the) actual density of the pure-air/air-pollutant mixture for  $\rho_{air}$ .

For a well-mixed zone containing a volume of air of mass  $M_{air}$  the mass rate of production (+) or removal (-) of a given air pollutant, say for species  $B$  again,  $R_B$  (grams-B·sec<sup>-1</sup>) is related to the time rate of change of species concentration  $[B]$  as:

$$R_B = \frac{M_{air} M_B}{N_A \rho_{air}} \frac{d[B]}{dt} \quad (18)$$

Using Equations 17 and 18 one may, then, convert each of the rate expressions presented above in conventional kinetics form to well-mixed zone mass generation or removal rate expressions as tabulated below:

Table 2. Well-Mixed Zone Chemical Generation/Removal Rate Expressions

Zero Order	$\frac{d[A]}{dt} = -k_0$	$R_A = -\frac{M_{air}M_A}{N_A\rho_{air}}k_0$ $K_{0A} \equiv \frac{M_A}{N_A\rho_{air}}k_0$ $R_A = -M_{air}K_{0A}$
First Order	$\frac{d[A]}{dt} = -k_1[A]$	$R_A = -\frac{M_{air}M_A}{N_A\rho_{air}}k_1\frac{N_A\rho_{air}}{M_A}C_A$ $R_A = -M_{air}k_1C_A$ $K_{1A} \equiv k_1$ $R_A = -M_{air}K_{1A}C_A$
Second Order Reactant A	$\frac{d[A]}{dt} = -n_Ak_2[A][B]$	$R_A = -n_A\frac{M_{air}M_A}{N_A\rho_{air}}k_2\frac{N_A\rho_{air}}{M_A}\frac{N_A\rho_{air}}{M_B}C_A C_B$ $R_A = -n_A M_{air}\frac{N_A\rho_{air}}{M_B}k_2 C_A C_B$ $K_{2A} \equiv n_A\frac{N_A\rho_{air}}{M_B}k_2$ $R_A = -M_{air}K_{2A}C_A C_B$
Second Order Reactant B	$\frac{d[B]}{dt} = -n_Bk_2[A][B]$	$R_B = -n_B\frac{M_{air}M_B}{N_A\rho_{air}}k_2\frac{N_A\rho_{air}}{M_A}\frac{N_A\rho_{air}}{M_B}C_A C_B$ $R_B = -n_B M_{air}\frac{N_A\rho_{air}}{M_A}k_2 C_A C_B$ $K_{2B} \equiv n_B\frac{N_A\rho_{air}}{M_A}k_2$ $R_B = -M_{air}K_{2B}C_A C_B$

---

Second Order  
Product C

$$\frac{d[C]}{dt} = n_C k_2 [A][B]$$

$$R_C = n_C \frac{M_{air} M_C}{N_A \rho_{air}} k_2 \frac{N_A \rho_{air}}{M_A} \frac{N_A \rho_{air}}{M_B} C_A C_B$$

$$R_C = n_C M_{air} M_C \frac{N_A \rho_{air}}{M_A M_B} k_2 C_A C_B$$

$$K_{2C} \equiv n_C M_C \frac{N_A \rho_{air}}{M_A M_B} k_2$$

$$R_C = M_{air} K_{2C} C_A C_B$$

---

Third Order  
Reactant A

$$\frac{d[A]}{dt} = -n_A k_3 [A][B][C]$$

$$R_A = -n_A \frac{M_{air} M_A}{N_A \rho_{air}} k_3 \frac{N_A \rho_{air}}{M_A} \frac{N_A \rho_{air}}{M_B} \frac{N_A \rho_{air}}{M_C} C_A C_B C_C$$

$$R_A = -n_A M_{air} \frac{(N_A \rho_{air})^2}{M_B M_C} k_3 C_A C_B C_C$$

$$K_{3A} \equiv n_A \frac{(N_A \rho_{air})^2}{M_B M_C} k_3$$

$$R_A = -M_{air} K_{3A} C_A C_B C_C$$

---

Third Order  
Product C

$$\frac{d[C]}{dt} = n_C k_3 [A][B][C]$$

$$R_C = n_C \frac{M_{air} M_C}{N_A \rho_{air}} k_3 \frac{N_A \rho_{air}}{M_A} \frac{N_A \rho_{air}}{M_B} \frac{N_A \rho_{air}}{M_C} C_A C_B C_C$$

$$R_C = n_C M_{air} M_C \frac{(N_A \rho_{air})^2}{M_A M_B} k_3 C_A C_B C_C$$

$$K_{3C} \equiv n_C M_C \frac{(N_A \rho_{air})^2}{M_A M_B} k_3$$

$$R_C = M_{air} K_{3C} C_A C_B C_C$$

---

Other cases follow, by example, from these generic possibilities.

#### 2.1.1.6. Example Application – Single Well-Mixed Zone with Bimolecular Chemistry

It is useful to place these equations in the full context that they will appear in indoor air quality analysis. To do so, consider a single well-mixed zone containing two reactants A and B, their products C and D, and a volume of air of mass  $M_{air}$ . For trace dispersal analysis (and no significant generation of air within the zone) mass conservation demands that the mass flow rate of air exiting the zone be equal to that flowing in,  $w_{air}$ . Given these conditions, mass balances for each of the four pollutant involved may be directly formed as:

$$w_{air} \begin{Bmatrix} C_A \\ C_B \\ C_C \\ C_D \end{Bmatrix} - \begin{Bmatrix} R_A \\ R_B \\ R_C \\ R_D \end{Bmatrix} + M_{air} \frac{d}{dt} \begin{Bmatrix} C_A \\ C_B \\ C_C \\ C_D \end{Bmatrix} = w_{air} \begin{Bmatrix} C_{Ao} \\ C_{Bo} \\ C_{Co} \\ C_{Do} \end{Bmatrix} + \begin{Bmatrix} G_A \\ G_B \\ G_C \\ G_D \end{Bmatrix} \equiv \begin{Bmatrix} E_A \\ E_B \\ E_C \\ E_D \end{Bmatrix} \quad (19)$$

where  $C_{Ao}$  is the outdoor air concentration of species A,  $G_A$  is the indoor generation rate of species A, and  $E$  is a new variable – the zone *excitation* – equal to the sum of species mass inflow and generation rates. Defining new constants  $K_{2i}$ ,  $i = A, B, C, D$  equal to the composite of the leading constants for each of the well-mixed zone rate expressions above (i.e., as tabulated in Table 2) then Equation (19) may be rewritten as:

$$w_{air} \begin{Bmatrix} C_A \\ C_B \\ C_C \\ C_D \end{Bmatrix} - M_{air} \begin{Bmatrix} -K_{2A}C_A C_B \\ -K_{2B}C_A C_B \\ +K_{2C}C_A C_B \\ +K_{2D}C_A C_B \end{Bmatrix} + M_{air} \frac{d}{dt} \begin{Bmatrix} C_A \\ C_B \\ C_C \\ C_D \end{Bmatrix} = \begin{Bmatrix} E_A \\ E_B \\ E_C \\ E_D \end{Bmatrix} \quad (20)$$

For a multizone building idealization where all or selected zones are subjected to the same bimolecular reaction, the system transport matrix will be the sum of a) the contribution due to zone-to-zone flow elements that model dilution dynamics  $[K_{dil}]$  and b) the contribution due to chemical kinetics  $[K_{kin}]$  which assumes the block-diagonal form, given the chemical kinetics is local to a given zone:

$$[K_{kin}] = \begin{bmatrix} M_{air-1}[K] & 0 & 0 & 0 \\ 0 & M_{air-2}[K] & 0 & 0 \\ 0 & 0 & \ddots & \vdots \\ 0 & 0 & \dots & M_{air-n}[K] \end{bmatrix} \quad (21)$$

for an  $n$  zone idealization, if concentration degrees of freedom are ordered by species first and zone thereafter as  $\{C_{A1}, C_{B1}, C_{C1}, C_{D1}, C_{A2}, C_{B2} \dots\}^T$ . Here,  $[K]$  is the zone kinetics transport matrix based, for example, on the second terms of Equation 20 for identical bimolecular kinetics in each zone. A similar block-diagonal form will result for termolecular kinetics as well.

#### 2.1.1.7. The Pseudo Uncoupled Linear Form

Differential equations governing single-zone chemistry based on the assembly of the kinetic rate expressions presented in Table 2 may be written in the following special *autonomous* form (15) that has the form (but not the substance) of an uncoupled, linear system of ordinary differential equations – the *pseudo uncoupled linear form*:

$$\frac{d}{dt}\{C\} = \{P(C_A, C_B, \dots)\} - [L(C_A, C_B, \dots)]\{C\} \quad (22)$$

where  $\{P(C_A, C_B, \dots)\}$  is a *production vector* and  $[L(C_A, C_B, \dots)]$  is a diagonal matrix of apparent system eigen values (i.e., inverse time constants) identified as the *loss rate matrix* – both, importantly, containing only nonnegative terms. This form is termed *autonomous* since the

production vector and loss rate matrix contain terms assumed to be time independent. Equation 21, is a form that, in essence, hides the nonlinearities and the implicit coupling of the system equations in the individual terms of the  $P$  and  $L$ .

For the system of differential equations used above to model bimolecular kinetics in a single, well-mixed zone, Equation 20, the pseudo uncoupled linear form becomes:

$$\frac{d}{dt} \begin{pmatrix} C_A \\ C_B \\ C_C \\ C_D \end{pmatrix} = \begin{pmatrix} \frac{E_A}{M_{air}} \\ \frac{E_B}{M_{air}} \\ K_{2C}C_A C_B + \frac{E_C}{M_{air}} \\ K_{2D}C_A C_B + \frac{E_D}{M_{air}} \end{pmatrix} - \begin{bmatrix} \frac{w_{air}}{M_{air}} + K_{2A}C_B & 0 & 0 & 0 \\ 0 & \frac{w_{air}}{M_{air}} + K_{2B}C_A & 0 & 0 \\ 0 & 0 & \frac{w_{air}}{M_{air}} & 0 \\ 0 & 0 & 0 & \frac{w_{air}}{M_{air}} \end{bmatrix} \begin{pmatrix} C_A \\ C_B \\ C_C \\ C_D \end{pmatrix} \quad (23)$$

It is important to note that, in spite of the apparent form of this equation:

- Bimolecular (and termolecular) kinetics couples the dynamic response of the reactants and products.
- Bimolecular (and termolecular) kinetics introduce nonlinearities in the resulting system of ordinary differential equations, here represented as nonlinear coefficients in a system having the form of a uncoupled system of linear equations.

At any instant, say  $t$ , during the dynamic response of the single-zone system being studied, however, a given *state* of reactant and product concentrations will exist  $\{C_A(t), C_B(t), C_C(t), C_D(t)\}$ , thus at that instant in time the behavior of the system may be described in terms of a linear, uncoupled system of equations with (instantaneous) species time constants  $(\tau_A, \tau_B, \tau_C, \tau_D)$  equal to the inverses of each of the diagonal terms of  $L$ :

$$\tau_A = \frac{1}{\left(\frac{w_{air}}{M_{air}} + K_{2A}C_B(t)\right)} ; \tau_B = \frac{1}{\left(\frac{w_{air}}{M_{air}} + K_{2B}C_A(t)\right)} ; \tau_C = \tau_D = \frac{1}{\left(\frac{w_{air}}{M_{air}}\right)} \quad (24a)$$

providing, of course, the nonlinear production terms for products C and D,  $K_{2C}C_A C_B$  and  $K_{2D}C_A C_B$  remain relatively constant (or insignificant) at the instant of time under consideration. Thus within the limitations of these caveats and the recognition that all terms are nonnegative, the characteristic species time constants of the system are bounded as:

$$\tau_A \approx \left\langle \frac{1}{K_{2A}C_B(t)} ; \frac{M_{air}}{w_{air}} \right\rangle ; \tau_B \approx \left\langle \frac{1}{K_{2B}C_A(t)} ; \frac{M_{air}}{w_{air}} \right\rangle ; \tau_C = \tau_D = \frac{M_{air}}{w_{air}} \quad (24b)$$

That is to say, the species time constants have an upper bound determined by the dilution time constant and, for the reactants, a lower bound that may approach zero when the product of the composite rate constants and species concentrations,  $K_{2A}C_B$  and/or  $K_{2B}C_A$ , greatly exceed the

dilution eigenvalue,  $w_{air}/M_{air}$ . From a numerical point of view, then, the dilution dynamics will tend to place a upper limit on the system time constants (i.e., a lower limit on the systems eigenvalue) which will tend to moderate the *stiffness* of the resulting system equations.

#### 2.1.1.8. Solution Methods – PSSA and Newton-Raphson Methods

The nonlinear, coupled, systems of equations that result when bimolecular, termolecular, or other nonlinear chemical kinetics are modeled may be solved by a number of techniques. Here we will consider two broad classes of methods – methods based on the so-called *pseudo-steady-state approximation* (PSSA) scheme and those based on the Newton-Raphson Method. To make these considerations concrete we will apply these methods to the single zone bimolecular example considered above and draw general conclusions from these applications.

*PSSA Scheme:* The *pseudo-steady-state approximation scheme* (also identified as the *asymptotic approximation scheme*) is based directly on the pseudo, uncoupled linear form presented above. If the production vector  $\mathbf{P}$  and the loss rate matrix  $\mathbf{L}$  characterizing the dynamic system's behavior remains constant then an exact solution of the system equations is available (15):

$$\{\mathbf{C}(t + \delta t)\} = e^{-\delta t[\mathbf{L}]} \{\mathbf{C}(t)\} + [\mathbf{I} - e^{-\delta t[\mathbf{L}]}][\mathbf{L}]^{-1} \{\mathbf{P}\} \quad (25)$$

This observation has lead to a number of explicit, time-stepping, integration schemes based on discrete approximations to Equation 25 (15) such as:

$$\{\mathbf{C}_{n+1}\} = e^{-\delta t[\mathbf{L}_n]} \{\mathbf{C}_n\} + [\mathbf{I} - e^{-\delta t[\mathbf{L}_n]}][\mathbf{L}_n]^{-1} \{\mathbf{P}_n\} \quad (26)$$

where a compact notation has been used:  $\{\mathbf{C}_n\} \approx \{\mathbf{C}(t_n)\}$ ,  $[\mathbf{L}_n] = [\mathbf{L}(\{\mathbf{C}(t_n)\})]$ ,  $\{\mathbf{P}_n\} = \{\mathbf{P}(\{\mathbf{C}(t_n)\})\}$ , and  $t_{n+1} = t_n + \delta t$ . Given the diagonal form of the loss rate matrix, the indicated matrix operations in Equation 26 are computationally trivial, consequently this algorithm is computationally very attractive. This scheme is similar to that used by Yamamoto (16) for the US EPA/AEERL IAQ model.

One may, conceivably, cast multizone contaminant dispersal analysis into the pseudo, uncoupled linear form (e.g., by including all off-diagonal dilution transport terms in the production vector) and achieve computational efficiency. The resulting loss of accuracy and stability when compared to more rigorous implicit and explicit approaches may be expected to become a problem however.

The PSSA scheme has been presumed to provide quick, computationally inexpensive solutions to (single-zone) chemical kinetics problems that provide sufficient accuracy for atmospheric urban air shed analysis (i.e., where the chemistry is modeled at a very large number of points in the atmosphere, over broad geographic regions such as the Los Angeles basin). Verwer and van Loon show results, however, that indicate implicit methods utilizing Newton-Raphson integration, while more complex, are computationally competitive and appear to be more reliable than the PSSA schemes considered (15).



*Newton-Raphson Method:* To apply the Newton Raphson Method, we begin by applying a finite difference algorithm to the system of differential equations described by Equation 20 to transform them to a nonlinear system of algebraic equations that will be solved in a step-by-step manner to approximate the dynamic solution of the original system. To this end, Equation 20 may be rewritten in *autonomous form* as:

$$\frac{d}{dt} \begin{Bmatrix} C_A \\ C_B \\ C_C \\ C_D \end{Bmatrix} = -\frac{w_{air}}{M_{air}} \begin{Bmatrix} C_A \\ C_B \\ C_C \\ C_D \end{Bmatrix} + \begin{Bmatrix} -K_{2A}C_A C_B \\ -K_{2B}C_A C_B \\ +K_{2C}C_A C_B \\ +K_{2D}C_A C_B \end{Bmatrix} + \frac{1}{M_{air}} \begin{Bmatrix} E_A \\ E_B \\ E_C \\ E_D \end{Bmatrix} \quad (27a)$$

or, in concise notation:

$$\frac{d}{dt}\{C\} = -\frac{w_{air}}{M_{air}}\{C\} + \{R(C_A, C_B)\} + \frac{1}{M_{air}}\{E\} \quad (27b)$$

where the vectors contained in Equation 27b are defined implicitly by comparison to Equation 27a.

To transform this system of differential equations, a general semi-implicit scheme will be employed based on the following consistent finite difference approximation:

$$\{C_{n+1}\} = \{C_n\} + (1 + \alpha\delta t)\frac{d}{dt}\{C_n\} + \alpha\delta t\frac{d}{dt}\{C_{n+1}\} \quad (28)$$

where  $\alpha$  is a parameter to control the nature of integration with  $0 \leq \alpha \leq 1$ ; the time domain has been divided into discrete steps  $t_{n+1} = t_n + \delta t$ ; and an abbreviated notation has, again, been used as  $C_n \equiv C(t_n)$ . Note that this difference approximation corresponds to the Forward Difference Scheme for  $\alpha = 0$ ; the Crank-Nicholson scheme for  $\alpha = 1/2$ ; and the Backward Difference Scheme for  $\alpha = 1$ .

Evaluating Equation 27 at time  $t_n$  and  $t_{n+1}$  and substituting the finite difference approximation, Equation 28, we obtain:

$$\begin{aligned} \left(1 + \alpha\delta t\frac{w_{air}}{M_{air}}\right)\{C_{n+1}\} - \alpha\delta t\{R(\{C_{n+1}\})\} &= \left(1 - (1 + \alpha\delta t)\frac{w_{air}}{M_{air}}\right)\{C_n\} + \\ (1 + \alpha\delta t)\left\{\frac{1}{M_{air}}\{E_n\} + \{R(\{C_n\})\}\right\} &+ \alpha\delta t\frac{1}{M_{air}}\{E_{n+1}\} \end{aligned} \quad (29)$$

This rather complicated expression defines a step-by-step integration algorithm where the vector of unknown concentrations at  $t = t_{n+1}$ ,  $\{C_{n+1}\}$  is approximated from the values of the other listed vectors on the right hand side that have known numerical values at time  $t_{n+1}$ . For our purposes here, the sum of these right hand terms will be identified as an effective dynamic excitation  $\{\hat{E}_{n+1}\}$  as:

$$\{\hat{E}_{n+1}\} \equiv \left(1 - (1 + \alpha\delta t)\frac{w_{air}}{M_{air}}\right)\{C_n\} + (1 + \alpha\delta t)\left\{\frac{1}{M_{air}}\{E_n\} + \{R(\{C_n\})\}\right\} + \alpha\delta t\frac{1}{M_{air}}\{E_{n+1}\} \quad (30)$$

so that Equation 29 will assume the apparently simpler form:

$$\boxed{\left(1 + \alpha \delta t \frac{w_{air}}{M_{air}}\right) \{C_{n+1}\} - \alpha \delta t \{R(\{C_{n+1}\})\} = \{\hat{E}_{n+1}\}} \quad (31)$$

With  $\alpha = 0$ , Equation 31 becomes an *explicit* integration scheme while with  $\alpha = 1$  it becomes a “fully” *implicit* scheme. For values between these extremes, the algorithm leads to so-called *semi-implicit* schemes.

The implicit variants of Equation 31 demand the solution of a system of nonlinear equations at each time step. This may be achieved using the Newton-Raphson method. To do so, we reformulate Equation 31 in residual form as:

$$\{f(\{C_{n+1}\})\} \equiv \left(1 + \alpha \delta t \frac{w_{air}}{M_{air}}\right) \{C_{n+1}\} - \alpha \delta t \{R(\{C_{n+1}\})\} - \{\hat{E}_{n+1}\} \quad (32)$$

and form the *Jacobian*  $[f'(\{C_{n+1}\})]$  of the residual  $\{f(\{C_{n+1}\})\}$  with individual terms defined as:

$$f'_{ij}(\{C_{n+1}\}) = \frac{\partial f_i(\{C_{n+1}\})}{\partial C_j} \quad (33)$$

and apply the following iterative algorithm based on Taylor’s formula:

$$\boxed{[f'(\{C_{n+1}\}^k)](\{C_{n+1}\}^{k+1} - \{C_{n+1}\}^k) + \{f(\{C_{n+1}\}^k)\} = \{0\}} \quad (34)$$

where  $k$  is an iteration index.

To summarize, the proposed algorithm involves a step-by-step integration of the discrete form of the system equations (Equation 31) using a Newton-Raphson iterative scheme (Equation 34) at each time step to solve the nonlinear algebraic problem defined these semidiscrete equations. To implement this algorithm one would follow the steps listed below:

Given the (approximate) value of the system concentration vector  $\{C_n\}$  at time step  $n$  (i.e.,  $t = t_n$ ):

1. Form the effective dynamic excitation for the next time step  $\{\hat{E}_{n+1}\}$ .
2. Initialize the iterative algorithm:
  - 2.1 Set  $k = 1$
  - 2.2 Set  $\{C_{n+1}\}^1 = \{C_n\}$
3. Iteratively solve Equation 34 until convergence:
  - 3.1 Form the current system Jacobian  $f'(\{C_{n+1}\}^k)$ .
  - 3.2 Form the current system residual  $f(\{C_{n+1}\}^k)$

3.3 Solve Equation 34 for  $\{\{C_{n+1}\}^{k+1} - \{C_{n+1}\}^k\}$

3.4 Update estimate for the system concentration vector:

$$\{C_{n+1}\}^{k+1} = (\{C_{n+1}\}^{k+1} - \{C_{n+1}\}^k) + \{C_{n+1}\}^k$$

3.5 Evaluate convergence  $\delta C$  of the system concentration vector by evaluating an appropriate norm of the solution from 3.3:

$$\delta C \equiv |\{C_{n+1}\}^{k+1} - \{C_{n+1}\}^k|$$

3.6 If  $\delta C$  is not sufficiently small, increment  $k$  (i.e., set  $k = k+1$ ) and go to

3.7 otherwise continue.

4. Step forward to the next time step:

4.1 Set  $\{C_{n+1}\} = \{C_{n+1}\}^{k+1}$ .

4.2 Set  $n = n+1$ .

4.3 Go to Step 1.

The system Jacobian  $[R']$  is central to the success of this method. First, the iterative algorithm can not proceed unless this matrix is nonsingular. For the system being considered the system Jacobian is the sum of a contribution due to the dilution transport and one due to the bimolecular kinetics:

$$[R'(\{C_{n+1}\})] = \left(1 + \alpha \delta t \frac{w_{air}}{M_{air}}\right) \begin{bmatrix} 1 & 0 & 0 & 0 \\ 0 & 1 & 0 & 0 \\ 0 & 0 & 1 & 0 \\ 0 & 0 & 0 & 1 \end{bmatrix} - \alpha \delta t \begin{bmatrix} -K_{2A} C_{B(n+1)} & -K_{2A} C_{A(n+1)} & 0 & 0 \\ -K_{2B} C_{B(n+1)} & -K_{2B} C_{A(n+1)} & 0 & 0 \\ K_{2C} C_{B(n+1)} & K_{2C} C_{A(n+1)} & 0 & 0 \\ K_{2D} C_{B(n+1)} & K_{2D} C_{A(n+1)} & 0 & 0 \end{bmatrix}$$

$$= \begin{bmatrix} \left(1 + \alpha \delta t \frac{w_{air}}{M_{air}}\right) + \alpha \delta t K_{2A} C_{B(n+1)} & \alpha \delta t K_{2A} C_{A(n+1)} & 0 & 0 \\ \alpha \delta t K_{2B} C_{B(n+1)} & \left(1 + \alpha \delta t \frac{w_{air}}{M_{air}}\right) + \alpha \delta t K_{2B} C_{A(n+1)} & 0 & 0 \\ -\alpha \delta t K_{2C} C_{B(n+1)} & -\alpha \delta t K_{2C} C_{A(n+1)} & \left(1 + \alpha \delta t \frac{w_{air}}{M_{air}}\right) & 0 \\ -\alpha \delta t K_{2D} C_{B(n+1)} & -\alpha \delta t K_{2D} C_{A(n+1)} & 0 & \left(1 + \alpha \delta t \frac{w_{air}}{M_{air}}\right) \end{bmatrix} \quad (35)$$

At this point little can be said about the general nature of this system Jacobian, although given all variables and constants in this Jacobian are nonnegative it may be concluded that this Jacobian will, in general, not be diagonally dominant.

It follows from this example that single-zone systems with any combination of bimolecular and termolecular chemistry will result in systems of nonlinear equations that may be solved using the Newton-Raphson method and the resulting system Jacobian will be the sum of the dilution contribution of the form  $\left(1 + \alpha \delta t \frac{w_{air}}{M_{air}}\right) [I]$  and relatively simple additive contributions for each

reaction considered (i.e., scaled by  $\alpha\delta t$ ). If the individual rate expressions tabulated in Table 2 are considered to be *elemental* then the reaction kinetics contributions to the system Jacobian may be directly assembled from *element Jacobians* formed by differentiating the elemental rate expressions with respect to each concentration variable involved and evaluating the resulting derivatives at the current state of the system concentration. For chemical kinetics described by other rate expressions, a solution may be realized using the algorithm outlined above by providing specific reaction subroutines that can, for the current state of species concentrations  $\{C_n\}$ , “report” the rate of production or removal of each species involved (i.e., to form the residual used in Equation 34) and the current value of the element Jacobian terms (i.e., to form the system Jacobian) to a master solver routine. Furthermore, given homogeneous chemistry is limited to each zone these general strategies extends as well to the multizone case.

#### 2.1.1.9. Initial Concentrations, Outdoor Concentrations, and Steady State Concentrations

The consideration of indoor homogeneous chemistry will demand, necessarily, the specification of initial conditions and outdoor concentrations for all species involved. Outdoor chemistry is photolytically driven and as a result is in constant flux, consequently the specification of outdoor concentrations will prove difficult for most users and may, in effect, limit the analysis of homogeneous chemistry to the research specialists. Furthermore, trace, immeasurable levels of some species may have a significant impact on indoor chemistry, yet it may be practically difficult to specify outdoor concentrations – again a specialist may be able to devise indirect strategies to estimate outdoor levels. If analysis is limited to indoor chemistry that has already been studied guidance is available (6, 8, 9, 17, 18) – in fact, code is available (e.g., the RADCAL routines from Nazaroff’s program MIAQ4 (19). If, on the other hand, the next generation NIST IAQ Model is to be general then general tools should be provided, but what can be done in these cases?

In atmospheric chemistry many reactions are so rapid – i.e., due to large rate constants and/or large concentrations of reactants such as oxygen or nitrogen – that it is often assumed that the reactions proceed instantaneously to steady-state. As a result, for such systems of reactions, the concentration of some species may be related to the dynamic variation of other species through so-called pseudo-steady-state approximations (PSSA) – not to be confused with, but related to, the PSSA integration scheme presented above. These approximations assume the form of algebraic expressions as, for example, for the photochemical cycle of  $\text{NO}_2$ ,  $\text{NO}$ , and  $\text{O}_3$  the PSSA concentration of the oxygen radical  $\text{O}$  is:

$$[\text{O}] = \frac{k_1[\text{NO}_2]}{k_2[\text{O}_2][\text{M}]}$$

or in the atmospheric chemistry of  $\text{CO}$  and  $\text{NO}_x$  the PSSA concentration of ozone  $\text{O}_3$  is:

$$[O_3] = \frac{k_1[NO_2]}{k_3[NO] + \frac{k_4}{\left(1 + \frac{k_5[M]}{k_6[H_2O]}\right)}}$$

where, in both cases,  $M$  represents a so-called third body such as nitrogen gas.

These PSSA algebraic expressions may, then, be used to establish the variation of some species in terms of other species whose variation may be easier to characterize. That is to say, PSSA algebraic approximations may be used to a) relate some initial concentrations to other better known concentrations and/or b) relate some outdoor concentrations to other better known concentrations. Furthermore, it may prove useful to use PSSA approximations to estimate the time variation of some indoor species concentrations to others. Numerically, this would involve mixing algebraic with ordinary differential equations demanding other solution strategies than those considered above.

√ To provide the greatest generality, the next generation CONTAMxx should, therefore, allow the user to define algebraic relations between air pollutant species for either a) specification of initial concentrations, b) specification of outdoor concentrations, and/or c) possibly, specification of steady-state dependencies of some indoor species on others.

#### 2.1.1.10. Heterogeneous Loss

Most gases that will be involved in homogeneous chemical reactions within rooms may also be expected to interact chemically or physically with building surfaces – that is to say, when modeling homogeneous chemistry one should also model the heterogeneous processes that may influence the reactants and products considered. For a variety of reasons – that will be discussed in section 2.3 of this report – it will prove difficult to model the details of these heterogeneous processes faithfully, consequently, these processes are commonly modeled as a *heterogeneous loss*  $R_{Ad}$  (mass-species-A·time<sup>-1</sup>) using first order approximations known as *deposition velocity models*:

$$R_{Ad} = -\rho_{air} \left( \sum_m \bar{v}_{Amd} A_{md} \right) C_A \quad (36)$$

where  $\bar{v}_{Amd}$  is the mean deposition *velocity* (cm·s<sup>-1</sup> or m·s<sup>-1</sup>) for species  $A$  to surface  $m$ , and  $A_{md}$  is the surface area available for deposition of surface  $m$ . Note that a sign convention has been associated with  $R_{Ad}$  that is consistent with that introduced for homogeneous gas-phase reaction rate  $R_A$  such that the mass rate of removal from the zone bulk-air phase is negative. Thus gas-phase deposition may be directly added to the zone rate vector  $\{R\}$  discussed above to include deposition transport in system equations governing transport of air pollutants in building systems (e.g., Equation 20).

Regrettably, the deposition velocity model is deceptively attractive – one can easily imagine loss to surfaces in terms of the “velocity” of a given species (e.g., molecule, radical, or ion) toward the

surface. Yet the actual mechanisms involved are likely to be far more complex involving a variety of diffusion processes to, through, and within porous surfaces complicated by sorption processes, change of phase, and surface chemistry. It should not come as a surprise, therefore, to discover that measured deposition velocities show extremely large variation – i.e., the “constant” of the deposition velocity model is not observed to be constant at all. Seinfeld (1) reports values of *dry deposition* measured in the outdoor environment that vary over four orders of magnitude for a range of chemical species and two orders for a given species yet show a clear trend related to the reactivity of the gas species considered. (In atmospheric modeling, *dry* deposition is distinguished from *wet* deposition, the latter associated with removal of gases due to water droplets in clouds or rain. Within the indoor environment wet deposition could conceivably play a role when water sprays are present (e.g., in showers) but is otherwise likely not to be important. On the other hand, water layers and absorbed water within building materials may be expected to play a key role in “dry” deposition.)

√ First order deposition velocity models are presently supported by CONTAM93/94 so the question of implementation is moot. Providing users with recommended values for deposition velocities is another matter. At this point in time it is probably best to simply point them to the literature – several investigators have measured and investigated the variation of deposition velocity in the indoor environment and have put forward (tentative) theories to explain and predict this variation (7, 20-27).

#### 2.1.1.11. Recommendations for the Next Generation NIST IAQ Model

√ At this point there seems to be two directions that could be taken for the next generation NIST IAQ Model – either implement specific chemistry – i.e., the indoor homogeneous chemistry that has already been studied – or provide tools for the investigation of indoor homogeneous chemistry, in general. Nazaroff’s model for indoor NO<sub>x</sub> gas-phase, homogeneous chemistry is far more complete than any other available model and could be used directly to implement the first strategy. This is an especially attractive strategy given his model is available as extremely well-documented FORTRAN77 routines within the MIAQ4 program (19).

Alternatively, general tools could be developed. To comprehensively cover all possibilities, the following general types of reactions would have to be considered (with user input specified for each type of reaction):

- *Zero Order Reactions*: specified in terms of:
  - a) a simple rate “constant”,  $k_0$ , defined to be either a (true) constant or temperature-dependent (i.e., as defined by an Arrhenius-type expression or a simple linear expression<sup>3</sup>) given either a schedule of temperature variation or a

<sup>3</sup>A simple linear expression of the form  $k = a + bT$  may be used to approximate any other temperature dependent relationship about some mean operating temperature (i.e., by a Taylor series about that mean).

matching temperature (i.e., thermal) solution for the system being considered, and

- b) a reactant and product species name(s) (i.e., identification strings), product stoichiometry, and reactant and product molecular weights.
- *Pseudo-Steady-State Reactions, Equation 9*: specified in terms of:
    - a) a rate “constant”  $k_1$  defined to be either:
      - i) a (true) constant,
      - ii) temperature-dependent (i.e., as defined by an Arrhenius-type expression or a simple linear expression) given either a schedule of temperature variation or a matching temperature (i.e., thermal) solution for the system being considered, or
      - iii) photochemically dependent, defined in terms of discretely defined absorption cross-sections, quantum yields, and actinic irradiance density (i.e., Equation 8) input as wavelength dependent schedules by the user.
    - b) a “steady-state” concentration  $[A]_{ss}$  defined in terms of an actual constant value or in terms of a schedule of concentration variation with time (e.g., ambient O<sub>2</sub> concentration in the first case or CO<sub>2</sub> in the second case – both available in relatively large amounts with the first remaining practically constant and the second varying with time of day to local auto traffic conditions, for example), and
    - c) a reactant and product species name(s) (i.e., identification strings), product stoichiometry, and reactant and product molecular weights.
  - *First Order (Unimolecular) Reactions, Equation 1*: specified in terms of:
    - a) a rate “constant”  $k_1$  defined to be either:
      - i) a (true) constant,
      - ii) temperature-dependent (i.e., as defined by an Arrhenius-type expression or a simple linear expression) given either a schedule of temperature variation or a matching temperature (i.e., thermal) solution for the system being considered, or
      - iii) photochemically dependent, defined in terms of discretely defined absorption cross-sections, quantum yields, and actinic irradiance density (i.e., Equation 8) input as wavelength dependent schedules by the user

- b) a reactant and product species name(s) (i.e., identification strings), product stoichiometry, and reactant and product molecular weights.
- *Pseudo First Order (Bimolecular) Reactions*, Equation 15: specified in terms of:
  - a) a rate “constant”  $k_2$  defined to be either a (true) constant or temperature-dependent (i.e., as defined by an Arrhenius-type expression or a simple linear expression) given either a schedule of temperature variation or a matching temperature (i.e., thermal) solution for the system being considered,
  - b) a “steady-state” concentration  $[B]_{ss}$  defined in terms of an actual constant value or in terms of a schedule of concentration variation with time,
  - c) a selection of either the general reaction type defined by Equation 2 or the special case defined by Equation 10, and
  - d) reactant and product species names (i.e., identification strings), reaction stoichiometry, and reactant and product molecular weights.
- *Second Order (Bimolecular) Reactions*, Equation 2: specified in terms of:
  - a) a rate “constant”  $k_2$  defined to be either a (true) constant or temperature-dependent (i.e., as defined by an Arrhenius-type expression or a simple linear expression) given either a schedule of temperature variation or a matching temperature (i.e., thermal) solution for the system being considered,
  - b) reactant and product species names (i.e., identification strings), reaction stoichiometry, and reactant and product molecular weights, and
  - c) a selection of either the general reaction type defined by Equation 2 or the special case defined by Equation 10.
- *Third Order (Termolecular) Reactions*, Equation 3: specified in terms of:
  - a) a rate “constant”  $k_3$  defined to be either a (true) constant or temperature-dependent (i.e., as defined by an Arrhenius-type expression or a simple linear expression) given either a schedule of temperature variation or a matching temperature (i.e., thermal) solution for the system being considered,
  - b) reactant and product species names (i.e., identification strings), reaction stoichiometry, and reactant and product molecular weights, and
  - c) a selection of either the general reaction type defined by Equation 3 or the special cases defined by Equations 11 and 12.
- *Third Body Combination Reactions*, Equation 14: specified in terms of:



- a) rate “constants”  $k_{20}$  and  $k_{2\infty}$  defined to be either (true) constants or temperature-dependent (i.e., as defined by an Arrhenius-type expression or a simple linear expression) given either a schedule of temperature variation or a matching temperature (i.e., thermal) solution for the system being considered,
  - b) reactant, product, and third body species names (i.e., identification strings), reaction stoichiometry, and reactant, product, and third body molecular weights, and
  - c) specification of a broadening factor  $F$  to use.
- *User-Specified Reactions*: specified in terms of:
    - a) a user supplied subroutine that can “report” production or removal rates of reactant and species and *element Jacobians* for the specific reaction for a given state of the system concentration vector, and
    - b) reactant and product species names (i.e., identification strings), reaction stoichiometry, and reactant and product molecular weights.
    - c) specification of a broadening factor  $F$  to use.

To provide the greatest flexibility, the user should be allowed to first specify a specific type of reaction that may be considered (i.e., in one of the categories presented above), then to indicate in which zones each specific reaction is to be applied. This will allow the user, for example, to specify different photochemical dissociation reaction for different zones depending on the actinic intensity variation within each zone. In addition, as discussed above, it would be most useful to provide an algebraic parser that would allow the user to define algebraic relations between gas-phase species for either a) specification of initial concentrations, b) specification of outdoor concentrations, or c) specification of (some) indoor concentrations in terms of others.

In addition, to facilitate the consideration of gas-phase homogeneous chemistry the next generation of the NIST IAQ Model could provide a) libraries of standard reactions (e.g., NO<sub>x</sub> chemistry to begin with), b) concentrations of components of the standard dry atmosphere, and c) a utility to convert between gas-phase water concentrations [ $H_2O$ ] and relative humidity RH given schedules of or computed values of either (Seinfeld’s Appendix 4.A.3 Calculation of Atmospheric Water Vapor Concentration provides one approach (1)).

### 2.1.2. Aqueous- & Aerosol-Phase Chemistry

Aerosol-phase chemistry, especially aqueous aerosol chemistry plays a very important role in the atmosphere (see, for example, Chapter 5 of (1)). Recent research points to the possibility that aerosol chemistry may play an important role in indoor air quality (7, 11-13, 17, 28, 29). Aqueous, acid aerosols may have a more significant impact on health than previously thought and

can, if present, have a devastating impact on electronic equipment, building materials, and contents. Consequently, we may begin to look to a future need for including aerosol-phase chemistry in indoor air quality modeling.

Two important classes of aerosol-phase chemistry are likely to be important – chemical reactions occurring homogeneously within aqueous droplets and chemical reactions occurring on surfaces and within the pores of solid particles. Diffusion transport through air-phase boundary layers separating aerosol particles from the bulk air-phase play a role in both cases and, for this reason, both classes of chemistry may be considered to be heterogeneous (i.e., occurring at the bounding surface) relative to the bulk air-phase even though homogeneously distributed through out the bulk air phase. Furthermore, gas-liquid absorption equilibrium for the aqueous-phase and gas-solid adsorption equilibrium for the solid-phase aerosols will prove important in these classes of chemistry – additional characteristics of this class of chemistry that supports the positions that these processes ought to be modeled as heterogeneous processes.

√ That is to say, while it is premature at this time to propose general modeling tools for indoor aerosol-phase chemistry, the modeling tools that will be presented in Section 2.4 for heterogeneous processes are likely to be useful for this purpose and should be developed with this application in mind.

## **2.2. Aerosol Transport & Fractional Particle Filtration**

Professor Bill Nazaroff has presented theory and developed the program MIAQ4 for modeling aerosol transport in multizone buildings that has established the state-of-the-art in the field (6, 19, 22, 23, 30-34). He provides the following general description of the MIAQ4 model:

“The indoor aerosol dynamics model predicts the time-dependent evolution of particle size distributions in buildings. The indoor aerosol is represented by a multicomponent sectional description (Gelbard and Seinfeld, 1980). The particle size distribution is divided into a number of discrete contiguous sections according to particle diameter. Within each size section, the particles comprise one or more classes of chemical constituents.

The Model employs a flexible multichamber description of a building. ... In simulating the evolution of particle size distribution, the model accounts for the influences of direct indoor emission, ventilation, filtration, mixing between chambers, coagulation, and deposition onto indoor surfaces. Evaporation, condensation, and homogeneous nucleation are not included in the model.” (33)

Nazaroff presents a practically complete description of his aerosol transport model formulation in (31). This section will simply follow and review the Nazaroff model formulation presented in this paper adding details to aid in the understanding of Nazaroff’s model and modifications needed to integrate the Nazaroff model into the framework of the current NIST IAQ model. As such, the organization of this section follows that used by Nazaroff – i.e., the level three headings (2.2.1,

2.2.2, ...) below are identical to those used by Nazaroff so that both this section and Nazaroff's key paper can be reviewed in parallel.

Fundamental principles of aerosol science and technology are presented in a number of texts (1, 35-39). Any of these texts should help to clarify unfamiliar concepts – the texts by Hind and Seinfeld are especially useful in this regard.

### 2.2.1 Aerosol Representation

Aerosols are suspensions of solid or liquid particles in air. In general, an aerosol may be expected to contain a continuous distribution of particle sizes (i.e., if a statistically significant population of particles are present), consequently to characterize an aerosol one must characterize the aerosol's size distribution. To this end, a size distribution function  $n(D_p)$  is defined so that the number of particles per volume (e.g., number·cm<sup>-3</sup>)  $N_j$  within a particle diameter  $D_p$  range "j" or section "j"  $\Delta D_{pj} \equiv \langle D_{pj1}, D_{pj2} \rangle$  is equal to the integral of the size distribution function over that range:

$$N_j = \int_{D_{pj1}}^{D_{pj2}} n(D_p) dD_p \quad (37)$$

The total number of particles per unit volume  $N$  is then:

$$N = \int_0^{\infty} n(D_p) dD_p \quad (38)$$

In addition to the distribution of number of particles, it is often useful to characterize the particle surface area distribution  $n_s$ , particle volume distribution  $n_v$ , and particle mass distribution  $n_m$ . Functions for these distributions may be derived from the basic number distribution functions if a) it is assumed that all particles are spherical and b) for the mass distribution, all particles have the same density  $\rho_p$  (e.g., see Chapter 7 of (1)):

$$n_s(D_p) = \pi D_p^2 n(D_p) \quad (39)$$

$$n_v(D_p) = \frac{\pi}{6} D_p^3 n(D_p) \quad (40)$$

$$n_m(D_p) = \rho_p \frac{\pi}{6} D_p^3 n(D_p) = \rho_p n_v(D_p) \quad (41)$$

The accumulated volume (fraction) of particles  $V_j$  (volume-particles-volume-air<sup>-1</sup>) in a given section  $j$  is, then:

$$V_j = \int_{D_{pj1}}^{D_{pj2}} n_v(D_p) dD_p \quad (42)$$

Nazaroff utilizes the mass concentration  $C^4$  (mass-particles-volume-air<sup>-1</sup>) of each of several (discrete) size fractions as the fundamental independent variable of his model. It then follows from the above definitions that the mass concentration of section  $j$  or  $C_j$  is:

$$C_j = \int_{D_{pj1}}^{D_{pj2}} \rho_p \frac{\pi}{6} D_p^3 n(D_p) dD_p = \int_{D_{pj1}}^{D_{pj2}} \rho_p n_v(D_p) dD_p \quad (43)$$

or, if it assumed that all particles have the same density:

$$C_j = \rho_p V_j \quad (44)$$

The fundamental independent variable of the NIST IAQ Model is concentration  $C$  expressed in terms of mass fraction, hence the (mass fraction) concentration  $C_j$  (mass-particles-mass-air<sup>-1</sup>) of a given section  $j$  of particles is related to the (volumetric) mass concentration  $C_j$  and the volume fraction  $V_j$  of that section as:

$$C_j = \frac{1}{\rho_{air}} C_j = \frac{\rho_p}{\rho_{air}} V_j \quad (45)$$

where  $\rho_{air}$  is the density of the air.

Thus the distribution of aerosol particles may be described in terms of the discrete distributions  $N_j$ ,  $C_j$ ,  $C_j$ , and/or  $V_j$ . While the last three are related by Equation 45 (i.e., assuming constant particle density), the link between the discrete number size distributions  $N_j$  and the remaining three depends on knowledge of the continuous size distribution function  $n(D_p)$  which will, generally, not be available. In Nazaroff's model, however, the distribution of particles within each section is assumed to be uniformly distributed with respect to particle diameter or, equivalently, with respect to the logarithm of particle mass. If, it is assumed that the distribution function is constant within a section  $n(D_{pj1}, D_{pj2}) \equiv n_j$  then:

$$N_j = \int_{D_{pj1}}^{D_{pj2}} n_j dD_p = n_j (D_{pj2} - D_{pj1}) \quad (46)$$

$$\begin{aligned} C_j &= \int_{D_{pj1}}^{D_{pj2}} \rho_p \frac{\pi}{6} D_p^3 n_j dD_p = \rho_p \frac{\pi}{24} n_j (D_{pj2}^4 - D_{pj1}^4) \\ &= \rho_p \frac{\pi}{24} N_j \frac{(D_{pj2}^4 - D_{pj1}^4)}{(D_{pj2} - D_{pj1})} = \rho_p \frac{\pi}{24} N_j (D_{pj2} + D_{pj1}) (D_{pj2}^2 + D_{pj1}^2) \end{aligned} \quad (47)$$

and

---

<sup>4</sup> An outline font will be used to distinguish mass concentration variables  $C$  (e.g. mass-particles per unit volume of air) from mass fraction variables  $C$  (e.g. mass-particles per unit mass of air).

$$C_j = \frac{\rho_p}{\rho_{air}} \frac{\pi}{24} N_j (D_{pj2} + D_{pj1}) (D_{pj2}^2 + D_{pj1}^2) \quad (48)$$

In addition to distinguishing concentrations of particles within a given particle diameter section, Nazaroff distinguishes chemical components – identified by index  $k$  – and chambers or well-mixed zones,  $i$ , so that  $C_{ijk}$  “represents the mass concentration of component  $k$  in section  $j$  contained within chamber  $i$ . Furthermore, “components are assumed to be mixed internally, i.e., within a section all particles have the same composition.” Finally, Nazaroff places a geometric constraint on the width of the section used in computation – the mass of the largest particle within a section must be at least twice that of the smallest particle within the section ((31) pages 157-158) or, assuming constant particle density:

$$D_{pj2}^3 \geq 2D_{pj1}^3 \quad \text{or} \quad D_{pj2} \geq 2^{1/3} D_{pj1} = 1.2599 D_{pj1} \quad (49)$$

Although the next generation of CONTAM will base computations on particle concentrations expressed in terms of mass fraction  $C_j$  (mass-particles-mass-air<sup>-1</sup>), users of CONTAMxx may prefer to review results in terms of the discrete distributions of  $C_j$ ,  $V_j$ , or  $N_j$ . The relations presented in this section define the conversions that will be required to report results in these alternative forms.

### 2.2.2 [Nazaroff’s] Basic Model Postulate

Nazaroff presents the form of the system equations that will be assembled from elemental or component equations for ventilation, filtration, coagulation, etc. in Equation 1 of his paper. The form used will be recognized as that of the pseudo, uncoupled linear form considered in the discussion of homogeneous gas-phase chemistry presented above, Equation 22. This form is the basis of the pseudo steady state approximation PSSA (or asymptotic approximation) scheme used for approximate, but computationally cheap, numerical integration in analysis of gas-phase atmospheric chemistry and is the solution method, in fact, used by Nazaroff (i.e., see **Computer Implementation Notes** on page 161 of Nazaroff’s paper (31)).

As discussed above, the PSSA scheme is not a rigorous approach to numerical integration and can not be expected to provide a reliable, accurate, and/or stable means to solve the (more general) types of nonlinear equations that may be expected to be encountered in the next generation of the NIST IAQ Model. For this reason, Nazaroff’s solution strategy will not be pursued here. Instead, we will extract the elemental and or component mass transport relations presented by Nazaroff and reformulate them, as necessary, for assembly in more rigorous solution schemes.

### 2.2.3 Ventilation and Filtration

The advective transport of aerosols in a multizone building may be treated in the same manner as that used for gaseous contaminants. That is to say, if it is assumed that within the bulk-air phase

of a given zone and at any section along discrete flow paths between zones the concentration of the aerosol is uniformly distributed (well-mixed), then the methods to model the advective transport of gases presently used may be directly applied to aerosols. Of course, as for advective transport of gases, there will be instances where these well-mixed assumptions may be inappropriate – e.g., for dense aerosols injected into a zone that will tend to behave more like a cloud than a well-mixed suspension of particles or the movement of even trace aerosols through flow passages, such as cyclone separators, that tend to separate the aerosol suspension from the gas phase.

Modeling of the advective transport of aerosols will, however, demand significantly larger systems of equations. For example, to faithfully capture the detailed nature of aerosol transport, one may have to consider from 10 to 30 sections – Nazaroff used 16 sections in his studies (31) – for each component considered. Thus for a single component, the number of equations to be solved may be expected to be 10 to 30 times the number of zones!

From a numerical perspective, it will prove difficult to order these equations to minimize either their bandwidth or their skyline and, as a result, sparse matrix equation solving techniques, that have fostered the use of implicit solution methods, may not be as effective as they have proven to be in simpler contaminant dispersal analysis. Nevertheless, some relatively obvious strategies are available to mitigate this problem. From the discussion presented above, it is clear that homogeneous chemistry will couple concentration degrees of freedom within zones but not between zones. We shall see that sorption transport, source models, and, for aerosols, coagulation modeling all have the same characteristic. Furthermore, these transport processes will, most often, be characterized by nonlinear couplings. Consequently, it may be most reasonable to order system degrees of freedom by zone. If this is done, the contributions of these *zone* processes  $[K_{zone}]$  to the system transport matrix  $[K]$ – or, perhaps, more importantly to the system Jacobian – will assume a block-diagonal form similar to that described by Equation 21. The patterns of coupling between these blocks due to advective (dilution) transport, then, will be identical to the coupling that would exist for if a single component. That is to say, the system transport matrix may be seen as the sum of dilution transport contributions following a skyline pattern and a block-diagonal form associated with the zone processes as:

$$[K] = \begin{bmatrix} [K_{dil}] & 0 & 0 & [K_{dil}] & \cdots & 0 \\ 0 & [K_{dil}] & 0 & 0 & \cdots & 0 \\ 0 & 0 & [K_{dil}] & 0 & \cdots & [K_{dil}] \\ 0 & [K_{dil}] & 0 & [K_{dil}] & \cdots & 0 \\ \vdots & \vdots & \vdots & \vdots & \ddots & \vdots \\ 0 & 0 & 0 & 0 & \cdots & [K_{dil}] \end{bmatrix} + \begin{bmatrix} [K_{zone}] & 0 & 0 & 0 & \cdots & 0 \\ 0 & [K_{zone}] & 0 & 0 & \cdots & 0 \\ 0 & 0 & [K_{zone}] & 0 & \cdots & 0 \\ 0 & 0 & 0 & [K_{zone}] & \cdots & 0 \\ \vdots & \vdots & \vdots & \vdots & \ddots & \vdots \\ 0 & 0 & 0 & 0 & \cdots & [K_{zone}] \end{bmatrix} \quad (50)$$

The bandwidth of the zone contribution will approach or equal the number of pollutants considered while the advective (dilution) contribution will necessarily have a larger bandwidth (more

exaggerated skyline) minimally twice that of the zone contribution but more likely several multiples of the zone contribution. Consequently, by ordering the zone numbering strategically, one may minimize the overall system bandwidth.

### 2.2.3.1 Fractional Aerosol Filtration

The single component filter model presently available in CONTAM93/94 is a particularly simple component. Given a filter of efficiency  $\eta_k$  for air pollutant component  $k$ , with a supply and, by continuity, an exhaust air flow rate  $w_{air}$  (mass-air-time<sup>-1</sup>), the supply and exhaust mass flow rates of component  $k$ :  $w_{ki}$  and  $w_{ko}$  respectively (both defined positive for flow into the filter) are related to the supply  $C_{ki}$  concentration as:

$$w_{ki} = w_{air}C_{ki} \quad (51a)$$

$$w_{ko} = -w_{air}(1 - \eta_k)C_{ki} \quad (52a)$$

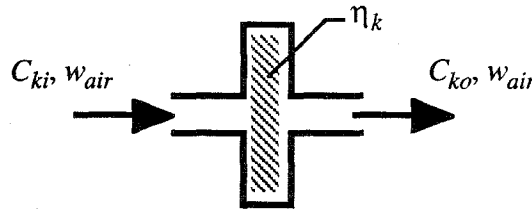


Figure 1. Single component filter idealization.

Expressed in terms of an element equation describing component  $k$  mass flow rates between discrete spatial nodes associated with the supply and exhaust concentrations, these equations may be written as:

$$\begin{Bmatrix} w_{ki} \\ w_{ko} \end{Bmatrix} = \begin{bmatrix} w_{air} & 0 \\ -w_{air}(1 - \eta_k) & 0 \end{bmatrix} \begin{Bmatrix} C_{ki} \\ C_{ko} \end{Bmatrix} \quad (53)$$

Demanding the conservation of component  $k$  mass, the mass rate of accumulation of component  $k$  on the filter  $w_{kf}$  is then:

$$w_{kf} = w_{air}\eta_k C_{ki} \quad (54a)$$

and the total mass of component  $k$  accumulated  $M_{kf}$  on the filter during a time interval  $\langle t_1, t_2 \rangle$  is:

$$M_{kf} = \int_{t_1}^{t_2} w_{air}\eta_k C_{ki} dt \quad (55a)$$

These relations are based on an implicit definition of the filter efficiency  $\eta_k$ :

$$\eta_k = \frac{C_{ki} - C_{ko}}{C_{ki}} \quad (56a)$$

These simple relations may be directly applied to each section  $j$  of  $n$  sections of an aerosol distribution  $j = 1, 2, \dots, n$  by simply adding an addition index for the section designation as:

$$w_{jki} = w_{air}C_{jki} \quad (51b)$$

$$w_{jko} = -w_{air}(1 - \eta_{jk})C_{jki} \quad (52b)$$

$$w_{jkf} = w_{air}\eta_{jk}C_{jki} \quad (53b)$$

$$M_{jkf} = \int_{t_1}^{t_2} w_{air}\eta_{jk}C_{jki}dt \quad (55b)$$

and, assuming again that aerosol particles are effectively spherical, of uniform density, and uniformly distributed with respect to diameter (i.e., by Equations 45 and 48):

$$\eta_{jk} = \frac{C_{jki} - C_{jko}}{C_{jki}} = \frac{C_{jki} - C_{jko}}{C_{jki}} = \frac{N_{jki} - N_{jko}}{N_{jki}} = \frac{V_{jki} - V_{jko}}{V_{jki}} \quad (56b)$$

√

The next generation of the NIST IAQ model should compute and report the distribution and total particulate mass accumulated on filters,  $M_{jkf}$  and  $\sum_{j,k} M_{jkf}$  given an initial (distribution) of accumulated particulate mass input by the user.

### 2.2.3.2 Fractional Filtration Efficiency – The Empirical Approach

In the practical application of the equations presented above a number of issues need to be considered – importantly, the variation of filter efficiency with particle size, *face velocity*, component, and *loading*. From results just now being disseminated from a major investigation of fractional aerosol filtration sponsored by the US EPA and being carried out by the Research Triangle Institute (RTI) (40), data is now becoming available to quantify the first three of these issues – the fourth remains problematic. Specifically, RTI is presently releasing data to characterize the dependency of the filter efficiency on particle size  $D_p$ , air flow expressed in terms of face velocity  $\overline{v_{air}}$ , and *loading* – determined by RTI indirectly in terms of the pressure drop measured across a filter due to the accumulation of a standard test dust. RTI is not attempting to discriminate filter efficiency variation with aerosol component type. The RTI data set – a data set that will clearly become the definitive (only?) data set available into the near future – can be used directly to specify the particle-size and face-velocity dependency of the filter efficiency for one of the several filters studied, i.e.,  $\eta_j(\overline{D_{pj}}, \overline{v_{air}})$  for single component analyses and  $\overline{D_{pj}}$  presumed to the mean diameter of a given section  $j$ . The variation with loading is another matter.

Ideally, in air quality analysis, it would be best to define loading in terms of the mass of aerosol accumulated on the filter. One possibility, would be to define loading as the accumulated sum of this mass across all sections  $\sum_j M_{jf}$ . While this could be computed directly during analysis it is not without shortcomings, e.g., the impact of the accumulation of large particles may be expected to differ from that of small particles; of solid particles from liquid particles, etc. Nevertheless,



given the state-of-the-art, this definition of loading is likely to prove practically useful, in that one may expect it to be well-correlated with both the change of fractional aerosol efficiency and the change in the pressure-drop across the filter. Unfortunately, as presented the RTI data can not be directly related to loading defined in this manner – there is some chance, however, that RTI has collected but not reported data (i.e., change of weight of filters upon loading) that would make this possible.

Unfortunately, there is an additional complication. The RTI investigators chose to evaluate filter efficiency in a somewhat unconventional manner. Instead of applying the conventional definition presented above, Equation 56b, they used the following definition:

$$\eta_{jk} = 1 - \frac{C_{jko} - C_{jko-background}}{C_{jki} - C_{jki-background}} \quad (57)$$

where  $C_{jki-background}$  and  $C_{jko-background}$  are supply and exhaust “background” concentrations – particle concentrations measured when the filters were not subjected to an aerosol-laden supply air flow. The measured supply “background” concentrations were always at or near zero, but the exhaust “background” concentrations were nonzero for loaded filters. A loaded filter will tend to shed particles creating nonzero exhaust concentrations even when supply concentrations are zero, thus this definition was employed to “remove the effect of shedding from the computed efficiency” ((40) page 173).

Given these less than ideal circumstances, the following recommendations are made for the use of measured data for aerosol transport analysis in the next generation of the NIST IAQ Model:

- following Nazaroff’s approach (31), it should be assumed that filter efficiency depends not on composition but only particle size – that is, for all components of the same size fraction, a given filter should be assumed to have the same filter efficiency, and
- minimally, efficiency data should be defined in terms of user input empirically measured profiles of efficiency versus mean particle size  $\eta_j(\overline{D_{pj}})$ , and
- better, users should be able to input profiles for a range of two or more discrete values of air face velocity through the filter  $\eta_j(\overline{D_{pj}}, \overline{v_{air}})$  and CONTAMxx would linearly interpolate between values, or
- ideally, users should be able to input profiles for a range of discrete values of both air face velocity through the filter and loading, i.e., as defined above,  $\eta_j(\overline{D_{pj}}, \overline{v_{air}}, \sum_j M_{jf})$  and CONTAMxx would estimate the loading, using Equation 55b, and linearly interpolate between values.

Data may be limited to values at the mean particle diameters of each size range used to represent the aerosol – to avoid the computational overhead of interpolation – or, alternatively, at any convenient

set of mean particle diameters that span the range used to represent the aerosol – thus demanding interpolation of values for computation.

### 2.2.3.3 Fractional Filtration Efficiency – The Theoretical Approach

Hinds presents well established theory to predict the fractional filtration efficiency of filters composed of fibers and the dependency of this efficiency on face velocity (see (39) Chapter 9). The details of this theory will not be presented here – the presentation in Hinds is concise and to the point and need not be replicated – but the general features of this theory will be reviewed.

The fractional efficiency of a fibrous filter may be estimated by considering the theoretical efficiency of a single fiber  $E_{\Sigma}$ . This single fiber efficiency may be estimated as the sum of five contributions:

$$E_{\Sigma} \approx E_R + E_I + E_D + E_{DR} + E_G \quad (58)$$

contributions due to interception (R), impaction (I), Brownian diffusion (D), interception of diffusing particles (DR), and gravitational settling (G). An additional term to account for electrostatic attraction may be included, but is often neglected given lack of knowledge regarding the state of charge of supply particles. Expression for each of these contributions are available – the face-velocity entering the expressions for all but the first contribution – that could be used directly to provide an analytical approach to the determination of  $\eta_j(\overline{D}_{pj}, \overline{v}_{air})$ . The results of the application of this theoretical approach show the same trends as the measured data reported so far by the RTI group for fibrous filters, thus encouraging serious consideration of this approach. Hinds also presents related expressions for the pressure drop across fiber filters that define pressure-flow relations that could be directly used in the airflow computations of the NIST IAQ Model – a very attractive added advantage of this theoretical approach.

Although the theory is limited to fiber filters – indeed the  $\eta_j(\overline{D}_{pj}, \overline{v}_{air})$  curves reported by RTI for other types of filters show quite different trends – and does not account for loading, it would appear wise to at least investigate comparisons between RTI measured and predicted profiles of  $\eta_j(\overline{D}_{pj}, \overline{v}_{air})$  using this theory and if this comparison is favorable to implement filter components based on this theory for the next generation of the NIST IAQ Model.

### 2.2.4 Aerosol Deposition onto [Room] Surfaces

As noted by Nazaroff, particle deposition to room surfaces is likely to be “of secondary importance” from a mass conservation perspective but may be primary when the deposition itself is of concern – e.g., for users studying air quality in museums or in facilities with valuable electronic equipment. Beyond this concern, however, it is likely that aerosol deposits play a key role in sorption transport and the surface chemistry that may be associated with it and their impact on, at least, the perceived air quality within buildings (41, 42).

The nature of particle deposition is understood, at least, qualitatively to involve the movement of aerosol particles through surface or boundary layers separating surfaces from the bulk air phase indoors. Rather obviously, the movement of an aerosol particle through surface boundary layers is strongly influenced by the detailed nature of room air flows near surfaces. Less obviously, the movement of such particles is also influenced by electrostatic charge differences between particles and surfaces, thermophoresis, photophoresis, diffusiophoresis, radiation pressure, and Stefan Flow (39). The three classes of -phoresis are due to momentum gradients associated with temperature gradients in the bulk air phase, caused by radiant absorption of individual aerosol particles, and due to concentration gradients, respectively. Stefan flow – the bulk flow of evaporating (or condensing) gases away from (or to) surfaces can also transfer momentum to aerosol particles accelerating them away (or toward) surfaces. In principle, then, aerosol deposition may be expected to be governed by the details of airflow, electrostatic charge, temperature, concentration, radiation, and bulk motion of evaporating or condensing gases near surfaces – details that must remain largely unknown for practical air quality analysis, given the analytical effort that would be required to predict them. Consequently, it has become common practice to model the net effect – i.e., the mass rate of deposition of particles in section  $j$  of component  $k$   $R_{jkd}$  – of these processes simplistically as a first order process (i.e., linearly dependent on the bulk air-phase fractional aerosol concentration  $C_{jk}$ ) using so-called *deposition* expressions of the form:

$$R_{jkd} = -\rho_{air} \left( \sum_m \bar{v}_{jkm} A_{md} \right) C_{jk} \quad (59)$$

where  $\bar{v}_{jkm}$  is the mean deposition *velocity* ( $\text{cm}\cdot\text{s}^{-1}$  or  $\text{m}\cdot\text{s}^{-1}$ ) for particles in size fraction  $j$  to surface  $m$ , and  $A_{md}$  is the surface area available for deposition of surface  $m$ . Note that a sign convention has been associated with  $R_{jkd}$  that is consistent with that introduced for both homogeneous gas-phase reaction rate  $R_A$  and gas-phase deposition rate  $R_{Ad}$ , i.e., for species  $A$ , such that mass rate of removal from the zone bulk-air phase is negative and rates adding species, component, or size section mass to the zone (i.e., production, generation, emission, etc.) are positive.

As noted by Nazaroff, vertical, horizontal upward facing, and horizontal downward surfaces must be distinguished. For each of these orientations, the Nazaroff model provides for deposition due to: 1) natural convection driven by a boundary layer temperature difference at surfaces, 2) homogeneous turbulence in the core of the room, or 3) forced laminar flow over the surface. Deposition velocity models for the first and second cases are discussed in the key paper paralleling this discussion (31); all three models are derived in earlier papers (22, 30); and comparisons of the use of the last two deposition models are presented in (34).

For forced laminar flow past planar surfaces, Nazaroff used the correlation in his earlier publication (30):

$$v_{jkd} = 0.678 D^{2/3} \left( \frac{u_\infty}{L} \right)^{1/2} v^{-1/6} \quad (60)$$

where  $u_\infty$  is the air velocity parallel to the surface beyond the boundary layer,  $L$  is the distance from the leading edge of the surface, and  $\nu$  is the kinematic viscosity of the air-phase. Later, Nazaroff approached the problem by solving boundary layer equations.

In addition to the relations defining the Nazaroff deposition models, one must integrate these relations over available surfaces and within each aerosol size section to compute a surface and section average deposition velocity to use in Equation 59. Finally three additional relations are needed to use Nazaroff's deposition models:

- The coefficient of Brownian diffusivity  $D$  can be estimated using the modified Stokes-Einstein relation (see (1, 39) page 324):

$$D = \frac{k T C_c}{3\pi\mu D_p} \quad (61)$$

where, here,  $k$  is the Boltzmann constant ( $1.381 \times 10^{-23} \text{ J}\cdot\text{K}^{-1}$ ),  $T$  is the absolute temperature ( $^\circ\text{K}$ ),  $\mu$  is the coefficient of viscosity (e.g., of air), and  $C_c$  is the *Cunningham* or *slip correction factor* that is dependent on the mean free path  $\lambda$  of the air-phase molecules (see (1) page 317):

$$C_c = 1 + \frac{2\lambda}{D_p} \left( 1.257 + 0.4 \exp \left( -1.1 D_p / 2\lambda \right) \right) \quad (62)$$

Nazaroff's function DIFFUS(DP, T) computes  $D$  given the particle diameter  $D_p$  and absolute temperature  $T$ . Within this function the mean free path is computed using function FREEMP(T) and the so-called *Knudsen* number  $Kn = 2\lambda/D_p$  is passed to the function SLIP(AKN) which returns the slip correction factor that is based on an alternative formulation by Phillips, rather than Equation 62, as noted in the code.

- Nazaroff estimates the turbulence intensity parameter  $K_e$  (34) using an empirical relation developed by Corner and Pendlebury:

$$K_e = k_o^2 \frac{0.073 \rho u^2}{\mu} \left( \frac{\mu}{\rho u x_s} \right)^{1/5} \quad (63)$$

with  $k_o$  the Von Kármán constant taken by Nazaroff to be 0.4,  $\rho$  is the density of air,  $u$  is the mean air velocity near a surface, and  $x_s$  is the direction along a surface in the direction of the mean air flow. Here the mean air velocity near a surface is indeterminate in meaning and, even if more precisely defined, would be difficult to estimate. As a practical compromise for estimating the boundary layer thickness, Nazaroff takes  $x_s$  to be the geometric mean of the dimensions of a surface.

√ For the next generation CONTAMxx, two approaches may be taken to implement aerosol deposition modeling – the user can provide profiles of (surface and section average) deposition velocity (possibly, using plotted results presented by Nazaroff as a guide) and/or the models for deposition velocity presented by Nazaroff may be directly implemented. As deposition may be

seen as a physical process, it is reasonable to assume that deposition velocity is independent of composition.

Given the current state of the CONTAM94 interface, it would be most reasonable to include data associated with deposition with the definition of individual building zones. This would allow zone-specific specification of deposition velocity, a level of flexibility that may be expected to be required to provide realistic deposition modeling.

As published, the Nazaroff deposition models are directed to researchers in the field rather than professional practitioners, as they contain a large number of relatively esoteric parameters that must be specified for use and provide estimates of deposition at specific points along a surface rather than a surface-average value. Nazaroff has, nevertheless, implemented these models in MIAQ4 for practical application so that it should be possible to use the input requirements and computational algorithms implemented within MIAQ4 to add these models to CONTAMxx. One communicates with the program MIAQ4 through a command-line interface. The following commands pertain to modeling aerosol deposition:

General

**PRINT DEPOSITION**

This commands the program to report computed average accumulation of aerosols on surface due to deposition.

**PRINT FLUX**

This commands the program to report averaged source and sink terms including among others deposition fluxes.

**SET WALLS**

This command allows the specification of numbers of surfaces for each zone or chamber.

Direct Specification of Deposition Velocities

**SET SURFACE LOSS DEPOSITION**

This command specifies that deposition velocities are to be directly specified.

**DATA DEPOSITION VELOCITY AEROSOL**

This commands allows direct specification of deposition velocities for each aerosol size section.

Forced Laminar Flow Model

**SET SURFACE LOSS FLOW**

This command specifies that the forced laminar flow model is to be used.

**DATA SURFACE FLOW**

This command allows specification of the air velocity outside of the boundary layer  $u_{\infty}$ , surface orientation, and geometry used for the computation of deposition velocities based on the forced laminar flow model.

### Natural Convection Model

#### SET SURFACE LOSS CONVECTION

This command specifies that the natural convection model is to be used.

#### DATA SURFACES

This command allows specification of surface temperatures, surface orientation, and geometry used for the computation of deposition velocities for the natural convection model.

#### DATA HEIGHT

This command allows specification of chamber (zone) height used in the calculation of deposition velocity for the natural convection model.

#### DATA THERMOPHORESIS

This command allows specification of the thermophoresis coefficient for each aerosol size section.

### Homogeneous Turbulence Model

#### SET SURFACE LOSS TURBULENCE

This command specifies that the forced laminar flow model is to be used.

#### DATA TURBULENCE

This command allows specification of the turbulence intensity parameter in each zone as a function of time.

The source code of MIAQ4 is extremely well-documented, consequently, it should take little effort to “port” this code to the CONTAMxx environment. The following functions implement Nazaroff’s model (taken directly from the MIAQ4.DOC file):

```
C DVPE - DEPOSITION: NATURAL CONV., HORIZONTAL, ENCLOSED SURFACE
C DVPI - DEPOSITION: NATURAL CONV., HORIZONTAL, ISOLATED SURFACE
C DVPL - PARTICLE DEPOSITION: FORCED LAMINAR FLOW ALONG SURFACE
C DVPTD - DEPOSITION: HOMOGENEOUS TURBULENCE, DOWNWARD SURFACE
C DVPTU - DEPOSITION: HOMOGENEOUS TURBULENCE, UPWARD SURFACE
C DVPTV - DEPOSITION: HOMOGENEOUS TURBULENCE, VERTICAL SURFACE
C DVPV - DEPOSITION: NATURAL CONVECTION, VERTICAL SURFACE
```

Users of these models would specify for each surface: a) the orientation of the surface, b) the model to apply to the surface – i.e., forced laminar flow, natural convection, or homogeneous turbulence – c) the mean air velocity outside of the boundary layer  $u_{\infty}$ , a value that could be based on computed flow results with some imagination, and d) the expected temperature drop across the boundary layer of the surface (the zone surface temperature would be specified when defining a zone).

### **2.2.5 Coagulation**

Aerosol particles in a state of motion tend to coalesce when they collide. This process is known as coagulation and may be driven by collisions due to Brownian motion, air velocity gradients (shear)

in either laminar or turbulent flow fields, differential gravitational settling, or force fields due to van der Waals forces or Coulomb forces. Again Seinfeld presents the fundamental theory related to these processes (see Chapter 10 of (1)) and, for practical modeling, we shall use the model presented by Nazaroff (6) based on an approach developed by Gelbard and Seinfeld.

Nazaroff writes:

“The treatment of aerosol coagulation in the model is best considered in two stages: the calculation of the collision frequency between two particles and the integration of these probabilities to obtain the growth and loss rates for the component masses within each section.” (section **Coagulation**, page 160 of (6))

The details of Nazaroff’s model will not be repeated here – section **Coagulation** of (6) should be reviewed before proceeding. In the Nazaroff model, sectional mean coagulation coefficients  $\beta$  are computed for four basic classes of collisions  $n = 1, 2, 3, 4$  – with two variants,  $a$  and  $b$ , of collision classes 1 and 2 distinguished. These coefficients are then used to compute the coagulation ( $c$ ) rate of mass accumulation  $R_{ijk}$  of each component  $k$  within each size section  $j$  of zone  $i$ :as:

$$\begin{aligned}
 R_{ijk} \equiv M_{iair} \frac{1}{2} & \left[ \sum_{p=1}^{j-1} \sum_{q=1}^{j-1} \left\{ [{}^1a\beta_{pqj}] C_{iqk} \left( \sum_k C_{ipk} \right) + [{}^1b\beta_{pqj}] C_{ipk} \left( \sum_k C_{iqk} \right) \right\} \right. \\
 & - \left. \left\{ \sum_{p=1}^{j-1} \left[ [{}^2a\beta_{pj}] C_{ijk} \left( \sum_k C_{ipk} \right) - [{}^2b\beta_{pj}] C_{ipk} \left( \sum_k C_{ijk} \right) \right] \right\} \right. \\
 & \left. - \frac{1}{2} [{}^3\beta_{ij}] C_{ijk} \left( \sum_k C_{ijk} \right) - C_{ijk} \left\{ \sum_{p=j+1}^s [{}^4\beta_{pj}] \left( \sum_k C_{ipk} \right) \right\} \right] \quad (64)
 \end{aligned}$$

where  $M_{iair}$  is the mass of air in zone  $i$  and all concentrations  $C_{ijk}$  are expressed in mass fraction rather than the volumetric mass concentration  $\mathbb{C}_{ijk}$  employed by Nazaroff (see Equation 45 in section 2.2.1 above).

The structure of this rather complex expression will become more evident if we limit it to the analysis of a single component aerosol in a single zone and drop the  $i$  and  $k$  indices – keep in mind that coagulation “transport” is limited to individual building zones anyway:

$$\begin{aligned}
R_{jc} \equiv & M_{air} \frac{1}{2} \left[ \sum_{p=1}^{j-1} \sum_{q=1}^{j-1} \left\{ [{}^1a\beta_{pqj}] C_q C_p + [{}^1b\beta_{pqj}] C_p C_q \right\} \right. \\
& - \left. \left\{ \sum_{p=1}^{j-1} \left[ [{}^2a\beta_{pj}] C_j C_p - [{}^2b\beta_{pj}] C_p C_j \right] \right\} \right. \\
& \left. - \frac{1}{2} [{}^3\beta_{jj}] C_j C_j - C_j \left\{ \sum_{p=j+1}^s [{}^4\beta_{pj}] C_p \right\} \right] \quad (65)
\end{aligned}$$

For this simpler case it is more clearly seen that:

- the first double summation accounts for the collision of smaller particles – i.e., in size sections lower than size section  $j$  – that will increase the concentration in the  $j$  size section,
- the next summation within the braces accounts for the collision of particles in the  $j$  size section with smaller particles that result in loss of particles in section  $j$  and a corresponding increase in particles in larger sections,
- the third term  $\frac{1}{2} [{}^3\beta_{jj}] C_j C_j$  accounts for the loss of particles due to the collision of particles in the  $j$  size section with other particles in section  $j$  and a corresponding increase in particles in larger sections, and
- the last term accounts for the collision of particles in the  $j$  size section with larger particles that result in loss of particles in section  $j$  and a corresponding increase in particles in larger sections.

From a numerical point of view, Equations 64 and 65 both describe processes that depend on simple sums of products of zone concentration degrees of freedom – analogous to modeling a number of bimolecular homogeneous reactions occurring simultaneously within the zone. Again, the rate quantity  $R_{ijkc}$  or  $R_{jc}$  has been defined with the same general sign convention sign convention as that used for homogeneous chemistry, gas-phase deposition, and aerosol deposition so that the contribution of coagulation to the system transport equations will be similar to that presented earlier (e.g., Equation 19). Anticipating considering the use of a Newton-Raphson method for the solution of system equations involving coagulation we may define a coagulation rate vector for a single zone  $\{R_c\} = \{R_{1c}, R_{2c}, R_{3c}, \dots, R_{sc}\}^T$  for  $s$  size sections and a *coagulation Jacobian*  $[R'_c]$  – with  $i,j$  components for the single component case:

$$R'_{ijc} \equiv \frac{\partial R_{ic}}{\partial C_j} \quad (66)$$

or:



$$\begin{aligned}
\frac{\partial R_{ic}}{\partial C_j} = M_{air} \frac{1}{2} & \left[ \sum_{p=1}^{i-1} \sum_{q=1}^{i-1} \left\{ [{}^1a\beta_{pqi}] \left( C_q \frac{\partial C_p}{\partial C_j} + C_p \frac{\partial C_q}{\partial C_j} \right) + [{}^1b\beta_{pqi}] \left( C_q \frac{\partial C_p}{\partial C_j} + C_p \frac{\partial C_q}{\partial C_j} \right) \right\} \right. \\
& - \left. \left\{ \sum_{p=1}^{i-1} \left[ [{}^2a\beta_{pi}] \left( C_i \frac{\partial C_p}{\partial C_j} + C_p \frac{\partial C_i}{\partial C_j} \right) - [{}^2b\beta_{pi}] \left( C_i \frac{\partial C_p}{\partial C_j} + C_p \frac{\partial C_i}{\partial C_j} \right) \right] \right\} \right. \\
& \left. - \frac{1}{2} [{}^3\beta_{ii}] \left( 2 C_i \frac{\partial C_i}{\partial C_j} \right) - \left\{ \sum_{p=i+1}^s [{}^4\beta_{pi}] \left( C_i \frac{\partial C_p}{\partial C_j} + C_p \frac{\partial C_i}{\partial C_j} \right) \right\} \right] \quad (67)
\end{aligned}$$

Recognizing:

$$\frac{\partial C_i}{\partial C_j} = \begin{cases} 1 & \text{for } i = j \\ 0 & \text{for } i \neq j \end{cases} \quad (68)$$

and carefully observing the limits on the summations we obtain:

$$\begin{aligned}
\frac{\partial R_{ic}}{\partial C_j} = M_{air} \frac{1}{2} & \left[ \sum_{q=1}^{i-1} [{}^1a\beta_{jq}] C_q + \sum_{p=1}^{i-1} [{}^1a\beta_{pji}] C_p + \sum_{q=1}^{i-1} [{}^1b\beta_{jq}] C_q + \sum_{p=1}^{i-1} [{}^1b\beta_{pji}] C_p \right. \\
\text{for } j < i & \left. - \left\{ [{}^2a\beta_{ji}] C_i - [{}^2b\beta_{ji}] C_i \right\} \right] \quad (69a)
\end{aligned}$$

$$\text{for } j = i \quad \frac{\partial R_{ic}}{\partial C_j} = M_{air} \frac{1}{2} \left[ - [{}^3\beta_{ii}] C_i - \sum_{p=i+1}^s [{}^4\beta_{pi}] C_p \right] \quad (69b)$$

$$\text{for } j > i \quad \frac{\partial R_{ic}}{\partial C_j} = M_{air} \frac{1}{2} \left[ - [{}^4\beta_{ji}] C_i \right] \quad (69c)$$

With these coagulation Jacobians in hand, then, system equations governing the dispersal of aerosols could be solved using a step-by-step implicit integration scheme with Newton-Raphson iteration within each step in a manner similar to that presented above (section 2.1.1.8). More will be said about this and other possibilities in Chapter 3 of this report.

√ Nazaroff's model for coagulation appears to be quite general and practically complete (i.e., for those cases where evaporation, condensation, and Coulomb attraction may be ignored). Furthermore, Nazaroff presents well-documented FORTRAN 77 code in MIAQ4 for the

computation of the sectional mean coagulation coefficients  $\bar{\beta}$  and for the evaluation of the coagulation rate vector  $\{R_c\}$  in the following routines:

C	BETCAL	- EVALUATE INNER INTEGRAL OF SECTIONAL COAGULATION COEFS.
C	COAGCO	- EVALUATE CURRENT COAGULATION COEFFICIENTS BY BILINEAR INT.
C	COAGUL	- EVALUATE CONTRIBUTION OF COAGULATION TO LOSS AND GAIN
C	COEF	- COMPUTE SECTIONAL AEROSOL COAGULATION COEFFICIENTS
C	GAUSBT	- EVALUATE OUTER INTEGRAL OF SECTIONAL COAGULATION COEFS.

Therefore, it will be a straightforward task to add this capability to the next generation of CONTAM<sub>xx</sub>.

That is not to say, however, that analysis of coagulation transport – or aerosol transport, in general – will be computationally inexpensive. It should be clear from the discussion presented above relating to aerosol representation, filtration, deposition, and coagulation that the analysis of aerosol transport is computationally intensive due in part to the large number of concentration degrees of freedom that must be considered and, in part, to the overhead of computing deposition velocities, mean sectional coagulation coefficients, and the nested sums associated with coagulation loss, gain, and, possibly, Jacobian calculations. If the next generation of the NIST IAQ Model is to include realistic aerosol transport analysis, then these computational demands will have to be accepted.

### 2.3. Heterogeneous Processes

Heterogeneous processes are, from the perspective of room air quality, mass transport processes associated with mass transfer to and from the surfaces bounding the room air. These surfaces may be liquid or solid, part of the building construction, furnishings, finishes or decorations, or even surfaces of aerosols suspended in the room air. While associated with surfaces, heterogeneous processes should not be assumed to be due to simple surface phenomena such as “deposition” or condensation to smooth surfaces but rather dependent upon dynamically linked and generally serial mass transfer processes including:

- diffusion transport through boundary layers separating the apparent, exposed surface and the bulk air-phase,
- diffusion transport along the actual surface which, for solids, is likely to be convoluted and irregular rather than plane and smooth,
- diffusion transport within the liquid or solid material below the surface involving, for liquids, molecular, Brownian and convective diffusion and, for solids, molecular, Knudsen and surface diffusion within the porous interstices,
- sorption transport from the near-surface or pore air-phase – i.e., absorption in both solids and liquids as well as adsorption and desorption transport to surface sites within the porous structure of solids – and, possibly

- chemical transformations occurring homogeneously within the solid- or liquid-phase below the exposed surface or heterogeneously at surface sites within the porous structure of solids.

Regrettably, the popularity of deposition velocity models have fostered a view of heterogeneous transport that is invariably simplistic – the movement of air pollutants from the bulk air-phase to an exposed surface implicitly assumed to be smooth, impervious, and of unlimited capacity. These models tacitly assume the rate of mass transfer is related to the pollutant concentration in the air-phase – an assumption that, we shall see, is not completely unreasonable – and the apparent, exposed surface area. For porous solids, the actual surface area available is likely to be several orders of magnitude greater than the apparent, exposed surface area and the surface capacity is generally limited. Furthermore, the serial nature of mass transfer from the bulk air-phase through the surface to the interior below will, generally, depend on several distinct, elemental mass transfer mechanisms any one of which may tend to limit the overall rate of mass transport.

This section of the report will attempt to look more fundamentally at heterogeneous processes in general considering, first, elemental mass transport processes that may play a role and then applying models of these elemental processes to develop models to investigate the dynamics of sorption transport in rooms and building filtration devices and models to simulate the behavior of a variety of pollutant sources. These objectives are somewhat ambitious, given the current state-of-the-art, so the present discussion will be limited to simple models of these heterogeneous processes.

### **2.3.1 Elemental Mass Transport Processes**

To gain a better understanding of heterogeneous transport in general, it is necessary to look microscopically at room “surfaces” – at the interface between the room air and the bounding solid or liquid, at the air *boundary layers* separating this interface from the bulk (core) air-phase, and deep into the solid or liquid below the interface. To do so, one must necessarily consider these the spatial dimension from the bulk air-phase, through the interface, and into the liquid or solid below considering the variation of pollutant concentration in both the air-phase and the solid- or liquid-phase as one moves along the spatial axis. While in reality these concentrations may vary continuously with distance, for our purposes we shall seek to approximate this variation with values at discrete locations as indicated in the diagram below.

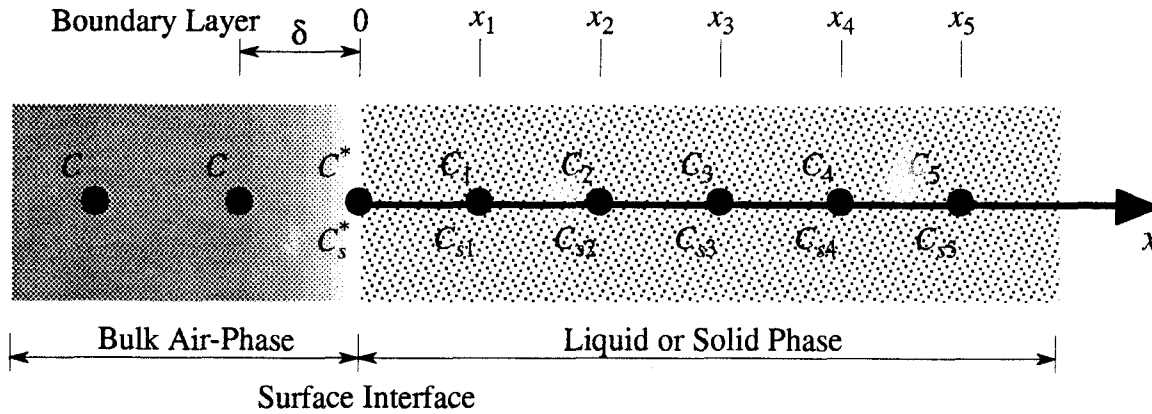


Figure 2. Spatial discretization of a region in the vicinity of a surface.

That is, we shall identify:

- air-phase concentrations in the room core  $C$ , at the interface of the surface  $C^*$ , and at discrete locations  $x_i$   $i = 1, 2, \dots$  within the solid or liquid below the surface  $C_i$ , recognizing that for liquids and nonporous solids these air-phase concentrations are likely to be negligible while for porous solids they will not, and
- solid-phase (or liquid-phase) concentrations at the interface of the surface  $C_s^*$  (or  $C_i^*$  for liquids), and at the same discrete locations  $x_i$   $i = 1, 2, \dots$  within the solid (or liquid) below the surface  $C_{si}$  (or  $C_{li}$  for liquids).

In the subsequent discussion, we will find it useful to consider two limiting cases, uniform distributions of either air-phase, solid-phase, or liquid-phase concentrations – i.e.,  $C_1 = C_2 = C_3 = \dots$ ,  $C_{s1} = C_{s2} = C_{s3} = \dots$  or  $C_{l1} = C_{l2} = C_{l3} = \dots$ . Also, we will most often assume the room core concentration is uniform – i.e., the familiar well-mixed zone assumption – although this will be done for convenience only, the elemental models presented may be applied as well to imperfectly-mixed room models.

### 2.3.1.1 Boundary Layer Diffusion

Diffusion through the air-phase boundary layer, sometimes called *external diffusion*, is intimately related to the details of airflow near the surface – details that must remain largely indeterminate due to the analytic challenge demanded to predict them. Nevertheless, the contaminant species mass transport,  $w$  ( $\text{g-species}\cdot\text{s}^{-1}$ ), through this boundary layer may be estimated using the discrete approximation from boundary layer theory :

$$w = \rho_{air} A_s \bar{h} (C - C^*) \quad (70)$$

where  $A_s$  is the exposed surface area of the surface ( $\text{m}^2$ ),  $\rho_{air}$  is the density of the air-phase ( $\text{g-air}\cdot\text{m}^{-3}$ ), and  $\bar{h}$  is the surface-average mass transfer coefficient ( $\text{m}\cdot\text{s}^{-1}$ ). For planar solid or liquid surfaces within rooms, the exposed surface area would normally be taken as the apparent or

projected area of the surface while for airflow over a bed of granules within an activated carbon filter, for example, the exposed area would be taken equal to the accumulated surface area of all the individual particles – both areas consistent with the correlation used to estimate the surface-average mass transfer coefficient.

Expressed in terms of an element equation describing species mass flow rates between discrete spatial nodes associated with the room core and surface air-phase concentrations, these equations may be written as:

$$\begin{Bmatrix} w \\ w^* \end{Bmatrix} = \rho_{air} A_s \bar{h} \begin{bmatrix} 1 & -1 \\ -1 & 1 \end{bmatrix} \begin{Bmatrix} C \\ C^* \end{Bmatrix} \quad (71)$$

where species mass flow from a node into the boundary layer element establishes the positive convention.

The average mass transfer coefficient may be measured directly, measured indirectly using the naphthalene sublimation technique (43), estimated from published heat transfer correlations using the so-called *heat and mass transfer analogy*, or estimated from published mass transfer correlations. Correlations are available for airflow through fixed beds of granules (44, 45) that may be used in some building sorption filtration systems.

√ For the next generation of CONTAMxx, a boundary layer element should be implemented. The user would have to specify:

- the exposed surface area  $A_s$ ,
- the surface average mass transfer coefficient  $\bar{h}$  or, ideally, would select from a choice of correlations for (at least) airflow over a planar surface (43) or through fixed beds of granules (44, 45), and
- the *connectivity* of the boundary layer element – that is, the discrete nodes corresponding to the core and surface concentrations.

Within the current interface conventions of CONTAM93/94 the specification of the *connectivity* of the boundary layer element and, indeed, the surface node itself presents a small problem. Limiting consideration, here, to modeling transport to surfaces of well-mixed zones – i.e., corresponding to rooms or, possibly, *tanks* of a *tanks-in-series* idealization of an air cleaning device (e.g., sorption filtration or wet scrubber devices) – then it would be useful to introduce a surface component represented by a *surface icon*. A *surface icon* could be placed in a CONTAM zone and *opened* to, metaphorically, reveal the micro-structure of the surface – the boundary layer, surface interface, and solid or liquid below, similar to Figure 2 above. The core and boundary layer nodes would be defined, by default, upon selection and placing of the surface icon in a zone and the user would,

with the icon open, specify the model parameters for boundary layer diffusion. In addition the user would have the option to:

- define additional spatially discrete nodes corresponding to layers below the surface,  $C_{si}$  or  $C_{li}$  ,
- define model parameters governing the nature of diffusion into these subsurface layers, if any,
- define mass transfer barriers or resistances,
- specify the nature of any equilibrium relations that may exist between air-phase and solid- or liquid-phase concentrations at the surface and each of the subsurface nodes, and
- specify initial concentrations and/or hypothetical ideal sources at each of the spatially discrete nodes.

That is to say, the introduction of a surface component would allow the user to, in essence, zoom-in and define the microscopic mechanisms governing the heterogeneous process of interest in terms of the boundary layer process of this subsection – which is fundamental to all heterogeneous processes – and the processes presented in the subsequent subsections of this section. This will not only allow a great deal of flexibility in modeling individual heterogeneous processes, but will allow the user to model more than a single heterogeneous process in each zone.

### 2.3.1.2 Mass Transfer Resistance

The use of so-called *vapor barriers* in building construction is commonplace. These *barriers* are designed to limit the transport of water vapor into building construction and materials and may be constructed of thin material layers or applied as paint. They may be expected to also limit the mass transport of other species as well and, therefore, may have to be modeled when considering some heterogeneous processes.

Following the example of the boundary layer mass transport, one may model these mass transport barriers as simple *resistances* to mass transfer of negligible thickness and across which the air-phase concentration drops from the one concentration  $C_i$  to another  $C_j$  as indicated in the diagram below:

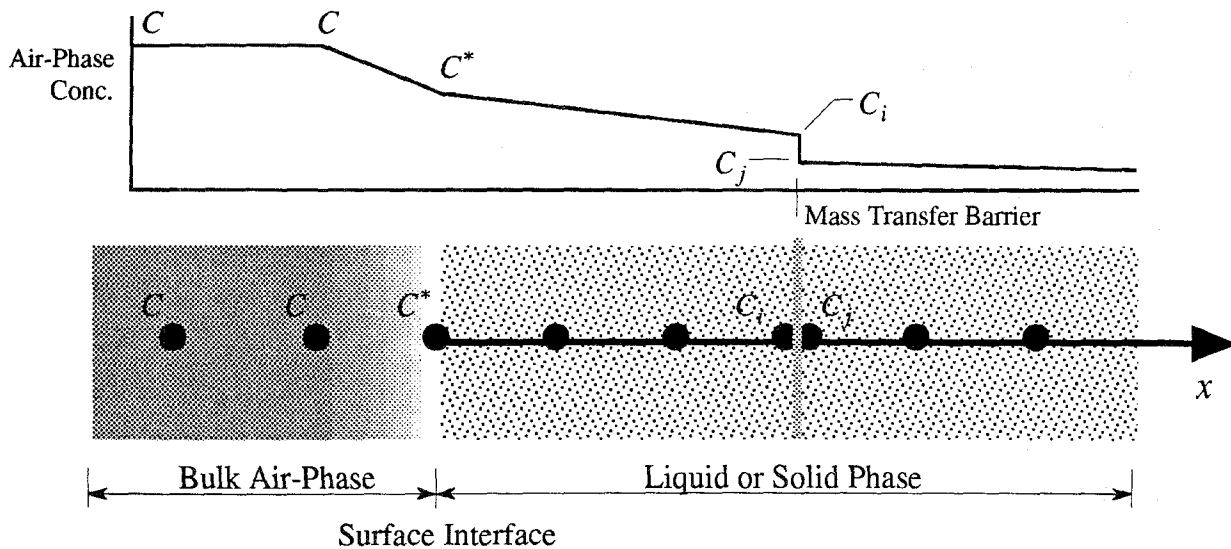


Figure 3. Mass transfer barrier or resistance.

For an ideal resistance, the contaminant species mass transport,  $w$  (g-species·s<sup>-1</sup>), through this layer may be modeled as:

$$w = \rho_{air} \frac{A_s}{R_m} (C_i - C_j) \quad (72)$$

where  $A_s$  is the surface area of the barrier (m<sup>2</sup>),  $\rho_{air}$  is the density of the air-phase (g-air·m<sup>-3</sup>), and  $R_m$  is the mass transfer resistance (s·m<sup>-1</sup>).

Expressed in terms of an element equation describing species mass flow rates between discrete spatial nodes, these equations may be written as:

$$\begin{Bmatrix} w_i \\ w_j \end{Bmatrix} = \rho_{air} \frac{A_s}{R_m} \begin{bmatrix} 1 & -1 \\ -1 & 1 \end{bmatrix} \begin{Bmatrix} C_i \\ C_j \end{Bmatrix} \quad (73)$$

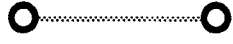
where again species mass flow from a node into the element establishes the positive convention.

In reality a barrier to mass transfer will have a finite thickness and could, therefore, be modeled as the porous solid that it is. This element allows the analyst to avoid considering this level of detail and is likely to provide an acceptable level of accuracy for typical vapor barriers. The use of this type of element may, however, introduce a small numerical problem. Often, a vapor barrier will be located at the exposed surface of a material – at the inner surface of the boundary layer. As a result, one would have to introduce the  $i$  and  $j$  nodes at this location leaving the room-side node without capacitance – that is to say a single algebraic, rather than differential, equation will be introduced thereby demanding a solution strategy that can handle mixed algebraic and differential equations.

√ For the next generation of CONTAMxx, a mass transfer resistance element should be implemented. Numerically, it is no different than a boundary layer element so implementation

would be trivial. The surface component interface strategy proposed above could be configured to allow the user to introduce the required coincident  $i, j$  nodes and specify the model parameters. To facilitate its use, the user should be allowed to define this element in terms of permeability or other parameters commonly used in the vapor barrier field.

### 2.3.1.3 Equilibrium Constraints



Sorption, vaporization, and sublimation mass transport are likely to be limited by diffusion processes that transport molecular species to or from the actual surface site where the sorption, vaporization, or sublimation processes take place. The kinetics of the actual sorption, vaporization, or sublimation processes is likely to be so rapid that for the purposes of indoor air quality analysis they may be treated as instantaneous. These processes are, however, limited by equilibrium constraints – that is to say, at the molecular level they may be assumed to be rapidly occurring reversible processes characterized by a) an equal exchange rate of molecules across the surface interface and, as a result, b) near-surface concentrations that effectively approach the levels that would exist at a steady, equilibrium state if the gas-liquid or gas-solid system were closed systems.

Somewhat ironically, therefore, we will not actually describe the mass transport for these key heterogeneous processes but instead establish algebraic constraints on near-surface concentrations based on empirical equilibrium measurements which, in general, will be identified using the functional notation:

$$C_{s0} = f_s(C^*) \text{ or } C_{l0} = f_l(C^*) \quad (74)$$

where  $f$  is a function that is unique for each species/solid (or liquid) system. It will prove useful to also identify the general inverse relation as well:

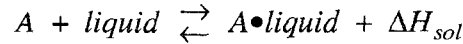
$$C^* = g_s(C_{s0}) \text{ or } C^* = g_l(C_{l0}) \quad (75)$$

As so often is the case, this seemingly benign modeling strategy of representing fast subprocesses with pseudo-steady-state, algebraic relations introduces numerical problems. Here the problems are threefold. First these types of constraints will result in mixed algebraic and differential system equations; second in several important cases – i.e., sorption modeling with effective sorbents – these algebraic constraints will introduce numerically challenging nonlinear couplings between system degrees of freedom; finally, by themselves, these constraints do not account for mass transfer from the air-phase to the solid or liquid-phase and their use may introduce violations of the conservation of contaminant species mass. We will attempt to address these problems as we proceed.



## Absorption $\hat{H}$

Gas-phase air contaminants will be soluble in liquids to a greater or lesser degree. If the contaminant does not chemically react with the liquid, the absorption of the contaminant may be represented as:



where  $A \bullet \text{liquid}$  is meant to represent the species  $A$  in solution with the liquid-phase and is the heat of solution. For dilute solutions, the equilibrium solubility of the gas in the liquid will be governed by Henry's law (see (46) Section 14.12 or (1) Section 5.1):

$$[A]_l = H_A p_A \quad (76)$$

where  $[A]_l$  is the liquid-phase concentration of species  $A$  (mass-A·mass-liquid<sup>-1</sup>),  $H_A$  is the Henry's law coefficient with units, here, of (mole-A·l-liquid<sup>-1</sup>·atm<sup>-1</sup>), and  $p_A$  is the vapor pressure of species  $A$  in the gas-phase above the liquid (atm). Henry's law coefficients are often related to so-called Bunsen absorption coefficients (46).

Henry's law coefficients have a temperature dependency defined by van't Hoff's relation (see (1) for details):

$$\frac{d \ln(H_A)}{dT} = \frac{\Delta H}{RT^2} \quad (77)$$

which leads to the approximate relation:

$$\ln(H_A(T_2)) \approx \ln(H_A(T_1)) + \frac{\Delta H}{R} \left( \frac{1}{T_1} - \frac{1}{T_2} \right) \quad (78)$$

If it is assumed that in the gas-phase species  $A$  is governed by the ideal gas law, then we can relate the gas-phase concentration  $C_A$  to the partial pressure as:

$$C_A = \frac{M_A}{\rho_{air} RT} p_A \quad (79)$$

where  $M_A$  is the molecular weight of species  $A$  (gram-A·mole-A<sup>-1</sup>),  $R$  is the ideal gas constant (8.31441 Pa·m<sup>3</sup>·°K<sup>-1</sup>·mole<sup>-1</sup>), and  $T$  is the absolute temperature of the gas-phase (°K). The mass-fraction liquid-phase concentration of species  $A$  is related to the molar concentration as:

$$C_{lA} = [A]_l \frac{M_A}{\rho_l} \quad (80)$$

Thus Henry's law may be written in a form more directly useful for our purposes as:

$$C_{lA} = \frac{M_A}{\rho_l} H_A \frac{\rho_{air} RT}{M_A} C_A = H_A \frac{\rho_{air} RT}{\rho_l} C_A \quad (81)$$

or:

$$C_{lA} = \hat{H}_A C_A \quad (82)$$

with:

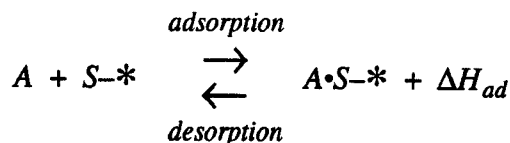
$$\hat{H}_A \equiv H_A \frac{\rho_{\text{air}} RT}{\rho_l} \quad (83)$$

If the gas contaminant chemically reacts with the liquid in a reversible manner that establishes an equilibrium state between the gas-phase species concentration and liquid-phase product concentrations it may still be possible to use Henry's law to describe the equilibrium state using a modified Henry's law coefficient (see Section 5.2 of (1) for examples).

For the next generation of CONTAMxx, an absorption equilibrium constraint should be provided. The surface component interface strategy proposed above could be configured to allow the user to specify the degrees of freedom to be constrained and the model parameters. It would be best to also automate the computation of the temperature dependency of this constraint.



The sorption of a species  $A$  to an active site  $S^*$  may be represented as (47-50):



where  $A \cdot S^*$  is the species in a bound state to an active site and  $\Delta H_{ad}$  is the heat of adsorption released. For closed systems under steady conditions the rate at which adsorbate molecules bind to active sites will eventually come to equal the rate at which they are released; the concentration of the adsorbate molecules in the air-phase  $C$  and the sorbed-phase  $C_s$  (mass-species/mass-sorbent) will remain constant at their respective equilibrium values. These equilibrium values depend on the nature of the adsorbate, adsorbent, and the thermodynamic state of the system. For isothermal conditions at atmospheric pressure equilibrium relations between these variables – identified as *adsorption isotherms* – may be represented functionally as given in Equation 74. Some isotherm models are tabulated below.

Table 4. Representative adsorption isotherm models.

Model	$C_{s0} = f(C^*)$	Constants
<i>Linear</i>	$C_{s0} = K_P C^*$	$K_P$ is the Partition Constant.
<i>Langmuir</i>	$C_{s0} = \frac{C_s^o K_L C^*}{1 + K_L C^*}$	$C_s^o$ is the molecular mono-layer sorbent concentration. $K_L$ is the Langmuir Constant.

<i>BET</i>	$C_{s0} = \frac{C_s^o K_{BET} \hat{C}^*}{(1 + \hat{C}^*) (1 - \hat{C}^* + K_{BET} \hat{C}^*)}$	$K_{BET}$ is the BET constant. $\hat{C}^*$ is the <i>reduced concentration</i> : – the ratio of the equilibrium to the saturation air-phase concentration $C_{sat}^*$ .
<i>Freundlich</i>	$C_{s0} = K_F (C^*)^{1/n}$	$K_F$ and $n$ are empirical Freundlich coefficients.
<i>Polanyi DR</i>	$C_{s0} = C_s^{o'} \exp \left( -D \left( \ln \left( \frac{C_{sat}^*}{C^*} \right) \right)^2 \right)$	$D$ is the Dubinin-Radushkevich parameter. $C_s^{o'}$ is the sorbed concentration corresponding to complete filling of micropores.

Modeling adsorption dynamics depends critically on modeling sorption equilibrium accurately. This may be achieved only through careful selection of a candidate isotherm model and empirical determination of model parameters using carefully measured experimental data. For the sorption of trace concentration air-pollutants on building materials the Langmuir model or its low-concentration asymptote, the Linear model, are reasonable first candidates. For sorption of water or other contaminants with concentrations within one order of magnitude of their saturated values the BET model should be considered. While the Freundlich isotherm is often employed for the sorption of volatile organic compounds (VOCs) on activated carbon, the Polanyi DR model is the model of choice for sorption of VOCs on granulated activated carbon (GAC) where capillary condensation in microporous interstices – *pore filling* – is important. In spite of recent progress in this area (51-54) there is very little data available for the sorption of indoor air pollutants, at low concentrations commonly found in buildings, on building materials or sorption filtration media.

The Polanyi DR approach, which is discussed in detail by Shen and Wang (55), is particularly attractive because, in principle, it may be used to describe sorption equilibrium for whole classes of compounds on a particular adsorbent and the variation of this equilibrium with temperature. This relation is most often presented as a so-called *characteristic curve* of the form:

$$W_e = W_o \exp \left( -k_\mu \left( \frac{RT}{b} \right)^m \left[ \ln \left( \frac{C_{sat}}{C_e} \right) \right]^m \right) \quad (84)$$

In this form, the (liquid) volume of adsorbate contained in micropores  $W_e$  ( $\text{cm}^3 \cdot \text{g-sorbent}^{-1}$ ) is related to the total volume of micropores available  $W_o$  ( $\text{cm}^3 \cdot \text{g-sorbent}^{-1}$ ) and the change in free energy of the sorbate from the gas-phase to the sorbed-phase as described by the Polanyi potential  $\phi = RT \ln(C_{sat}/C_e)$ , where  $R$  is the universal gas constant and  $T$  is the absolute temperature of the sorbate/sorbent system. Within this Polanyi relation, three constants,  $W_o$ ,  $k_\mu$  (a constant associated with the microporosity of the sorbent) and  $m$  (which is 2 for activated carbons), relate only to the character of the adsorbent and the other terms, the *affinity*  $b$  and the gas-phase

concentration at saturation  $C_{sat}$ , relate only to the adsorbate. The affinity provides a relative measure of the affinity of the sorbate for the adsorbent and is thought to be related to the molecular volume  $V_M$  ( $\text{cm}^3 \cdot \text{mol}^{-1}$ ) of the liquid adsorbate.

On this basis Shen and Wang have proposed the following general form of the Polanyi isotherm relation:

$$W_e = W_o \exp \left( -K \left( \frac{T}{V_M} \right)^m \left[ \ln \left( \frac{C_{sat}}{C_e} \right) \right]^m \right) \quad (85)$$

and have fitted this form to measured data for a set of six hydrocarbons on two sorbents – a petroleum-based activated carbon identified as BAC and an organic sorbent based on polystyrene (55). These authors provide a comparison between the characteristic curve they developed for the BAC activated carbon with several other characteristic curves for other activated carbons. While these curves differ, as expected, the curves presented for a variety of coconut shell-based activated carbons, commonly used in building applications, are similar to each other and to the curve obtained for the BAC. Regrettably, however, all of the curves presented were developed for relatively high air-phase concentrations ranges (i.e., on the order of 100 to 20,000 ppm).

The author adapted the Shen/Wang general formulation by adjusting the sorbate parameters  $W_o$  and  $K$  to better fit the few equilibrium measurements available that approach the concentration levels found in buildings (i.e., on the order of 1 - 500 ppb) to obtain (56):

$$C_{se} = 0.496 \rho \exp \left( -0.0016 \left( \frac{T}{V_M} \right)^2 \left[ \ln \left( \frac{C_{sat}}{C_e} \right) \right]^2 \right) \quad (86)$$

with  $W_o = 0.496 \text{ cm}^3 \cdot \text{g-sorbent}^{-1}$ ,  $K = 0.0016$ , and  $C_s = W_e \rho$  ( $\rho$  is the density of the liquid form of the adsorbate,  $\text{g} \cdot \text{cm}^{-3}$ ). This general Dubinin-Radushkevich isotherm – plotted for isobutyl methyl ketone, toluene, and benzene (with normal boiling points of 117 °C, 111 °C and 80.3 °C, respectively) – is compared, in Figure 4, with measured data and several (higher level) isotherms reported in the literature for room temperature conditions. Figure 5. compares toluene isotherms for three temperatures, based on Equation 6, with isotherms reported by Yeh (57).

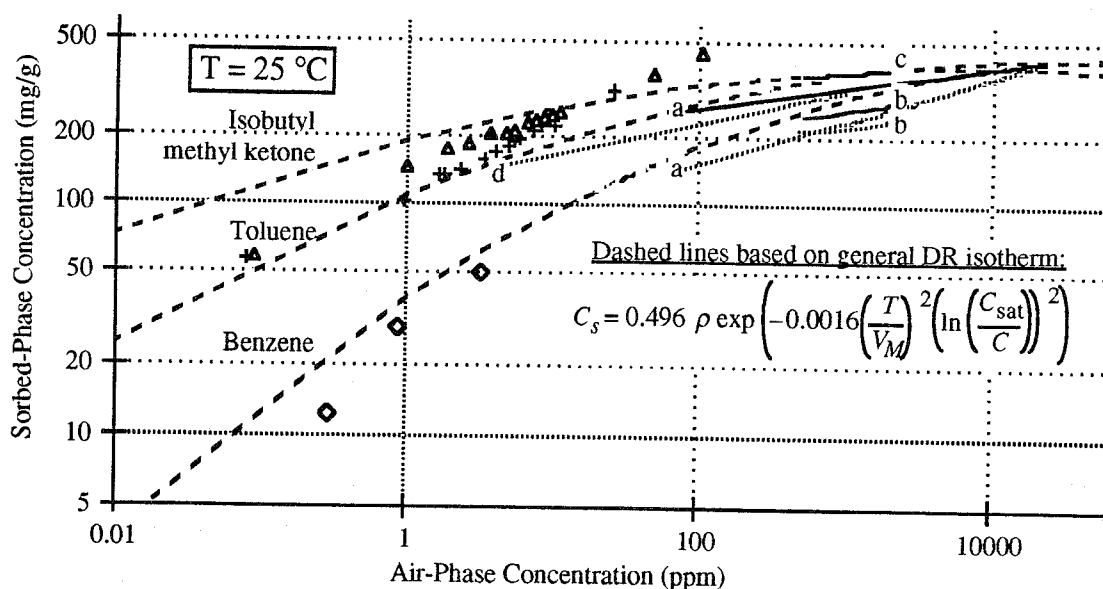


Figure 4. Representative General Dubinin-Radushkevich isotherm compared to: (a) isotherms reported in the literature for toluene (solid line) and benzene (dotted line) – (a. on petroleum-based activated carbon (58), b. on coal-based activated carbon (59), c. on coconut shell-based activated carbon (60), and d. on phenolic-based activated carbon fiber (61)); (b) measured data for isobutylmethyl ketone (triangles) and toluene (crosses) on coal-based activated carbon (59) and benzene (diamonds) on coconut shell-based activated carbon (62).

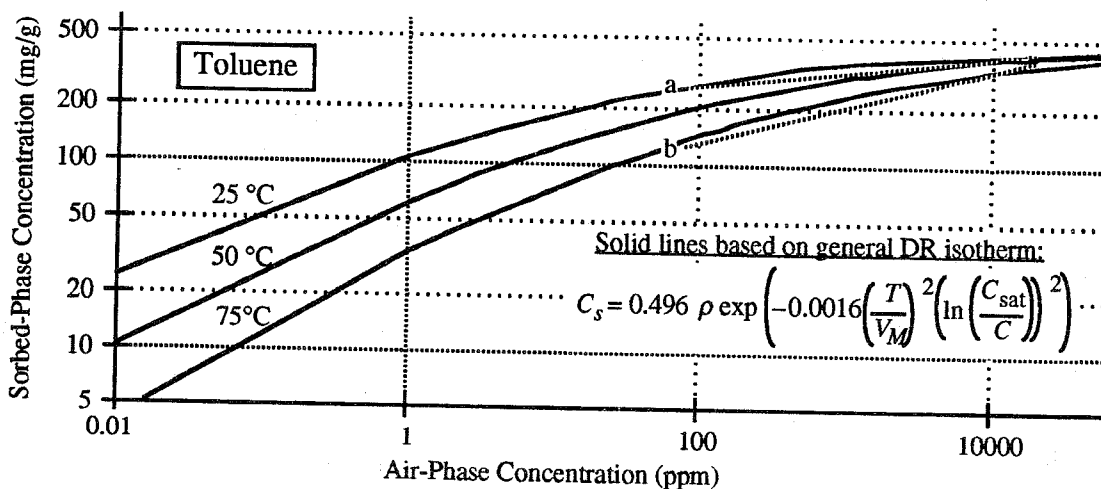


Figure 5. Representative General Dubinin-Radushkevich isotherm compared to Freundlich isotherms reported by Yeh for toluene on petroleum-based activated carbon at 25 °C (a.) and 75 °C (b.) (57).

It is important to stress measured data is simply not available to establish a single sorption isotherm for any VOC, or other air pollutant for that matter, at the 0-1000 ppb levels commonly encountered in buildings. The strategy used here of adjusting an available, high-concentration level isotherm to fit the few low-concentration measured data points available must be considered to be a method of last resort and not a recommended procedure for obtaining needed low-concentration range isotherms.

More recently, Wood published correlations for the coefficients of the Polanyi DR isotherm for some 140 compounds and 15 different activated carbons (63). While the data is "limited to vapors of organic compounds that exists as liquids at ordinary temperatures and pressures" and is based on higher concentration level measures than that found in indoor air, this data should prove useful in extending the scope of available data to a broader variety of VOCs.

So-far, the discussion above has been limited to *single-component* sorption. In practical situations building materials and sorption filtration media will be exposed to multi-component mixtures of compounds that will tend to compete for available active sites, consequently, *multi-component sorption* equilibrium will have to be accounted for. A variety of multi-component equilibrium relations have been developed and their efficacy for industrial applications has been investigated (44, 64). Liu has successfully demonstrated the application of a multi-component approach based on Polanyi's potential theory and a technique known as *component grouping* to the sorption of low-concentration VOC mixtures on activated carbon (65).

In general, for multi-component mixtures (under isothermal conditions at atmospheric pressure) the equilibrium sorbed concentration for component  $i$ ,  $C_{se,i}$ , will depend upon not only on the air-phase concentration of component  $i$ ,  $C_{e,i}$ , but the air-phase concentrations of all other components, as:

$$C_{se,i} = g(C_{e,1}, C_{e,2}, \dots, C_{e,i}, \dots, C_{e,n}) \quad (87)$$

The *Extended Langmuir Equation* developed by Markham and Benton for component molecules that do not influence each other provides one example of a multi-component model:

$$C_{se,i} = \frac{C_{so,i} K_{L,i} C_{e,i}}{1 + \sum_{j=1}^n K_{L,j} C_{e,j}} \quad (88)$$

The model parameters are defined for each component as presented above in Table 4. For very low air-phase concentrations (i.e.,  $1 \gg \sum K_{L,j} C_{e,j}$ ) this multi-component model simplifies to a series of  $n$  uncoupled single-component Linear isotherms and, therefore, for this limiting case, multicomponent competition may be ignored.

√ For the next generation of CONTAMxx, an adsorption equilibrium constraint should be provided. The surface component interface strategy proposed above could be configured to allow the user to specify the degrees of freedom to be constrained and the model parameters. It would be best to offer the user a choice of isotherm model to use – e.g., from the table of models presented above – and also automate the computation of the temperature dependency of this constraint.

### Vaporization and Sublimation

Liquid molecules with sufficient kinetic energy can escape the surface of a liquid to enter the gas phase and, conversely, gas molecules may enter the liquid phase. For closed systems of a single-

component  $A$  under steady conditions these reversible opposing processes of vaporization and condensation may be represented as:



where  $\Delta H_{vap}$  is the heat of vaporization. Eventually this system will come into a state of equilibrium – i.e., saturated conditions in the gas phase will prevail – at which point the saturation vapor may be estimated using the Clausius-Clapeyron equation:

$$p_A = p_{A\infty} \exp\left(\frac{-\Delta H_{vap}}{RT}\right) \quad (90)$$

The constant in this expression  $p_{A\infty}$  is conveniently determined from boiling point data for the pure liquid  $A$  (see (46) Sections 5.9 and 12.4. (Sublimation of a gas from the single-component solid phase follows a similar rule.)

Assuming, again, ideal gas behavior for  $A$  – Equation 79 – we obtain the saturation (equilibrium) concentration of species  $A$  above the pure liquid  $A$ :

$$C_{A-sat} = \frac{p_{A\infty} M_A}{\rho_{air} RT} \exp\left(\frac{-\Delta H_{vap}}{RT}\right) \quad (91)$$

For closed multicomponent systems, Raoult's law describing the equilibrium behavior of ideal solutions may be used to estimate the (partial) vapor pressure  $p_i$  of each component  $i$ :

$$p_i = x_i p_i^o \quad (92)$$

where  $x_i$  is the mole fraction of component  $i$  in the liquid solution:

$$x_i = \frac{C_{li}/M_i}{\sum_j C_{lj}/M_j} \quad (93)$$

Assuming ideal gas behavior and combining Equations 90, 92, and 93:

$$C_{i-sat} = \frac{p_{i\infty}}{\rho_{air} RT \sum_j C_{lj}/M_j} \exp\left(\frac{-\Delta H_{ivap}}{RT}\right) C_{li} \quad (94)$$

where  $\Delta H_{ivap}$  is the heat of vaporization,  $M_j$  the molecular weight, and  $C_{lj}$  is the liquid-phase (mass fraction) concentration of component  $j$ . For a single-component (pure) liquid  $C_{li} = 1.0$  and Equation 94 simplifies to 91.

Note, to apply Equation 94 to multicomponent evaporation modeling, one must track the change of liquid concentration  $C_{li}$ . Guo and Tichenor have put forward a model for emissions from wet sources (e.g., VOCs from wet interior architectural coatings) based on the assumption that the vapor pressure of a given VOC component will vary in proportion to the mass of the VOC

component remaining in the coating at any time (66-68). Their assumption may be considered to provide a crude approximation to Equation 94 above.

#### 2.3.1.4 1D Simple Diffusion

Diffusion transport within nonporous solids or liquids may be modeled using Fick's Law with the diffusivity  $D$  based on molecular or convective transport processes. For one-dimensional diffusion into planar nonporous solid sheets or bulk liquids with a single free surface – i.e., as opposed to spherical droplets – the resulting partial differential equations assume the form of the classic 1D diffusion equation:

$$\text{Nonporous Solids} \quad \rho_s A_s D \frac{\partial^2 C_s}{\partial x^2} + \rho_s A_s r_s = \rho_s A_s \frac{\partial C_s}{\partial t} \quad (95a)$$

$$\text{Bulk Liquids} \quad \rho_l A_l D \frac{\partial^2 C_l}{\partial x^2} + \rho_l A_l r_l = \rho_l A_l \frac{\partial C_l}{\partial t} \quad (95b)$$

where  $\rho_s$  and  $\rho_l$  are the density of the solid and liquid respectively ( $\text{g}\cdot\text{m}^{-3}$ ),  $A_s$  and  $A_l$  are the cross-sectional areas of the 1D liquid or solid domain ( $\text{m}^2$ ),  $x$  is the spatial dimension into the solid or liquid (m), and  $r_s$  and  $r_l$  are specific generation rates of the contaminant ( $\text{g}\cdot\text{species}\cdot\text{g}^{-1}$ ) introduced to account for the possibility of distributed generation (+) or removal (-) of the diffusing species.

A solution to this partial differential equation may be approximated using Finite Element procedures by discretizing the solid or liquid into a number of layers (see Chapter 10 of (69) for an introduction to these procedures). Using the simplest 1D finite element approximation based on linear *shape functions* and a lumped capacitance approximation, we obtain element equations that describe the species mass transport rate ( $\text{g}\cdot\text{species}\cdot\text{s}^{-1}$ ) from adjacent nodes,  $i, j$ , into the element,  $w_i$ , and  $w_j$ , as:

$$\begin{Bmatrix} w_i \\ w_j \end{Bmatrix} = -\frac{A_s \delta x \rho_s r_s}{2} \begin{Bmatrix} 1 \\ 1 \end{Bmatrix} + \frac{\rho_s A_s D_s}{\delta x} \begin{bmatrix} 1 & -1 \\ -1 & 1 \end{bmatrix} \begin{Bmatrix} C_{si} \\ C_{sj} \end{Bmatrix} + \frac{A_s \delta x \rho_s}{2} \begin{bmatrix} 1 & 0 \\ 0 & 1 \end{bmatrix} \begin{Bmatrix} \frac{dC_{si}}{dt} \\ \frac{dC_{sj}}{dt} \end{Bmatrix} \quad (96)$$

where  $\delta x$  is the element (discrete layer) thickness. To model diffusion transport in liquids we simply switch the  $s$  subscripts to an  $l$  subscripts.

Higher order finite element approximations and so-called *consistent* capacitance matrices could be used to gain accuracy while maintaining computational efficiency here. It is likely, given the current uncertainty in the field regarding species diffusivities and, especially, specific generation rates, that this simpler finite element approximation will, however, be sufficient for the time being. Numerically, then, subassemblies of elements defined by Equation 96 may be directly assembled with equations from existing CONTAM93/94 mass transport elements to form system equations



that include this class of diffusion transport. Given these equations are linear first order differential equations, CONTAM's current solution method may be applied to the solution of these equations and the only problem that may be expected to arise will relate to the "stiffness" of the resulting equations. The ratio of the element capacitance and the element conductance  $(\delta x^2 / (2D_s))$  provides a nominal measure of the time constant associated with this element.

To apply these equations to practical problems of analysis, initial conditions must be established for all nodal concentrations. Setting these conditions to zero corresponds to modeling an initially uncontaminated solid (or liquid). By setting these conditions to an appropriate high (initial) value, one may model an emission "source" governed by diffusion transport. For this case, research is needed to establish reasonable "appropriate" initial values. For both cases, experimental work is needed to establish effective diffusivities and/or to verify available techniques to estimate them.

### 2.3.1.5 1D Equilibrium-Constrained Diffusion in Porous Solids

Diffusion transport within porous solids invariably involves a complex variety of processes including molecular diffusion, Knudsen diffusion, surface diffusion, and, possibly, Poiseuille flow (44, 70). Molecular diffusion in the larger pores and Knudsen diffusion in the smaller pores, where the mean free path of the diffusing species is limited by the pore dimensions, are diffusion processes that occur in series. They may be modeled analogously to Fick's Law through the introduction of an *effective diffusion coefficient*  $D_e$  ( $m^2 \cdot s^{-1}$ ) (see section 4.2.2 of (44) for details). Surface diffusion, involving the motion of the diffusing species along the pore wall surfaces, occurs in parallel to the molecular and Knudsen diffusion processes. It may, also, be modeled analogously to Fick's law but with the complication that the effective surface diffusivity, in general, depends on the local sorbed concentration. Yang asserts:

*"Surface diffusion can be important, and dominating, in the total flux in porous material, provided: (1) surface area is high, and (2) surface concentration is high."* (44) page 113

For industrial sorption separation processes this is likely to be the case. In indoor air quality analysis where air-phase concentrations and material's specific surface areas are relatively low this is not likely to be the case and, therefore, surface diffusion will not be modeled directly.

#### Sheet-Like Porous Solids

Unlike simple diffusion, diffusion in porous solids may be expected to be constrained by the equilibrium sorption conditions discussed above in section 2.3.1.3. By assuming a) the sorbed-phase concentration remains in equilibrium with the porous air-phase concentration and b) surface and solid-phase diffusion are both negligibly small, one may obtain a partial differential equation that describes one-dimensional diffusion into sheet-like porous solids, as:

$$\rho A_s D_e \frac{\partial^2 C}{\partial x^2} + \rho_s A_s r_s = \rho A_s \epsilon \frac{\partial C}{\partial t} + \rho_s A_s \frac{\partial C_s}{\partial t} \quad (97)$$

where:

- the first term accounts for the diffusion of the air pollutant species in the porous gas-phase with  $\rho$  being the gas-phase density (g-air·m<sup>-3</sup>),
- the second term is included to account for distributed generation of the pollutant species as before,
- the fourth term accounts for the accumulation of the pollutant species in the pore gas-phase with  $\epsilon$  being the porosity of the solid (volume-pores-volume-total<sup>-1</sup>), and
- the last term accounts for the accumulation of pollutant species in the sorbed-phase with  $\rho_s$  being the bulk density of the porous solid. (In other formulations, the solid-phase density  $\rho_s^*$  is used so that  $\rho_s = (1-\epsilon)/\epsilon\rho_s^*$  would replace the bulk density used above.)

Imposing the equilibrium condition (see Equation 74 above):

$$C_s = f_s(C) \quad \text{or} \quad \frac{\partial C_s}{\partial t} = \frac{\partial f_s}{\partial C} \frac{\partial C}{\partial t} \quad (98)$$

Equation 97 may be transformed to assume the form of the classic 1D diffusion equation:

$$\rho A_s D_e \frac{\partial^2 C}{\partial x^2} + \rho_s A_s r_s = \left( \rho A_s \epsilon + \rho_s A_s \frac{\partial f_s}{\partial C} \right) \frac{\partial C}{\partial t} \quad (99)$$

Again we may apply Finite Element procedures to approximate a solution to this equation by discretizing the porous solid sheet into a number of layers. Using the simplest 1D finite element approximation based on linear *shape functions* and a lumped capacitance approximation, we obtain element equations that describe the species mass transport rate from adjacent nodes,  $i, j$ , into the element,  $w_i$ , and  $w_j$ , as:

$$\begin{Bmatrix} w_i \\ w_j \end{Bmatrix} = -\frac{A_s \delta x \rho_s r_s}{2} \begin{Bmatrix} 1 \\ 1 \end{Bmatrix} + \frac{\rho A_s D_e}{\delta x} \begin{bmatrix} 1 & -1 \\ -1 & 1 \end{bmatrix} \begin{Bmatrix} C_i \\ C_j \end{Bmatrix} + \frac{A_s \delta x}{2} \left( \rho \epsilon + \rho_s \frac{\partial f_s}{\partial C} \right) \begin{bmatrix} 1 & 0 \\ 0 & 1 \end{bmatrix} \begin{Bmatrix} \frac{dC_i}{dt} \\ \frac{dC_j}{dt} \end{Bmatrix} \quad (100)$$

Note that each element has an effective capacity  $M_{eff}$  equal to the sum of the mass of air within the discrete layer plus the mass of the porous solid within the discrete layer scaled by the tangent slope of the equilibrium relation as:

$$M_{eff} = \frac{A_s \delta x}{2} \left( \rho \epsilon + \rho_s \frac{\partial f}{\partial C} \Big|_{C = \frac{C_i + C_j}{2}} \right) \quad (101)$$

For effective adsorbents the gas-phase capacitance will prove negligible:

$$\rho_s \frac{\partial f}{\partial C} \Big|_{C = \frac{C_i + C_j}{2}} \ll \rho \epsilon \quad \text{so} \quad M_{eff} \approx \frac{A_s \delta x \rho_s}{2} \frac{\partial f}{\partial C} \Big|_{C = \frac{C_i + C_j}{2}} \quad (102)$$

and it becomes numerically strategic to employ an alternative formulation expressed in terms of the sorbed-phase concentration, ignoring the gas-phase capacitance altogether:

$$\begin{Bmatrix} w_i \\ w_j \end{Bmatrix} = -\frac{A_s \delta x \rho_s r_s}{2} \begin{Bmatrix} 1 \\ 1 \end{Bmatrix} + \frac{\rho A_s D_e}{\delta x} \begin{bmatrix} 1 & -1 \\ -1 & 1 \end{bmatrix} \begin{Bmatrix} g_s(C_{si}) \\ g_s(C_{sj}) \end{Bmatrix} + \frac{A_s \delta x \rho_s}{2} \begin{bmatrix} 1 & 0 \\ 0 & 1 \end{bmatrix} \begin{Bmatrix} \frac{dC_{si}}{dt} \\ \frac{dC_{sj}}{dt} \end{Bmatrix} \quad (103)$$

The inverse equilibrium model  $g_s(C_{si})$  used in this formulation may be expanded in a first order Taylor series  $g_s(C_{si}) \approx C_{sio} + \left(\frac{1}{K}\right)C_{si}$  to “linearize” the resulting equation about the current estimates of nodal concentrations and, thereby, effect a solution.

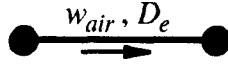
When the sorption equilibrium condition is defined by the linear model (see Table 4 above), Equation 100 (or 103) becomes a system of two linear ordinary differential equations and, again, the inclusion of this element equation in the CONTAM framework presents no special problem other than numerical “stiffness.” For all other sorption equilibrium models these equation become nonlinear and, consequently, alternate solution methods must be applied. One possibility, possibly the most attractive, is again to employ a time-stepping scheme utilizing the Newton-Raphson method. If this tack is taken, element Jacobians may be directly evaluated once a particular equilibrium sorption model is specified.

#### Granulated Porous Solids

Porous diffusion within the granules or pellets of sorption filtration media may, in a similar manner, be modeled using a partial differential equation describing radially symmetric diffusion within a spherical sorbent particle. The *Linear Driving Force (LDF)* model has been developed, however, to provide a computationally simpler alternative (44). To form an element equation using the LDF lumped-parameter approximation, a single node associated with the surface location of all sorption granules and a node associated with the overall mean concentration of all sorption granules,  $\bar{C}_s$ , must be introduced to yield:

$$\begin{Bmatrix} w^* \\ w_s \end{Bmatrix} = \frac{15D_e M_s}{R_p^2} \begin{bmatrix} 1 & -1 \\ -1 & 1 \end{bmatrix} \begin{Bmatrix} C_{se}^* \\ \bar{C}_s \end{Bmatrix} + M_s \begin{bmatrix} 0 & 0 \\ 0 & 1 \end{bmatrix} \begin{Bmatrix} \frac{dC_{se}^*}{dt} \\ \frac{d\bar{C}_s}{dt} \end{Bmatrix} \quad (104)$$

where  $R_p$  is the sorbent particle radius and  $C_{se}^*$  is the sorbed-phase concentration in equilibrium with the near-surface air-phase concentration. An appropriate sorption isotherm may be introduced to transform  $C_{se}^*$  to the near-surface air-phase concentration  $C^*$ .



### 2.3.1.6 1D Convection-Diffusion

#### Porous Solid Sheets

Air pressure differences across sheet-like porous materials will result in airflows through the materials and an added mass transport process – convective mass transport. The superposition of parallel 1D convection and diffusion mass transport is governed by the partial differential equation given above, Equation 99, with one additional term to account for convective mass transport:

$$\rho A_s D_e \frac{\partial^2 C}{\partial x^2} + \rho_s A_s r_s - w_{air} \frac{\partial C}{\partial x} = \left( \rho A_s \varepsilon + \rho_s A_s \frac{\partial f_s}{\partial C} \right) \frac{\partial C}{\partial t} \quad (105)$$

where  $w_{air}$  is the mass flow rate of air through the porous sheet ( $\text{g-air}\cdot\text{s}^{-1}$ ). Again, Finite Element procedures may be used to transform this differential equation into a discrete approximation. Using the simplest 1D finite element approximation based on linear *shape functions* and a lumped capacitance approximation, we obtain element equations that describe the species mass transport rate from adjacent nodes,  $i, j$ , into the element,  $w_i$ , and  $w_j$ , as (see (69) section 10.4):

$$\begin{Bmatrix} w_i \\ w_j \end{Bmatrix} = -\frac{A_s \delta x \rho_s r_s}{2} \begin{Bmatrix} 1 \\ 1 \end{Bmatrix} + \left[ [k_{diff}] + [k_{conv}] \right] \begin{Bmatrix} C_i \\ C_j \end{Bmatrix} + \frac{A_s \delta x}{2} \left( \rho \varepsilon + \rho_s \frac{\partial f_s}{\partial C} \right) \begin{bmatrix} 1 & 0 \\ 0 & 1 \end{bmatrix} \begin{Bmatrix} \frac{dC_i}{dt} \\ \frac{dC_j}{dt} \end{Bmatrix} \quad (106a)$$

where:

diffusion transport is modeled as: 
$$[k_{diff}] = \frac{\rho A_s D_e}{\delta x} \begin{bmatrix} 1 & -1 \\ -1 & 1 \end{bmatrix} \quad (106b)$$

convection transport is modeled as: 
$$[k_{conv}] = \frac{w_{air}}{2} \begin{bmatrix} 1 & 1 \\ -1 & -1 \end{bmatrix} + \frac{\phi w_{air}}{2} \begin{bmatrix} 1 & -1 \\ -1 & 1 \end{bmatrix} \quad (106c)$$

with the so-called upwind parameter,  $0 \leq \phi \leq 1$ , is introduced to control numerical stability/stiffness (at the cost of artificial diffusion) during the solution phase.

Equation 106 defines a set of linear, ordinary differential equations that may, therefore, be directly implemented in the current CONTAM93/94 system. That is not to say, the use of these convection diffusion element equations is not without pit falls. In fact, assemblages of these Equations are likely to lead to stiff system equations. The upwind parameter may be adjusted, with experience, to mitigate these problems, but may introduce error.

To be complete, Equation 106 would have to be complemented with pressure-flow relations for porous sheet-like materials – i.e., to determine  $w_{air}$ . The Poiseuille equation is a good candidate for those cases where the flow is likely to be laminar. Manufacturer literature is available for porous sheet material used for particle filtration in the turbulent regime.

Packed Beds of Porous Adsorbents

Axial convection-diffusion in packed beds of porous adsorbents (e.g., activated carbon) may be modeled with a convection-diffusion equation that includes a term to account for boundary-layer mass transport between the bed void-space and the surface of the adsorbent pellets (see (44) section 4.1):

$$\rho A \epsilon D_x \frac{\partial^2 C}{\partial x^2} - w_{air} \frac{\partial C}{\partial x} - \rho A \hat{A}_p \bar{h} (C - C^*) = \rho A \epsilon \frac{\partial C}{\partial t} \quad (107)$$

where  $A$  is the cross sectional area of the bed,  $\epsilon$  is the bed void fraction,  $D_x$  is the axial dispersion coefficient of the bed,  $\hat{A}_p$  is the surface area of the adsorbent pellets per volume of bed,  $\bar{h}$  is the average boundary layer mass transfer coefficient for the void-to-pellet interface, and  $C^*$  is the air-phase concentration at the pellet surface. This equation would then be coupled to a model for the diffusion transport within the adsorbent pellets – e.g., Equation 104.

Following the examples presented above, Equation 107 could be modeled with a discrete Finite Element convection-diffusion approximation with boundary layer transport elements linking each of the nodal, air-phase degrees of freedom to a two-node element corresponding to Equation 104. Diagrammatically, the idealization would take the following form:

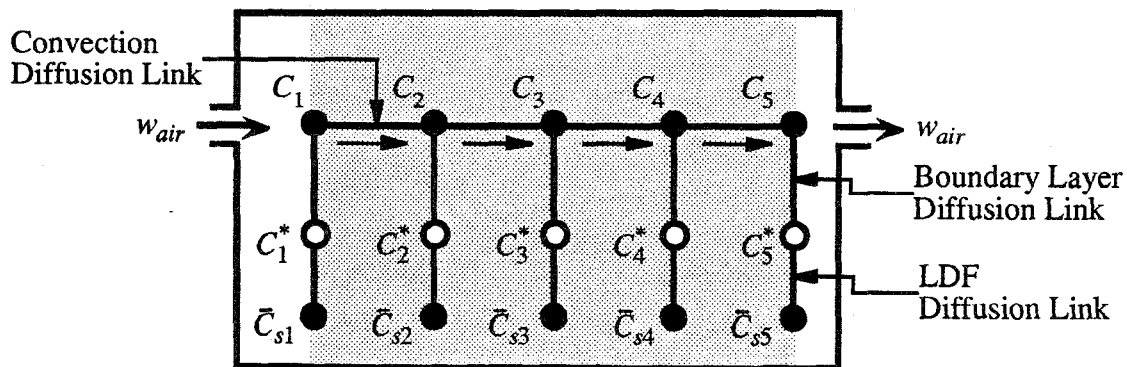


Figure 6. Packed bed adsorber idealization based on an assembly of conduction-diffusion Finite Elements, boundary layer elements, and Linear Driving Force elements.

The author has employed a *tanks-in-series* approach, without recirculation, to model both fixed bed adsorbents and distributed sorption filtration devices more commonly used in buildings using individual tanks that account for the boundary layer transport to the adsorbent pellets and intrapellet diffusion transport modeled with the linear driving force model (56). This alternative *tanks-in-series* approach, diagrammed below, is completely equivalent to the approach suggested by the diagram above when full upwinding ( $\phi = 1$ ) is employed. A *tanks-in-series* model with recirculation between the tanks would provide an equivalent means to model partial upwinding.

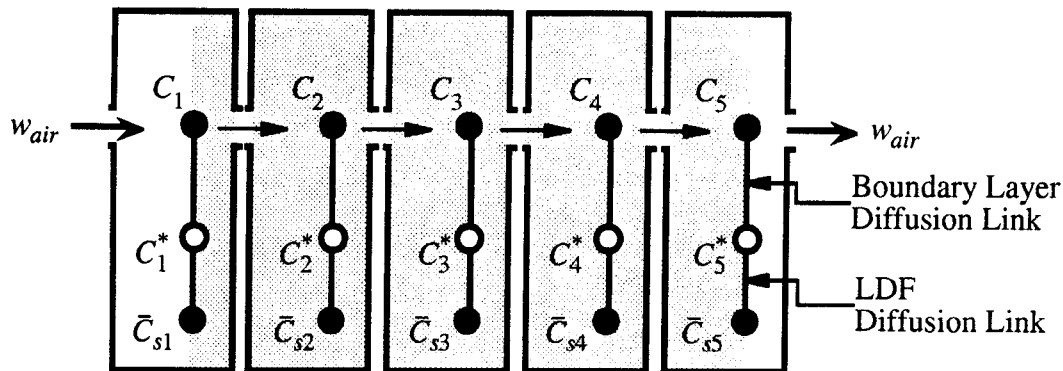


Figure 7. Packed bed adsorber *tanks-in-series* idealization based on an assembly of *filter cells* models of assemblies of well-mixed chambers with boundary layer elements and Linear Driving Force elements.

√ To provide the means to model sorption filtration devices, the next generation NIST IAQ Model should include the *tanks-in-series* (family of) model(s). The paper (56) provides all necessary details for implementation. This modeling approach provides capabilities equivalent to the mixed Finite Element-Lumped Element approach diagrammed above, when configured appropriately, yet is intuitively more direct and may accommodate the extended surface, distributed sorption filtration devices found more commonly in building applications.

The *tanks-in-series* approach leads to linear systems of ordinary differential equations when the sorption equilibrium relation upon which the filter cells are based are linear and nonlinear systems for nonlinear sorption equilibrium models. Given, effective sorbents are best characterized by nonlinear sorption equilibrium relations, realistic sorption filtration modeling will demand nonlinear equation solving techniques.

### 2.3.1.7 Surface Chemistry

Surface chemical transformations are likely to be important for all reactive air pollutants – i.e., those air pollutants that may be expected to be involved in homogeneous chemical transformations in indoor air. The list of this class of air pollutants is very long and includes nitrogen oxides and their radicals, oxygen, ozone, and oxygen radicals, sulfur dioxide and sulfate ions, organic and inorganic acids, and a large number of volatile organic compounds. The dynamics of surface chemistry is determined not only by the kinetics of the surface chemistry but the diffusion and sorption processes that lead reactants to the surface and products away. In the indoor air field surface chemistry has most often been modeled using the highly simplified *deposition velocity* approach (see section 2.1.1.10 of this report), even though, more complete models are available from the fields of catalysis and surface science. This section will, therefore, present an introduction to these models and present element models for the simplest cases.

Hudson classifies surface reactions into three broad classes (71):

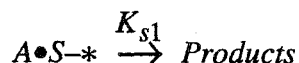
- *corrosion reactions* where the adsorbate reacts with the surface to either form volatile products, thereby consuming the surface, or a more or less stable compound – e.g., the formation of metal oxides on exposed metals,
- *crystal growth reactions* where the adsorbate is deposited on the surface extending the crystalline structure of the existing surface, and
- *catalytic reactions* where the surface does not directly react or combine with the adsorbate but, instead acts to catalyze a reaction between the adsorbate and either itself or another adsorbate.

In the indoor context corrosion and catalytic growth reactions have, possibly, important consequences – the former damaging surfaces, an especially important problem for electronic equipment, and the latter altering the chemical composition of the indoor air that may be beneficial or detrimental from a health point of view.

Here we will limit consideration to two relatively simple surface reaction mechanisms – *unimolecular decomposition* and *bimolecular interactions* – based on the introductions to the area given by Castellan and Steinfeld (14, 46).

#### Unimolecular Decomposition

The simplest surface reaction involves the sorption of a single species, say  $A$ , to an active site,  $S^*$ , bonding the species to the site,  $A \bullet S^*$ , modifying the bonding potentials of  $A$ 's electrons and thereby altering its chemical activity. The bound species may then undergo decomposition to form product compounds that may or may not be important from an indoor air quality point of view:



The rate of decomposition,  $R_A$ , may be assumed to be proportional to the mass of  $A$  sorbed on the surface:

$$R_A = -K_{s1} M_s C_s \quad (108)$$

where  $K_{s1}$  is the first order rate constant in mass units (i.e., see 2.1.1.5.),  $M_s$  is the mass of surface material involved, and  $C_s$  is the sorbed concentration of the adsorbate. The rate of generation of product species may be determined from the specific stoichiometry of the surface reaction following the same procedures used in section 2.1.1.5 for homogeneous chemistry.

If the specie's sorption is governed by a linear adsorption isotherm  $C_s = K_P C^*$ , with  $C^*$  being the near-surface air-phase concentration then the rate of decomposition will be first order with respect to this near surface air-phase concentration (i.e., assuming isothermal conditions):

$$R_A = -(K_{s1} M_s K_P) C^* \quad (109)$$

If, in addition, the rate of diffusion transport (e.g., boundary layer and porous diffusion transport) to the surface is rapid relative to the rate of reaction then the near surface concentration will approach the bulk air-phase concentration,  $C^* \approx C$ , and the rate of decomposition will be first order with respect to the bulk air-phase concentration:

$$\text{Linear Sorption; Rapid Diffusion} \quad R_A = -\left(K_{s1}M_sK_P\right)C \quad (110)$$

Under these rather restrictive conditions, then, the first order assumption of the *deposition velocity* approach is realized (see Equation 36). When diffusion transport is non-instantaneous, the surface chemistry dynamics will be spatially distributed, even though first order relative to near-surface concentrations locally and the behavior predicted by the *deposition velocity* approach will not be realized.

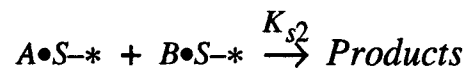
For sorption governed by other equilibrium relations the rate of decomposition will, strictly speaking, be nonlinearly dependent on near-surface concentrations, although, for all physically consistent equilibrium relations that approach linear behavior at near-zero concentration levels, first order behavior will prevail at low concentration levels. For example, the Langmuir isotherm model leads to following surface decomposition rate expression:

$$\text{Langmuir Sorption} \quad R_A = -\left(K_{s1}M_s\right)\frac{C_s^oK_L C^*}{1 + K_L C^*} \quad (111)$$

which, at low concentration levels  $K_L C^* \ll 1$ , approaches first order behavior with respect to  $C^*$  and, at high concentration levels  $K_L C^* \gg 1$ , approaches zero-order behavior. That is to say, as active sites become completely filled – *saturated* – the rate of reaction approaches a constant rate. Even this relatively simple isotherm model leads to rather complex surface decomposition kinetics; other models will introduce even more complex behavior.

### Bimolecular Interactions

A more complex surface reaction involves the sorption of two species, say *A* and *B*, to two active sites,  $S-*$ . The bound species may then react to form product compounds that may or may not be important from an indoor air quality point of view:



The rate of consumption of, say, species *A*,  $R_A$ , may be assumed to be proportional to the product of the mass of *A*,  $M_s C_{As}$ , and *B*,  $M_s C_{Bs}$ , sorbed on the surface:

$$R_A = -K_{s2}\left(M_s C_{As}\right)\left(M_s C_{Bs}\right) = -K_{s2}M_s^2 C_{As} C_{Bs} \quad (112)$$

where  $K_{s2}$  is the second order rate constant in mass units. As a bimolecular reaction, this class of reaction has all the variant special cases considered in section 2.1 for homogeneous bimolecular chemistry. Again, the rate of generation of product species may be determined from the specific



stoichiometry of the surface reaction following the same procedures used in section 2.1 .1.5 for homogeneous chemistry.

If both species' sorption is governed by a linear adsorption isotherm  $C_s = K_P C^*$ , with  $C^*$  being the near-surface air-phase concentration then the rate of decomposition will be second order with respect to the near surface air-phase concentrations (i.e., assuming isothermal conditions):

$$R_A = -\left(K_{s2} M_s^2 K_{AP} K_{BP}\right) C_A^* C_B^* \quad (113)$$

If, in addition, the rate of diffusion transport (e.g., boundary layer and porous diffusion transport) to the surface is rapid relative to the rate of reaction then the near surface concentrations will approach the bulk air-phase concentrations,  $C^* \approx C$ , and the rate of decomposition will be second order with respect to the bulk air-phase concentrations:

$$\text{Linear Sorption; Rapid Diffusion } R_A = -\left(K_{s2} M_s^2 K_{AP} K_{BP}\right) C_A C_B \quad (114)$$

For this bimolecular case, application of the Langmuir isotherm model to each reactant independently leads to following surface rate expression:

$$\text{Independent Langmuir Chemisorption } R_A = -\left(K_{s1} M_s^2\right) \left(\frac{C_{As}^o K_{AL} C_A^*}{1 + K_{AL} C_A^*}\right) \left(\frac{C_{Bs}^o K_{BL} C_B^*}{1 + K_{BL} C_B^*}\right) \quad (111a)$$

which,

- at low concentration levels  $K_{AL} C_A^* \ll 1$  &  $K_{BL} C_B^* \ll 1$ , approaches second order behavior
- at high concentration levels  $K_{AL} C_A^* \gg 1$  &  $K_{BL} C_B^* \gg 1$ , approaches zero-order behavior, and
- when one species is at a high concentration level and the other is at a low level  $K_{AL} C_A^* \ll 1$  &  $K_{BL} C_B^* \gg 1$ , assumes a first order behavior.

Alternatively, accounting for competition of sorption sites yet applying the basic Langmuir approach leads to the so-called *Langmuir-Hinshelwood* model (14):

$$\text{Langmuir -Hinshelwood Chemisorption } R_A = -\left(K_{s2} M_s^2\right) \left(\frac{C_s^o K_{AL} C_A^* K_{BL} C_B^*}{\left(1 + K_{AL} C_A^* + K_{BL} C_B^*\right)^2}\right) \quad (111b)$$

√ The use of these surface chemistry models for practical air quality analysis is certainly marginal at the present time since not one relevant surface reaction has been elucidated to the point that the mechanism is understood and the rate and sorption equilibrium constants are known – air cleaning devices employing TiO<sub>2</sub> are arguably the exception to this position. On the other hand, it is clear that surface chemistry plays a significant role in the transport of chemically active air pollutants indoors and is central to the effectiveness of some methods of air cleaning (e.g., removal of active

air pollutants using activated carbon or other chemically treated filters). Research results reported by Spicer suggest a catalytic conversion of NO<sub>2</sub> to NO on some surfaces and results reported by Ryan indicate the “deposition” of ozone on latex paints is governed by a bimolecular surface reaction with sorbed water (26, 72). These surface chemistry models could then be included in the next generation NIST IAQ Model to support research in the area.

From a numerical point of view, the inclusion of surface chemistry in the NIST IAQ Model will lead to systems of nonlinear equations for all but the special unimolecular case defined by Equations 108, 109, and 110. Consequently, implementation will require a general purpose nonlinear solution procedure. The Newton-Raphson method outlined above presents one possibility.

### 2.3.2 Applications of the Elemental Transport Equations

The elemental transport and constraint relations presented above may be assembled – e.g., as indicated in Figures 6 and 7 above – in a great variety of ways to model a number of generic transport processes. The icons associated with each section title above will be used in this section to illustrate a few of the many possibilities. In these icons:

- ● or ○ a circle indicates a *node* – i.e., a discrete spatial location within a building or building component at which pollutant species concentrations will be estimated or, more rigorously, with which a local species concentration distribution will be approximated (e.g., a node in a well-mixed chamber is associated with the magnitude of a uniform distribution of concentration in the chamber; a node of a Finite Element approximation based on linear shape functions is associated with the magnitude of a concentration distribution that varies linearly from adjacent nodes).
- ● a filled circle indicates a *capacitance node* – a node that inherently has a capacitance associated with it given the defining mass transfer relation.
- ○ an open circle indicates *zero capacitance node* – a node that does not inherently have a capacitance associated with it, given the defining relation.
- ● a gray circle indicates a *dependent, constrained, or specified node* – a node associated with concentrations that are either dependent or constrained to another node or are have values that are specified – from a mathematical point a view a node defining concentration boundary conditions rather than system degrees of freedom.
- ————— a solid line indicates a *mass transfer link* – i.e., mathematical relation that establishes the rate of transport of mass from one “node” to another
- ..... a dotted or gray line indicates a *constraint link* – i.e., a mathematical relation that establishes an algebraic constraint between linked nodal degrees of freedom (concentrations) but, importantly does not directly define a mass transfer relation.

Assemblies of the elemental relations presented above define the so-called *topology* of a given mass transport model – a graph of the (sub)system equations associated with the model that completely defines (quantitatively) the structure and (qualitatively) the character of the (sub)system equations. Given the icon descriptions above, one may anticipate two difficulties that may arise in the use of these elemental relations – the practical use of the constraint relations and zero capacitance nodes.

### 2.3.2.1 Practical Use of Constraint Relations

The equilibrium constraints presented above do not define mass transport relations by themselves, consequently, they can not be directly assembled with the elemental mass transport relations to form mass conservation equations governing the system as a whole. Instead, these equilibrium constraints allow one to express mass transport relations in terms of alternative concentration degrees of freedom.

For example, consider the simple, single-zone model with a planar sorption sheet shown below:

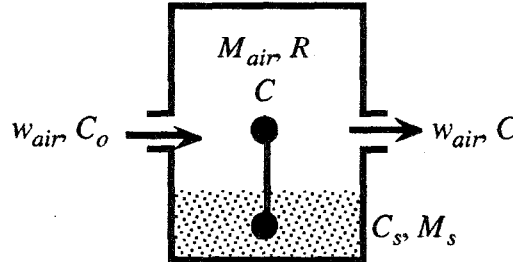


Figure 8. Simple, single-zone model with a planar sorption sheet – diffusion transport assumed to be instantaneous (“Equilibrium Adsorption Model”).

If it is assumed that diffusion transport is practically instantaneous and, therefore, sorbed concentrations  $C_s$  remains in equilibrium with the zone air-phase concentrations  $C$  – the basis of the *Equilibrium Adsorption Model* (47-49, 73) – then three equations will be associated with this model:

$$\text{Zone Mass Conservation} \quad w_{air}C + w_{ads} + M_{air} \frac{dC}{dt} = w_{air}C_o + R \quad (112)$$

$$\text{Equilibrium Constraint} \quad C_s = f(C) \text{ or } C = g(C_s) \quad (113)$$

$$\text{Sorbent Mass Conservation} \quad -w_{ads} + M_s \frac{dC_s}{dt} = 0 \quad (114)$$

where  $w_{ads}$  is the pollutant adsorption mass transport rate,  $C_o$  is the outdoor concentration, and  $R$  is the zone pollutant generation rate.

From the third equation  $w_{ads} = M_s \frac{dC_s}{dt}$  and from the sorption equilibrium constraint relation we note:

$$\frac{dC_s}{dt} = \frac{\partial(f(C))}{\partial C} \frac{dC}{dt} \quad (115)$$

Consequently:

$$w_{ads} = M_s \frac{\partial(f(C))}{\partial C} \frac{dC}{dt} \quad (116)$$

With this result the first conservation relation, Equation 112, becomes:

$$w_{air}C + \left( M_s \frac{\partial(f(C))}{\partial C} + M_{air} \right) \frac{dC}{dt} = w_{air}C_o + R \quad (117)$$

Alternatively, using the inverse equilibrium relation, Equation 117 may be rewritten in terms of the sorbed-phase concentrations as:

$$w_{air}g(C_s) + \left( M_s + M_{air} \frac{\partial(g(C_s))}{\partial C_s} \right) \frac{dC_s}{dt} = w_{air}C_o + R \quad (118)$$

That is to say, this equilibrium constraint relations allow the elimination of one conservation relation – i.e., it constrains one concentration degree of freedom to another.

For adsorption and absorption mass transport, we may impose the equilibrium constraint relations within the element-assembly framework of the NIST IAQ Model by introducing the following mass transport relations:



Adsorption mass transport from a near-surface air-phase node to an adjacent sorbent node is described by Equation 116, reproduced below:

$$w_{ads} = M_s \frac{\partial(f(C))}{\partial C} \frac{dC}{dt} \quad (119)$$


Given a solution for the near-surface air-phase concentration  $C(t)$ , the sorbed phase concentration  $C_s(t)$  may be recovered using the inverse equilibrium relation.



In a similar manner, absorption mass transport from a near-surface air-phase node to an adjacent liquid node is described by:

$$w_{abs} = M_l \hat{H} \frac{dC}{dt} \quad (120)$$

where  $M_l$  is the mass of liquid associated with the liquid node and  $\hat{H}$  is the Henry's law coefficient (see Equation 82). Given a solution for the near-surface air-phase concentration  $C(t)$ , the liquid-phase concentration  $C_l(t)$  may be recovered using the inverse equilibrium relation.

Evaporative Transport 

Evaporative mass transport introduces a new complication – loss of mass from a liquid can not be treated as a trace mass transport processes. For example, consider the simple, single-zone model with an evaporating liquid layer shown below:

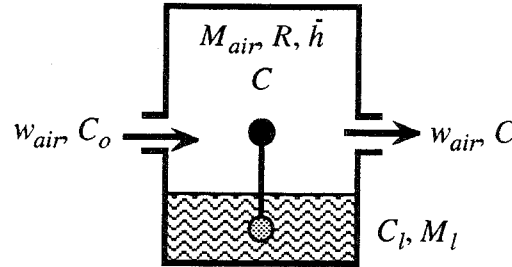


Figure 9. Simple, single-zone model with a evaporating liquid layer – boundary layer diffusion transport included.

If it is assumed that the gas-phase concentration at the liquid surface remains at the saturation value  $C_{sat}$  then three equations will be associated with this model:

$$\text{Zone Mass Conservation} \quad w_{air}C - w_{evap} + M_{air} \frac{dC}{dt} = w_{air}C_o + R \quad (121)$$

$$\text{Boundary Layer Transport} \quad w_{evap} = -\rho_{air}A_s\bar{h}(C - C_{sat}) \quad (122)$$

$$\text{Liquid Mass Conservation} \quad -w_{evap} + \frac{d(M_l C_l)}{dt} = 0 \quad (123)$$

where  $w_{evap}$  is the evaporative mass transport rate,  $M_l$  is the mass of liquid that varies with time, and  $C_l$  is the liquid concentration of the pollutant species being studied.

For a pure (single component) liquid the saturation concentration is determine independently of concentration degrees of freedom by Equation 91 as:

$$C_{A-sat} = \frac{p_{A\infty}M_A}{\rho_{air}RT} \exp\left(\frac{-\Delta H_{vap}}{RT}\right)$$

and the liquid concentration is unity  $C_l = 1.0$ . Consequently, we are left with two uncoupled equations that govern the behavior of this system:

$$w_{air}C + \rho_{air}A_s\bar{h}(C - C_{sat}) + M_{air} \frac{dC}{dt} = w_{air}C_o + R \quad (124)$$

and

$$\frac{dM_l}{dt} = -\rho_{air}A_s\bar{h}(C - C_{sat}) \quad (125)$$

To generalize: for pure liquid evaporation, the equilibrium condition Equation 91 simply establishes a boundary condition for boundary layer mass transport. The system equations would

be used to solve for the bulk air-phase concentration and the changing mass of liquid may be computed by simple direct (numerical) integration of Equation 125.

For multicomponent liquid evaporation, we must consider mass conservation of each component  $i$  as:

$$w_{air}C_i + \rho_{air}A_s\bar{h}_i(C_i - C_{sat,i}) + M_{air}\frac{dC_i}{dt} = w_{air}C_{o,i} + R_i \quad (126)$$

where (strictly) a different boundary layer mass transport coefficients must be evaluated for each component and the component saturation concentrations are coupled to all component concentrations – i.e., by Equation 94:

$$C_{i-sat} = \frac{p_{i\infty}}{\rho_{air}RT\sum_j C_{lj}/M_j} \exp\left(\frac{-\Delta H_{ivap}}{RT}\right) C_{li}$$

Practically, however, one may gain sufficient accuracy by estimating current,  $t_n$ , saturation concentrations from liquid component concentrations from a previous integration time step,  $t_{n-1}$ , as:

$$C_{i-sat}(t_n) = \frac{p_{i\infty}}{\rho_{air}RT\sum_j C_{lj}(t_{n-1})/M_j} \exp\left(\frac{-\Delta H_{ivap}}{RT}\right) C_{li}(t_{n-1}) \quad (127)$$

If this is done, then the mass conservation of each liquid component species will remain uncoupled as:

$$\frac{dM_{l,i}}{dt} = -\rho_{air}A_s\bar{h}_i(C_i - C_{sat,i}) \quad (128)$$

where  $M_{l,i}$  is the mass of liquid component  $i$ . Equations 128 may, thus, be directly integrated to determine total liquid mass and species concentrations as:

$$M_l = \sum_i M_{l,i} \quad (129)$$

$$C_{l,i} = \frac{M_{l,i}}{M_l} \quad (130)$$

### 2.3.2.2 Zero-Capacitance Nodes:

Certain assemblies may leave some system nodes without capacitance – that is to say nodes whose behavior will be defined in terms of algebraic, rather than ordinary differential, equations that will be coupled to other system nodes. If such nodes are to be allowed, the next generation version of CONTAM will need solution routines for mixed differential and algebraic equations.

This problem can quite naturally arise at near-surface nodes associated with a boundary layer. For example, the filter cell idealization shown above in Figures 7 includes a near-surface air-phase

node for which species mass conservation is described in terms of an algebraic equation (see (56) for details).

When mass conservation for an *algebraic* node is defined by a linear algebraic relation, the node may be algebraically eliminated. When a nonlinear algebraic relation is involved this may prove difficult. Alternatively, one may formulate models in such a way as to avoid a zero capacitance node.

### 3. SOLUTION OF SYSTEM EQUATIONS

This section will briefly consider methods to solve system equations assembled from the proposed new mass transport elements and note special structural characteristics of these system equations that may lead to computational strategies that minimize computational effort and storage requirements.

#### 3.1 Solution Methods

The new mass transport elements introduced in section 2. of this report differ from those currently available in the NIST IAQ Model in three critical respects:

- *Nonlinearities* Several of the proposed elements are based on nonlinear formulations (i.e., the mass transport/transformation being modeled depends nonlinearly on system concentration degrees of freedom). When assembled to form system equations, the resulting system equations will be nonlinear as well.
- *Stiffness*: The use of several of the proposed elements will result in system equations that may prove to be very *stiff*. That is to say, at any instant in time the eigen values corresponding to the current state of the system equations may have values differing by several orders of magnitude. As a result, the garden variety equation solving techniques will demand integration step sizes so small as to be impractical – so-called *stiff* equation solvers will be needed.
- *Algebraic Equations*: As presented, some of the proposed elements may introduce algebraic equations that will be coupled to the (more common) ordinary differential equations governing the behavior of the systems being studied.

The earlier generations of CONTAM have used, by numerical standards, first or second generation equation solving techniques that are relatively easy to understand and implement. The proposed elements will introduce truly significant numerical challenges, consequently the time has arrived to turn to the specialist in the field for guidance. A useful and, apparently, up-to-date reference is the new edition of J. Stoer and R. Bulirsch's *Introduction to Numerical Analysis: Second Edition* translated by R. Bartels, W. Gautschi, and C. Witzgall (importantly, of NIST's Center for Applied Mathematics) (74) – a reference that is hardly introductory by most standards.

Stoer and Bulirsch distinguish the following general types of ordinary differential equations (using notation and sign conventions consistent with the systems considered in this report) ordered in terms of general difficulty to solve:

$$\text{Linear Explicit Systems} \quad \frac{d\{C\}}{dt} = [A]\{C(t)\} + \{F(t)\} \quad (131)$$

$$\text{Linear Implicit Systems} \quad [M]\frac{d\{C\}}{dt} = -[K]\{C(t)\} + \{E(t)\} \quad (132)$$



$$\text{Linear-implicit Nonlinear Systems} \quad [M] \frac{d\{C\}}{dt} = \{G(t, C(t))\} \quad (133)$$

$$\text{Quasilinear-implicit System} \quad [M(C)] \frac{d\{C\}}{dt} = \{G(t, C(t))\} \quad (134)$$

Importantly, the solution of quasilinear-implicit type of system “is still the subject of research,” (74) page 495. In addition, mixed systems of differential and algebraic equations may also be encountered.

The current and earlier versions of CONTAM assembles linear element equations to form linear implicit system equations of the form shown above:

$$[M] \frac{d\{C\}}{dt} = -[K]\{C(t)\} + \{E(t)\} \quad (135)$$

where  $[M]$  is the contaminant capacitance matrix,  $[K]$  is the contaminant concentration matrix,  $\{E(t)\}$  is the contaminant *excitation* vector (e.g., due to internal sources and contaminant infiltration), and  $\{C(t)\}$  are the nodal concentration degrees of freedom. For these versions of CONTAM, the concentration capacitance matrix has been a diagonal matrix so, in principle, the transformation of Equation 135 to the linear explicit would be trivial:

$$\frac{d\{C\}}{dt} = -[M]^{-1}[K]\{C(t)\} + [M]^{-1}\{E(t)\} \quad (136)$$

The proposed new mass transport elements may be implemented in a number of different ways so as to result in system equations of one or another of these general forms. It is, therefore, strategic to avoid the more challenging forms. As discussed in section 2.3.2.1 and 2.3.2.2, it should be possible to limit element formulations to mass transport relations and to avoid zero capacitance nodes so as to avoid algebraic equations. If this is accomplished, yet all other possibilities are admitted we would, in general, need to solve system equations of the following form:

$$[M(C(t))] \frac{d\{C\}}{dt} = -[K(C(t))]\{C(t)\} + \{E(t, C(t))\} \quad (137)$$

The nonlinear contributions to the capacitance matrix would result from the modeling sorption transport to sorbents characterized by nonlinear sorption equilibrium behavior (isotherms).

By limiting element equations (e.g., for 1D diffusion) to lumped mass formulations and thus obtaining diagonal capacitance matrices, we may avoid this difficult class of differential equation and address instead the better understood explicit nonlinear form:

$$\frac{d\{C\}}{dt} = -[\text{diag}(M(C(t)))]^{-1}[K(C(t))]\{C(t)\} + [\text{diag}(M(C(t)))]^{-1}\{E(t, C(t))\} \quad (138)$$

For the types of problems that will be considered when using the proposed new mass transport elements, however, the system equations may be expected to be very stiff.

Stoer and Bulirsch review relatively recent methods to solve stiff differential equations of the explicit nonlinear form (technically, their discussion is related to a close cousin of this form the *autonomous form*) and note two important requirements:

- to assure stability the method must be *absolutely stable* – as defined mathematically – which forces one to choose implicit or semi-implicit methods,
- to maximize computational efficiency the method must include automatic time stepping.

Ironically, these authors use one of the chemical kinetics problem addressed above in section 2.1.1 – the decomposition of ozone to oxygen – as an example of a stiff system.

Quoting directly from Stoer and Bulirsch, (74) page 491:

“Taking A-stability into account, one can then develop one-step, multistep, and extrapolation methods .... All these methods are implicit or semi-implicit, since only these methods have the proper rational stability function. All explicit methods considered earlier ... cannot be A-stable. The implicit character of all stable methods for solving stiff differential equations implies that one has to solve a linear system of equations in each step at least once (semi-implicit methods), sometimes even repeatedly, resulting in Newton-type iterative methods. In general, the [solution] matrix ... of these linear equations contains the Jacobian matrix....”

The implicit solution method used in the single-zone example of section 2.1.1.8., based on the so-called generalized trapezoid rule for integration with Newton-Raphson integration applied at each integration time step provides an example of such a, A-stable implicit method. Importantly, this example demonstrates that the system Jacobian may be directly assembled from elemental contributions. This method did not include, however, automatic time stepping.

At this point in time it would seem most appropriate to follow the recommendations of Stoer and Bulirsch and investigate the use of one of the methods they proposed. The one-step method developed by Kaps and Rentrop “are distinguished by a simple structure, efficiency, and robust step control” (74) page 491 appears to be a particularly attractive candidate. As in the example presented in section 2.1.1.8, the system Jacobian used in this particular method may be directly assembled from elemental contributions.

Press, Teukolsky, Vetterling, and Flannery, in the second edition of their very useful *Numerical Recipes in C* (75), recommend the Kaps and Rentrop algorithm (identified as one instance of a *Rosenbrock Method*), using, however, a set of algorithm parameters developed by Shampine. Press, et al. provide C routines implementing their preferred variant of the Kaps/Rentrop method as well as practical advice in its use (see pages 738-742 of (75)). These authors imply that semi-implicit extrapolation methods may be more appropriate for larger systems and/or higher accuracy and provide C routines and advice for these methods as well (see pages 742-747 of (75)).

Within the routines offered by Press et al., LU decomposition is used to solve the linearized system equations within each time step. For large sparse systems, the LU decomposition routines (i.e., ludcmp and lubksb) should be replaced by appropriate sparse matrix procedures. These authors, again, provide guidance – see section 2.7 of (75). An interesting approach that should be considered for larger problems is the *biconjugate gradient method* presented on pages 84 to 89 of (75) – this iterative method is unique in that it may be applied to systems that are not necessarily symmetric, positive definite systems<sup>5</sup>.

√ It is difficult to make specific recommendations with great confidence here. Nevertheless, it would seem reasonable to consider employing the following C routines provided by Press et al.:

- stiff – the Kaps/Rentrop algorithm using Shampine’s parameters (see pages 738-742 of (75)), with the equation solving routines ludcmp and lubksb replaced by:
- linbcg – the iterative biconjugate gradient method (see pages 84-89 of (75)) to solve the linearized system equations within each time step using
- the indexed storage routines for sparse systems also supplied by Press et al. (see pages 78-83 of (75)).

Press et al. have developed their various equation solving routines to be “plug-compatible” to facilitate the use of alternative routines. Using this “plug-compatibility” the solution phase may, in principle, be directed to one of several solvers depending on the nature of the system assembly. For the next generation of CONTAM, the use of nonlinear elements or components may be readily monitored so that, in principle, a nonlinear or linear solver may be selected as appropriate. Practically, however, the Kaps/Rentrop algorithm may be applied to both linear or nonlinear systems – the latter demanding iteration within each time step and the former not. Furthermore, the stiffness of a given assembly – linear or nonlinear – will not be readily evident so, again, to be safe a stiff solution method such as the Kaps/Rentrop algorithm should be used. Within the Kaps/Rentrop algorithm, however, it may be strategic to use a direct (linear) equation solver for small systems and the proposed implicit one for larger systems.

### 3.2 Structure of System Equations

Given the diagonal form of the capacitance matrix, the structure of the conductance matrix alone becomes relevant when considering the structure of the system equations and its impact on storage and solution time requirements. The discussion of section 2.3.3 applies generally to system equations assembled from the proposed mass transport elements with a single caveat – (nonlinear) equilibrium constrained convection diffusion between building zones will not be admitted. That is

---

<sup>5</sup> Press et al. note that a variant of this method for symmetric but non-positive definite systems “has been generalized in various ways for unsymmetric matrices” but the citations noted have not been investigated.

to say, assemblies of any or all the proposed new mass transport elements will couple intra-zone degrees of freedom only – providing we do not allow convection diffusion transport through adsorbents separating zones so that the system transport matrix can be expressed as the sum of a zone-zone dilution transport contribution and an (intra) zone contribution as given in Equation 50 and reproduced here:

$$[K] = \begin{bmatrix} [K_{dil}] & 0 & 0 & [K_{dil}] & \dots & 0 \\ 0 & [K_{dil}] & 0 & 0 & \dots & 0 \\ 0 & 0 & [K_{dil}] & 0 & \dots & [K_{dil}] \\ 0 & [K_{dil}] & 0 & [K_{dil}] & \dots & 0 \\ \vdots & \vdots & \vdots & \vdots & \ddots & \vdots \\ 0 & 0 & 0 & 0 & \dots & [K_{dil}] \end{bmatrix} + \begin{bmatrix} [K_{zone}] & 0 & 0 & 0 & \dots & 0 \\ 0 & [K_{zone}] & 0 & 0 & \dots & 0 \\ 0 & 0 & [K_{zone}] & 0 & \dots & 0 \\ 0 & 0 & 0 & [K_{zone}] & \dots & 0 \\ \vdots & \vdots & \vdots & \vdots & \ddots & \vdots \\ 0 & 0 & 0 & 0 & \dots & [K_{zone}] \end{bmatrix}$$

providing, system degrees of freedom are numbered in the order discussed in section 2.3.3.

The dilution contribution will be linear while the zone contribution will include nonlinearities if any of the nonlinear element types are employed. That is to say, system nonlinearities will be isolated to the zone matrices of the block-diagonal zone conductance contribution and will, therefore, have a relatively limited bandwidth. Furthermore, updating the system Jacobian will involve only these block-diagonal zone contributions and will, in general, be limited to just a few degrees of freedom within each individual zone conductance matrix.

## 4. USER INTERFACE STRATEGIES

To implement the proposed new mass transport elements and components it will be necessary to devise additional user interface conventions to complement those presently established by the current generation of the CONTAM program – CONTAM93/94. Currently, to communicate input CONTAM93/94 uses a graphic user interface called a *sketchpad* to, in essence, define the *topology*<sup>6</sup> of a given building idealization and *data entry screens* to associate data with individual icons of the sketchpad diagram. In many instances a cascade of several data screens are associated with a given icon of the sketchpad diagram that are organized in a tree-like hierarchy with the *root* data screen directly associated with the icon. In some instances, the data entry screens support graphical input of data or graphical representation of input data (e.g., for operation schedules). To communicate computed results to the user, CONTAM again provides both a graphical representation of results on a sketchpad diagram of the building and cascades of data screens that provide both tabular data and plotted results.

Additional interface conventions will need to be developed for each of the three general areas considered in this report – homogeneous chemistry, aerosol transport and fractional particle filtration, and heterogeneous processes.

### 4.1 Homogeneous Chemistry

Section 2.1.1.11 of this report outlines the basic input data that would be required to define homogeneous chemical reactions within building zones. Two reasonable alternatives should be considered for the specification of this chemistry – definition at the project level or at the zone level of data input.

#### 4.1.1 Project-Level Definition

The general reaction rate expressions summarized in Table 2 above are expressed in terms of the product of a) the mass of air in a given zone  $M_{air}$ , b) a rate “constant”  $K_0$ ,  $K_1$ , or  $K_2$ , and c) the product of zero or more (current) zone concentrations. Furthermore, for realistic modeling a given homogeneous chemical reaction should be expected to occur in each and every zone of a building idealization. Consequently, reactants, products, stoichiometry, and rate “constants” could be defined at the project level for all zones for each of the reactions to be modeled. Rates of transformation would then be computed specifically for each zone given  $M_{air}$ .

The specification of rate “constants” introduces a few complications. Temperature-dependent rate “constants” could also be defined generally at the project level and evaluated for each specific zone during computation given either specified zone temperature schedules or computed zone

---

<sup>6</sup> *Topology* here is the geometric configuration of a given assembly of elements and/or components used to idealize a given building/HVAC system including the relative position of these elements or components and their connectivity (e.g., as defined by discrete airflow paths).



temperatures (i.e., for a future generation version of CONTAM that models the coupled thermal-airflow problem). Photolytic rate constants depend on discretely defined distributions of absorption cross-sections, quantum yields, and actinic irradiance density. The first two distributions may, again, be input at the project level for all zones in general. The actinic irradiance density depends on the illumination level and spectral distribution – which may be expected to vary from zone to zone and with time – thus, this should be specified uniquely for each zone in terms of time schedules.


Specified and dependent concentrations add another wrinkle. As discussed in Section 2.1.1.9, it would be most convenient to allow:

- a) the specification of specific outdoor concentration time histories (i.e., boundary conditions for the independent concentration degrees of freedom) as constants or discrete time histories (e.g., for O<sub>2</sub>, N<sub>2</sub>, CO<sub>2</sub>, O<sub>3</sub>, NO, NO<sub>2</sub>, etc.),
- b) the specification of other outdoor concentrations in terms of these boundary conditions (e.g., the specification of algebraic relations resulting from PSSA approximations),
- b) the specification of specific indoor concentration time histories as constants or discrete time histories (e.g., for H<sub>2</sub>O), and/or
- c) the specification of dependent indoor concentration in terms of computed independent zone concentrations (e.g., the specification of algebraic relations resulting from PSSA approximations).

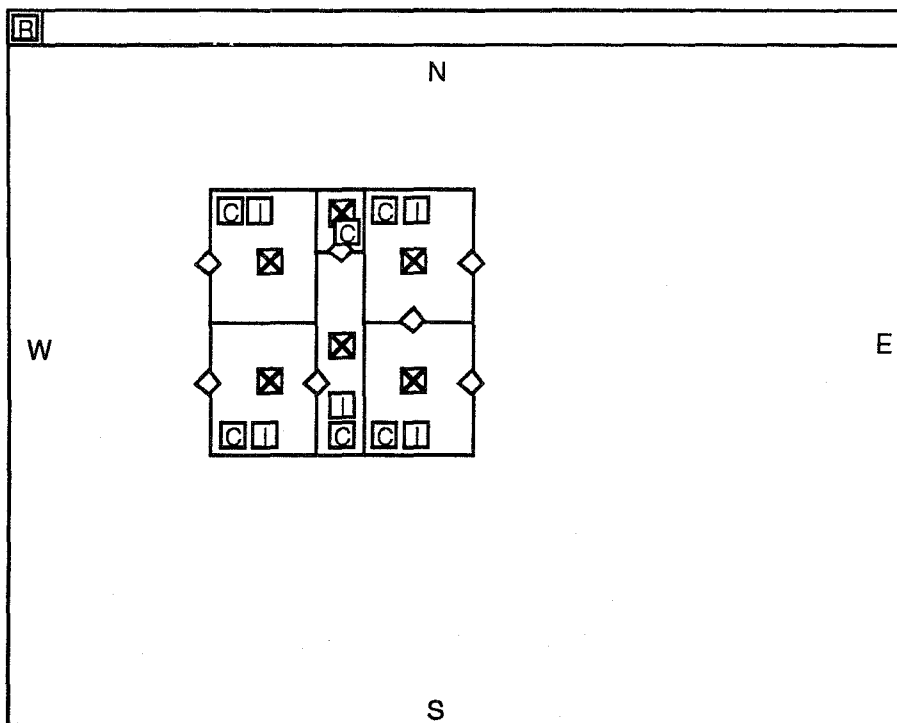
To achieve these objectives, a distinction should be made between independent and dependent concentration degrees of freedom at the project level. That is, when specifying the contaminants to be included in a given analysis, the user should be asked to distinguish independent and dependent concentration degrees of freedom. The specification of outdoor (independent) concentrations, presently provided for in CONTAM93/94, should be extended to allow the specification of dependent outdoor concentrations in terms of these independent concentrations. Finally, the user should be able to specify either dependent concentration time histories or equations defining the dependency of dependent concentrations on the computed (independent) zone concentrations.




To maintain a graphical link between icons on the sketchpad and the associated data screens icons should be provided for the following:



-  An icon associated with the general, project-level specification of reactions to be considered. This icon has a double box to distinguish it from icons associated with a specific location in the sketchpad diagram. Reasonably, project-level icons could be arranged along one edge (e.g., the top edge) of the sketchpad window to graphically distinguish them from the building diagram.
-  An icon associated with the specification of time schedules of actinic irradiance density discrete distributions.


-  An icon associated with the specification of independent concentration time histories or their dependency on dependent concentration degrees of freedom. This icon would be automatically placed in the outdoor “zone” waiting for user definition and could be placed by the user in (selected) building zones as required.

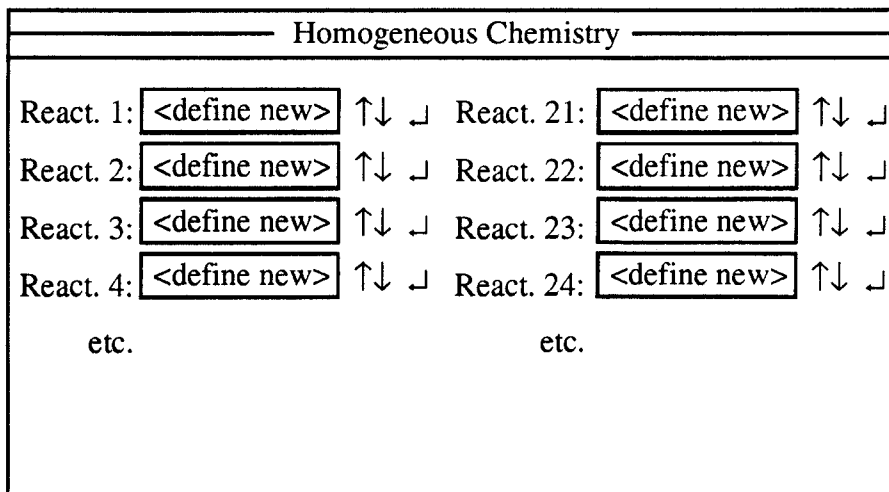
A representative sketchpad diagram including these icons is shown below:



The  icon at the upper left indicates homogeneous chemistry has been defined. The  icons in selected zones indicate actinic irradiance density has been defined for these zones; its absence in some zones indicates the zero actinic irradiance. The  icons in indoor and the outdoor zones provides the link to data screens used to specify dependent concentrations.

In most instances dependent concentration relations (e.g., PSSA approximations) may be expected to defined identically in all zones. For this reason, it may be strategic to allow definition of these relations globally – i.e., at the project-level, perhaps through the introduction of a  icon – leaving the  icon to be associated only with specification of concentration time histories for both dependent and, possibly, independent concentrations in selected zones.

“Selecting” the  icon would “open” a root data screen for reaction definitions. This root screen would reasonably provide a summary of the reactions that have been defined allowing on the order of 25 to 50 distinct elementary reactions and would allow either selection from a list of standard elementary reactions ( $\uparrow\downarrow$ ) or definition of new reactions ( $\rightarrow$ ) as suggested by the data screen shown below:




If the user selects to define a new reaction he/she would then enter a cascade of data screens organized as outlined in Section 2.1.1.11 of this report.

#### 4.1.2 Zone-Level Definition

As presented, homogeneous chemistry is limited to well-mixed zones, consequently this chemistry could be defined uniquely for each zone. A single icon placed within a zone could indicate the modeling of this chemistry within a given zone. While this approach allows greater flexibility, it will generally require unnecessary duplication of input and contribute to the congestion of icons on sketchpad diagrams. Alternatively, homogeneous reactions could be defined globally as in Section 4.4.1 and turned on or off selectively through the use of the zone icon.

### 4.2 Aerosol Transport and Fractional Particle Filtration

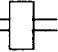

The interface for aerosol transport will demand first the specification of the aerosol representation – the number of size fraction bins and their particle size limits (i.e., within the constraint of Equation 49). Reasonably this specification should be done globally and could be associated with a project-level icon, say, . Here the users should be able to select to represent the distribution in terms of  $N_j$ ,  $C_j$ ,  $C_j$ , or  $V_j$  (see Section 2.2.1).

#### 4.2.1 Fractional Particle Filtration

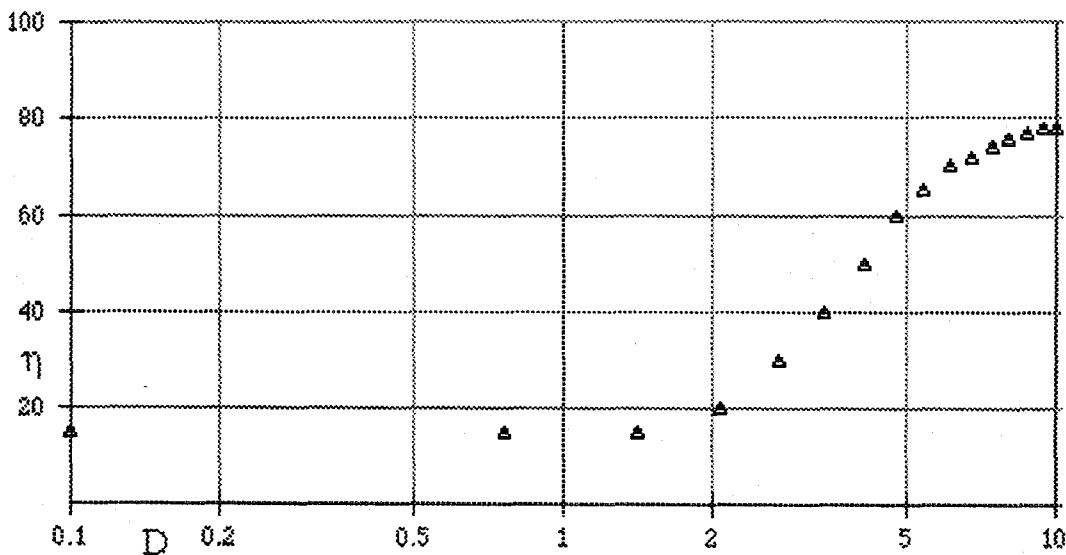
As presented in Section 2.2.3, two approaches to modeling fractional particle efficiencies are available – an empirical approach based on measured fractional particle efficiencies of filters and a theoretical model that is appropriate for fibrous filters. Not discussed in this report, are theoretical models for particle deposition in narrow flow paths that effectively act as filters. As presently implemented, CONTAM93/94 allows the user to specify single filter efficiency values to all discrete flow paths. For those cases where an aerosol is specified globally, then reasonably fractional particle efficiencies would have to be specified for all filters. The addition of duct modeling tools in the next generation of CONTAM provides another means to specify particle



filtration. To avoid redundancy and to improve the correspondence between the actual building/HVAC system and the CONTAM idealization, I would propose the following:


-  A filter icon, available in the set of icons used to define duct systems, that, when selected, allows direct specification of the distribution of filter efficiencies or the specification of theoretical model parameters for the fibrous filter model.
-  A flow path icon shaded to indicate it acts as a filter that, when selected, allows direct specification of the distribution of filter efficiencies or the specification of theoretical model parameters for the particle deposition model.

Direct specification of fractional particle efficiencies should be supported by either (or both) graphical representation of tabular input or direct graphical input (i.e., by “clicking” data on a graph). Following the standard convention, this data should be represented on a semi-log plot of efficiency versus particle diameter in the range of 0.1  $\mu\text{m}$  to 10  $\mu\text{m}$  as shown below:



For the near future a single distribution as shown may be sufficient. For more refined analysis, distributions at different filter face velocities and at different loadings may be necessary with CONTAM linearly interpolating between values automatically during computation.

#### 4.2.2 Aerosol Deposition

Aerosol deposition is most reasonably defined uniquely for each zone. This could be achieved by either using the current zone icon or a new deposition icon, say,  to access appropriate data screens. The former choice avoids screen clutter, the latter makes the modeling of deposition evident. In either case, the associated data screens should allow either the direct specification of deposition velocities for each size bin or the implementation of Nazaroff's deposition models. Surface areas would have to be associated with each deposition distribution, if the former path is taken, or, for the Nazaroff models, the orientation of the surface models would have to be specified.


### 4.2.3 Coagulation

Coagulation is an homogeneous process, not unlike homogeneous chemistry, that is described generally for all zones and made specific to a zone by the scaling parameter of the mass of the air in the zone  $M_{air}$  (i.e., see Equation 64). Consequently, the user need do no more than specify the aerosol representation to effect coagulation modeling.

### 4.2.4 Aerosol Source Models

Aerosols may be generated within a zone due to in-zone occupant activity, due to resuspension resulting from cleaning, for example, or due to tracking of dust from one zone to another. Naive empirical models have been proposed for these sources that have not been considered in this report – possibly these models could be used here. Alternatively, the user may simply specify time histories of aerosol generation rates, by fraction sizes, in much the same way that (molecular) sources are now specified.

## 4.3 Heterogeneous Processes

The heterogeneous processes discussed in Section 2.3 of this report are unique in that spatial discretization at the microscopic level is associated with the models of the processes considered. Furthermore, heterogeneous transport is inherently zone-specific. For these reasons, it may be reasonable to provide an icon, say  , that provides the user with the means to access a *micro-sketchpad* – as if zooming in on a zone surface to view the microscopic character of the surface. At the *micro-sketchpad* level the user may be offered a choice of standard heterogeneous models – e.g., evaporation or sublimation from a single component reservoir, one of three Axley sorption transport models, etc. – or the ability to define a unique 1D spatial discretization similar to those represented in Figures 2, 3, 6, 7, 8, and 9 of this report. General finite element analysis programs provide models for accomplishing the latter.

For the modeling of gas-phase air cleaning devices based on microscopic models of heterogeneous transport processes, it would be best for most users to be able to simply select from a library of device components. CONTAM, would therefore, assume the responsibility to automatically choose an appropriate spatial discretization and provide the user with appropriate response results (i.e., supply and exhaust concentrations of the device rather than internal, spatially distributed concentration results).

As the approach to modeling heterogeneous processes is unusual, if not innovative, the application of the proposed elemental models to various heterogeneous processes will have to be more exploratory and, consequently, the development of interfaces to support these process models will have to follow these explorations.

## REFERENCES

1. Seinfeld, J., *Atmospheric Chemistry and Physics of Air Pollution*. 1986, New York: John Wiley.
2. Finlayson-Pitts, B.J. and J.N.J. Pitts, *Atmospheric Chemistry: Fundamentals and Experimental Techniques*. 1986, New York: John Wiley & Sons.
3. Atkinson, R., A.M. Winer, and J.N.J. Pitts, *Estimation of Nighttime N<sub>2</sub>O<sub>5</sub> Concentration from Ambient NO<sub>2</sub> and NO<sub>3</sub> Radical Concentrations and the Role of N<sub>2</sub>O<sub>5</sub> in Night-time Chemistry*. *Atmospheric Environment*, 1986. **20**(2): p. 331-339.
4. Atkinson, R., *Kinetics and Mechanisms of the Gas-Phase Reactions of the NO<sub>3</sub> Radical with Organic Compounds*. *Journal of Physical and Chemical Reference Data*, 1991. **Vol 20**(No. 3): p. pp. 459-507.
5. Weschler, C.J., H.C. Shields, and D.V. Naik. *Interplay Among Ozone, Nitric Oxide and Nitrogen Dioxide in an Indoor Environment: Results from Synchronized Indoor-Outdoor Measurements*. in *IAQ '93: The 6th International Conference on Indoor Air Quality and Climate*. 1993. Helsinki, Finland.
6. Nazaroff, W.W. and G.R. Cass, *Mathematical Modeling of Chemically Reactive Pollutants in Indoor Air*. *Environmental Science and Technology*, 1986. **Vol. 20**(No. 9): p. pp. 924-934.
7. Salmon, L.G., *et al.*, *Nitric Acid Concentrations in Southern California Museums*. *Environmental Science and Technology*, 1990. **24**(7): p. 1004-1013.
8. Axley, J.W., J.B. Peavey, and A. Hartzell. *Homogeneous and Heterogeneous Processes in the Transport of Outdoor Air Pollution Indoors*. in *Indoor Air Quality Problems - From Science to Practice*. 1993. Warsaw, Poland.
9. Weschler, C.J., H.C. Shields, and D.V. Naik, *Indoor Chemistry Involving O<sub>3</sub>, NO and NO<sub>2</sub> as Evidenced by 14 Months of Measurements at a Site in Southern California*. (submitted to) *Environmental Science and Technology*, 1994.
10. Weschler, C.J., H.C. Shields, and D.V. Naik, *Fourteen Months of Ozone and Oxides of Nitrogen Measurements at a Telecommunications Office in Southern California*, . 1993, Bellcore, Redbanks, NJ.
11. Liang, C.S.K. and J.M. Waldman, *Indoor Exposures to Acidic Aerosols at Child and Elderly Care Facilities*. *Indoor Air: International Journal of Indoor Air Quality and Climate*, 1992. **Vol. 2**(No. 4): p. pp. 196-207.
12. Spengler, J.D., *et al.*, *Nitrous Acid in Albuquerque, New Mexico, Homes*. *Environmental Science and Technology*, 1993. **Vol. 27**(No. 5): p. pp. 841-845.
13. Brauer, M., *et al.*, *Nitrous Acid Formation in an Experimental Exposure Chamber*. *Indor Air*, 1993. **1993**(3): p. pp. 94-105.
14. Steinfeld, J.I., J.S. Francisco, and W.L. Hase, *Chemical Kinetics and Dynamics*. 1989, Englewood Cliffs, New Jersey: Prentice-Hall, Inc. 548 pages.
15. Verwer, J.G. and M. van Loon, *NOTE: An Evaluation of Explicit Pseudo-Steady-State Approximation Schemes for Stiff ODE Systems from Chemical Kinetics*. *Journal of Computational Physics*, 1994. **Vol. 113**: p. pp. 347-352.
16. Yamamoto, T., *et al.* *Fast Direct Solution Methods for Multizone Indoor Model*. in *Building Systems: Room Air and Air Contaminant Distribution*. 1989. Allerton House, University of Illinois at Urbana-Champaign: ASHRAE.
17. Weschler, C.J., M. Brauer, and P. Koutrakis, *Indoor Ozone and Nitrogen Dioxide: A Potential Pathway to the Generation of Nitrate Radicals, Dinitrogen Pentoxide, and Nitric Acid Indoors*. *Environmental Science and Technology*, 1992. **Vol. 26**: p. pp. 179-184.

18. Axley, J.W., J.P. Peavey, and A.L. Hartzell, *Transport Of Reactive Gas Phase Outdoor Air Pollutants Indoors*. Indoor Environment, 1994. (submitted for publication).
19. Nazaroff, W.W., *MIAQ4 --- A Model for Airborne Pollutants in Buildings*, . 1988, Nazaroff, William W.: Pasadena, CA & Berkeley, CA.
20. Cano-Ruiz, J.A., *et al.*, *Removal of Reactive Gases at Indoor Surfaces: Combining Mass Transport and Surface Kinetics*. Atmospheric Environment, 1993. Vol. 27A(No. 13): p. pp. 2039-2050.
21. Gadgil, A.J., D. Kong, and W.W. Nazaroff, *Deposition of Unattached Radon Progeny Under Natural Convection: Effect of Progeny Lifetimes*, . 1991, LBL Indoor Environment Program.
22. Nazaroff, W.M. and G.R. Cass, *Mass Transfer Aspects of Pollutant Removal at Indoor Surfaces*. Environment International, 1989. Vo. 15: p. pp. 567-584.
23. Nazaroff, W.W., A.J. Gadgil, and C.J. Weschler. *Critique of the Use of Deposition Velocity in Modeling Indoor Air Quality*. in *ASTM Symposium on Modeling of Indoor Air Quality and Exposure, April 27-28, 1992*. 1992. Pittsburg, PA.
24. Nazaroff, W.W., D. Kong, and A.J. Gadgil, *Numerical Investigations of the Deposition of Unattached <sup>218</sup>Po and <sup>212</sup>Pb from Natural Convection Enclosure Flow*. Journal of Aerosol Science, 1992. Vol. 23(No. 4): p. pp. 339-353.
25. Scott, A.G. *Radon Daughter Deposition Velocities Estimated from Field Measurements*. in *Health Physics*. 1983. U.S.A.: Pergamon Press.
26. Spicer, C.W., R.W. Coutant, and G.F. Ward, *Investigation of Nitrogen Dioxide Removal From Indoor Air*. 1986, Chicago, Ill: Gas Research Institute: GRI-86/0303.
27. Weschler, C.J., *Predictions of Benefits and Costs Derived from Improving Indoor Air Quality in Telephone Switching Offices*. Indoor Air: International Journal of Indoor Air Quality and Climate, 1990. Vol. 0(No. 0): p. pp. 23-36.
28. Harris, G.W., *et al.*, *Observations of Nitrous Acid in the Los Angeles Atmosphere and Implications for Predictions of Ozone-Precursor Relationships*. Environmental Science and Technology, 1982. 16(7): p. 414-419.
29. Coutant, R.W., *et al. (DRAFT) Control of Indoor NO2 and Nitrogen Acids*. in *IAQ '94 Engineering Indoor Environments*. 1994. St. Louis, Mo: ASHRAE.
30. Nazaroff, W.M. and G.R. Cass. *Mass Transfer Aspects of Pollutant Removal at Indoor Surfaces*. in *Indoor Air '87*. 1987. West Berlin: Institute for Water, Soil, and Air Hygiene, Berlin.
31. Nazaroff, W.W. and G.R. Cass, *Mathematical Modeling of Indoor Aerosol Dynamics*. Environ. Sci. Technol., 1989. Vol. 23(No. 2): p. pp. 157-166.
32. Nazaroff, W.W., L.G. Salmon, and G.R. Cass, *Concentration and Fate of Airborne Particles in Museums*. Environmental Science and Technology, 1989. Vol. 24(No. 1): p. pp. 66-77.
33. Nazaroff, W.W., *et al.*, *Predicting Regional Lung Deposition of Environmental Tobacco Smoke particles*. Aerosol Science and Technology, 1993. Vol. 19: p. pp. 243-254.
34. Nazaroff, W.W., *et al.*, *Particle Deposition in Museums: Comparison of Modeling and Measured Results*. Aerosol Science and Technology, 1990. Vol. 13: p. pp. 332-348.
35. Dennis, R., ed. *Handbook on Aerosols*. . 1976, National Technical Information Service: Springfield, VA. pages 142.
36. van de Hulst, H.C., *Light Scattering by Small Particles*. 1981, New York: Dover Publications, Inc. 470 pages.

37. Friedlander, S.K., *Smoke, Dust and Haze: Fundamentals of Aerosol Behavior*. 1977, New York: John Wiley & Sons. 317 pages.
38. Fuchs, N.A., *The Mechanics of Aerosols*. 1964, New York: Dover Publications, Inc.
39. Hinds, W.C., *Aerosol Technology: Properties, Behavior, and Measurement of Airborne Particles*. 1982, New York: John Wiley & Sons.
40. Hanley, J.T., D.D. Smith, and D. Ensor. *Fractional Aerosol Filtration Efficiency of Air Cleaners*. in *Indoor Air '93: Proceedings of the 6th International Conference on Indoor Air Quality and Climate*. 1993. Helsinki, Finland: Indoor Air '93, Helsinki.
41. Hirvonen, A., et al., *Thermal Desorption of Organic Compounds Associated with Settled House Dust*. *Indoor Air*, 1994. Vol. 4(No. 4): p. pp. 255-264.
42. Wolkoff, P. and C.K. Wilkins, *Indoor VOCs from Household Floor Dust: Comparison of Headspace with Desorbed VOCs; Method for VOC Release Determination*. *Indoor Air*, 1994. Vol. 4(No. 4): p. pp. 248-254.
43. White, F.M., *Heat and Mass Transfer*. 1988, New York: Addison-Wesley Pub. Co. 718 pages.
44. Yang, R.T., *Gas Separation by Adsorption Processes*. Butterworths Series in Chemical Engineering, ed. H. Brenner. 1987, Boston: Butterworths. 352 pages.
45. Noll, K.E., V. Gounaris, and W.-S. Hou, *Adsorption Technology for Air and Water Pollution Control*. 1992, Chelsea, Michigan: Lewis Publishers, Inc. 347 pages.
46. Castellan, G.W., *Physical Chemistry*. Third Edition ed. 1983, Menlo Park, CA: Benjamin/Cummings Publishing Co., Inc. 944 pages.
47. Axley, J.W. and D.M. Lorenzetti. *Sorption Transport Models for Indoor Air Quality Analysis*. in *ASTM Symposium on Modeling Indoor Air Quality and Exposure*. 1992. Pittsburg, PA: American Society for Testing and Materials.
48. Axley, J.W. *Reversible Sorption Modeling for Multi-Zone Contaminant Dispersal Analysis*. in *Building Simulation '91, August 20-22, 1991*. 1991. Nice - Sophia Antipolis, France: IBPSA: International Building Performance Simulation Association.
49. Axley, J.W., *Adsorption Modeling For Building Contaminant Dispersal Analysis*. *Indoor Air: International Journal of Indoor Air Quality and Climate*, 1991. Vol. 1(No. 2): p. pp. 147-171.
50. Axley, J.W., *Adsorption Modeling for Macroscopic Contaminant Dispersal Analysis*, . 1990, National Institute of Standards and Technology.
51. Borrazzo, J.E. and C.I. Davidson. *Sorption of Organic Vapors to Indoor Surfaces of Synthetic and Natural Fibrous Materials*. in *Indoor Air '90: The 5th International Conference on Indoor Air Quality and Climate*. 1990. Toronto, Canada: Canada Mortgage and Housing Corporation.
52. Liu, R.-T. *Removal of Volatile Organic Compounds in IAQ Concentrations with Short Bed Lengths*. in *Indoor Air '90: The 5th International Conference on Indoor Air Quality and Climate*. 1990. Toronto, Canada: Canada Mortgage and Housing Corporation.
53. Borrazzo, J.E. and C.I. Davidson. *The Influence of Sorption to Fibrous Surfaces on Indoor Concentrations of Organic Vapors*. in *Eighty-third Annual Meeting of the Air and Waste Management Association*. 1990. Pittsburg, PA.
54. Seifert, B. and H.J. Schmahl. *Quantification of Sorption Effects for Selected Organic Substances Present in Indoor Air*. in *Indoor Air '87*. 1987. West Berlin: Institute for Water, Soil, and Air Hygiene, Berlin.
55. Shen, T. and D.H. Wang, *Chapter XIII Application of Potential Theory for Gas Adsorption Systems*, in *Adsorption Technology for Air and Water Pollution Control*, K.E. Noll, V.

- Gounaris, and W.-S. Hou, Editors. 1992, Lewis Publishers, Inc.: Chelsea, Michigan. p. pp. 256-277.
56. Axley, J.W., *Tools For The Analysis of Gas Phase Air Cleaning Systems In Buildings*. ASHRAE Transactions (to be published), 1994.
  57. Yeh, M.C., *Chapter XII Thermodynamic Analysis of Adsorption Systems*, in *Adsorption Technology for Air and Water Pollution Control*, K.E. Noll, V. Gounaris, and W.-S. Hou, Editors. 1992, Lewis Publishers, Inc.: Chelsea, Michigan. p. pp. 229-255.
  58. Sarlis, J.N., *Chapter IV Gravimetric Differential Reactor for Gas Adsorption Studies*, in *Adsorption Technology for Air and Water Pollution Control*, K.E. Noll, V. Gounaris, and W.-S. Hou, Editors. 1992, Lewis Publishers, Inc.: Chelsea, Michigan. p. pp. 72-85.
  59. Yu, J.-W., *Adsorption of Trace Organic Contaminants in Air*, . 1987, Royal Institute of Technology, Department of Chemical Engineering, Stockholm, Sweden.
  60. Chiang, P.C., *et al. Comparison of Adsorption Capacity of VOCs on Various Adsorbents*. in *Indoor Air '93: Proceedings of the 6th International Conference on Indoor Air Quality and Climate*. 1993. Helsinki, Finland: Indoor Air '93, Helsinki.
  61. Rood, M.J., *et al. Adsorption Properties of Activated Carbon Fibers: Applications to Indoor Air Quality*. in *Indoor Air '93: Proceedings of the 6th International Conference on Indoor Air Quality and Climate*. 1993. Helsinki, Finland: Indoor Air '93, Helsinki.
  62. Graham, J.R. and M.A. Bayati. *The Use of Activated Carbon for the Removal of Trace Organics in the Control of Indoor Air Quality*. in *Indoor Air '90: The 5th International Conference on Indoor Air Quality and Climate*. 1990. Toronto, Canada: Canada Mortgage and Housing Corporation.
  63. Wood, G.O., *Activated Carbon Adsorption Capacities for Vapors*. Carbon, 1992. Vol. 30(No. 4): p. pp. 593-599.
  64. Trogen, A., *Prediction of Binary Adsorption Equilibria From Single Component Data*, . 1992, The Royal Institute of Technology, Sweden.
  65. Liu, R.-T. *Modeling Activated Carbon Adsorbents for the Control of Volatile Organic Compounds in Indoor Air*. in *Far East Conference on Environmental Quality, November 1991*. 1991. Hong Kong: ASHRAE.
  66. Tichenor, B.A., Z. Guo, and L.E. Sparks. *Fundamental Mass Transfer Model for Indoor Air Pollution Sources*. in *Indoor Air '93: The 5th International Conference on Indoor Air Quality and Climate*. 1993. Helsinki, Finland: Helsinki University of Technology.
  67. Guo, Z.S. and B.A. Tichenor. *Fundamental Mass Transfer Models Applied to Evaluating the Emissions of Vapor-Phase Organics From Interior Architectural Coatings*. in *EPA/AWMA Symposium*. 1992. Durham, NC.
  68. Chang, J.C.S. and Z. Guo, *Characterization of Organic Emissions from a Wood Finishing Product*. Indoor Air, 1992. 2(3): p. pp. 146-153.
  69. Huebner, K.H. and E.A. Thornton, *The Finite Element Method for Engineers, Second Edition*. 1982, New York: John Wiley & Sons.
  70. Ruthven, D.M., *Principles of Adsorption and Adsorption Processes*. 1984, New York: John Wiley & Sons. 433 pages.
  71. Hudson, J.B., *Surface Science: An Introduction*. 1992, Boston: Butterworth-Heinemann. 321 pages.
  72. Ryan, P.B. and P. Koutrakis, *The Reactive Chemistry of Ozone in Indoor Environments*, in *CIAR Currents: The Newsletter of the Center for Indoor Air Research*. 1993: Linthicum, MD USA. p. pp. 1,3.

73. Axley, J.W. *Modeling Sorption Transport in Rooms and Sorption Filtration Systems for Building Air Quality Analysis*. in *Indoor Air '93: The 6th International Conference on Indoor Air Quality and Climate*. 1993. Helsinki, Finland: Indoor Air '93, Helsinki.
74. Stoer, J. and R. Bulirsch, *Introduction to Numerical Analysis: Second Edition*. Second Edition ed. 1993, New York: Springer-Verlag. 660 pages.
75. Press, W.H., *et al.*, *Numerical Recipes in C: The Art of Scientific Computing - Second Edition*. Second Edition ed. 1992, Cambridge: Cambridge University Press. 994 pages.